1968

A study of the behavior of beam-to-column connections

John W. Peters
Lehigh University

A STUDY OF THE BEHAVIOR OF BEAM-TO-COLUMN CONNECTIONS

by

John W. Peters

A thesis

Presented to the Graduate Committee

of Lehigh University

in Candidacy for the Degree of

Master of Science

in Civil Engineering

Lehigh University

1968

CERTIFICATE OF APPROVAL

This thesis is accepted and approved in partial fulfillment of the requirements for the degree of Master of Science.

May 15, 1968
Date

George C. Driscoll, Jr.
Dr. George C. Driscoll, Jr.
Professor in Charge

David A. VanHorn
Dr. David A. VanHorn
Chairman, Department of
Civil Engineering

TABLE OF CONTENTS

ACKNOWLEDGEMENTS

This thesis was prepared in connection with a research project on beam-to-column connections conducted by the Department of Civil Engineering, Fritz Engineering Laboratory, Lehigh University, Bethlehem, Pennsylvania. Dr. David A. VanHorn is the Chairman of the Department and Dr. Lynn S. Beedle is the Director of the Laboratory.

The work described here was sponsored jointly by the American Iron and Steel Institute and the Welding Research Council.

The author wishes to sincerely thank Dr. George C. Driscoll, Jr., the thesis advisor, for his patience and advice during his critical review of this work. Sincere appreciation is expressed for the unselfish help extended to the author by his colleagues, Messrs. James O. Armacost, III, and Leo H. Van Zuilen.

Finally, the author wishes to express his thanks to Mr. Kenneth Harpel, laboratory foreman, and his staff for their aid in the test program, Mr. Richard Sopko for the preparation of photographs, Miss Sharon Gubich for her help with the drawings, and Mrs. Diane Kroohs for her care in typing the manuscript.

ABSTRACT

This thesis presents the results of a theoretical and experimental investigation on fully rigid beam-to-column connections. Of primary importance is the effect of high axial load in a column on the behavior of beam-to-column connections.

Both upper and lower bound theoretical plastic analysis relations are derived and discussed. The theoretical investigations are compared against actual test results.

The results of an experimental investigation are presented and discussed. Conclusions are made as to how a connection behaves plastically.

The report is concluded with the presentation of a practical design method for some types of beam-to-column connections.

1. INTRODUCTION

In a multi-story frame, methods have been found to predict the behavior of the frame and most of its components.(1) However, the plastic method of analysis and design presently used neglects the combined effect of shear and axial load on the behavior of beam-to-column connections.(2)

During tests on multi-story frames at Lehigh University, it was observed that high column axial load and shear resulting from beam moments significantly affect the behavior of beam-to-column connections.(3) In some instances the diagonal stiffener, which was used in an exterior connection to resist the shear caused by a large beam moment, actually yielded before the plastic moment was reached in the beam. This behavior was observed in the lower stories of a frame where axial load was higher. In a test in which diagonal stiffeners were not used for an exterior connection, the shear deformation was largest in the connection with the highest axial load even though the shear force was the same in all the connections.

As a result of the observations from the frame tests and because of other unanswered questions about beam-to-column connections, a project on Beam-to-Column Connections

was initiated at Lehigh University in 1966 by the American Iron and Steel Institute and the Welding Research Council. This thesis is based on information obtained and work done on the research project.

1.1 Background

There are basically two types of beam-to-column connections. Both are characterized by the intersection of beam and column elements into a single joint. Interior and exterior beam-to-column connections form the two basic types of connections covered in this report (see Figure 1).

Under normal conditions a beam-to-column connection is subjected to axial load, moment, and shear from both of its component elements the beam and the column. Figure 2 shows an exploded view of an exterior connection subjected to the most general two-dimensional loading. A simplification can be made to the force system by noting that the axial load in the beam is generally low even when the frame is laterally loaded. The beam moment is also changed into two concentrated forces acting as a couple through the two beam flanges. This couple is the major factor in causing a highly stressed shear condition to occur in the central web region of the connection (this region will be referred to as the web panel). If the effect of the beam moment is concentrated in the beam flanges, normal stresses will only be applied to two of the four sides of the web panel. The

normal stresses result from the column moments and axial loads. The lower normal stress on the web panel will be larger than the upper normal stress. This effect is due to the shear in the beam.

When any of the forces applied to a beam-to-column connection reach a critical magnitude, the connection may fail in any of four failure modes. Three of the most common failure modes for beam-to-column connections are shown in Figure 3. Figure 3a shows a compressive type failure in which the concentrated compressive force from the beam couple crushes a zone of the column web. A tension failure, as is shown in Figure 3b, is characterized by the pulling out of a column flange due to the concentrated tensile force from the beam couple. The third effect is that in which a shear displacement occurs. This type of failure is shown in Figure 3c and can be described as "shear racking". It is believed that this type of failure is most sensitive to the action of axial load. Therefore, a shear failure mode is of prime importance, when the effect of high axial load is being studied in beam-to-column connections. Buckling is the fourth possible failure mode. However, almost all practical connections are made of thick enough elements that this type of failure will be neglected in the study to be presented. Previous work has resulted in suggestions for proportions adequate to prevent buckling failures.(1)

1.2 Past Work

Previous work done in the area of beam-to-column connections has not considered the combined effect of high axial load and shear resulting from beam moments. Solutions were developed by Beedle, et al. for the problem of shear failure of a corner connection neglecting the effect of axial load.(4) A slight modification of this formula is presently being used for the design of beam-to-column connections of multi-story frames.(1) The additional problem of instability or localized failure of a beam-to-column connection was studied by Jensen, et al.(5) Figure 3 shows the relationships presently being used and the type of failure they are designed to prevent. The solutions which are presently available provide a satisfactory prediction of beam-to-column connection behavior with low axial load in the column.

There is very little literature available which deals with the ultimate strength under the combined shear-axial load-moment interaction for connections. However, in Reference 6 a group from the University of Tokyo has examined in great detail the elastic solution of the combined shear-axial load-moment interaction for beam-to-column connections.

Work is currently being conducted at the University of California at Berkeley on the behavior of beam-to-column connections subjected to lateral loadings and high axial

loads in the column. An attempt is being made at California to solve the connection behavior problem using a finite element type approach. If this should prove successful, it could serve as a valuable check to the methods presented in this report or prove as a valuable aid in developing more accurate design relationships.

This report makes use of the findings and many of the results and procedures described in Reference 5.

2. THEORETICAL APPROACH

The theoretical work presented is an attempt to consider the combined effects of shear, axial load, and moment on the behavior of beam-to-column connections. The manner in which this problem was approached has taken two paths. As in most plastic analysis approaches, both an upper and a lower bound type solution should be performed.

All plastic analysis methods must satisfy three conditions: 1) fully yielded cross-section, 2) equilibrium, 3) failure mechanism. The difference between the upper and lower bound solutions is in the conditions from which the bound solution is started.

The lower bound solution is started by assuming a stress distribution which will not exceed the yield condition in the element under consideration. The ultimate load is computed by satisfying equilibrium across the element. If the lower bound solution so calculated causes a mechanism condition, the solution is the true solution.

The upper bound solution is started by assuming a mechanism condition which will cause failure of the element under consideration. The ultimate load is computed by satisfying equilibrium across the section. If this

ultimate load causes no violation of the yield condition at any point on the element, the ultimate load is the true solution.

The results of performing the two solutions outlined will usually give a range within which the answer must lie. The upper bound will always give a solution which is equal to or greater than true answer. The lower bound is always conservative and will give results lower than or equal to the true solution. Only when the upper and lower bound are equal can it be certain that the solution found is the true solution. Therefore, this report will attempt to outline upper and lower bound solutions in an attempt to narrow the range between the two bounds and in an attempt to better understand the true behavior of beam-to-column connections.

2.1 Lower Bound Approach

In order to help formulate a test program and provide an insight into the behavior of beam-to-column connections subjected to high axial load in the column, a preliminary lower bound theoretical investigation was attempted. The preliminary investigation has taken the same type approach as that used to determine the interaction of thrust, shear, and moment in beams.[7,8] This type of solution follows the lower bound type of solution outlined in the previous section of this report. Using a lower bound approach, it is necessary to begin the analysis with a description of

the force distribution applied to the connection. This is a complex problem for a solution in the elastic or plastic range. The problem is further complicated by the residual stress pattern due to welding in the fabrication process. As a result, the solutions developed in this study have attempted to formulate an equilibrium solution for the strength of the connection which will reflect the effect of normal force in the column on the shear capacity of a connection web panel.

The following is a list of assumptions made in developing the lower bound solution:

1. The connection under examination has no shear stiffening.
2. All shear in the column is distributed uniformly across its web.
3. All bending moment in the beam is taken by the beam flanges.
4. Axial load in the beam is neglected.
5. All normal force in the beam flange is transmitted directly to the horizontal stiffener.
6. The flanges of the column do not contribute any additional strength to the connection by their participation in the bending deformation of the connection.

7. No specific steps have been taken to account for residual stresses.

8. A connection will fail when its most critically stressed cross section becomes fully yielded.

9. The yield surface of the connection is defined by the von Mises Yield Theory.

10. Strain-hardening is not taken into account.

11. The connection is considered to be made of an elastic, perfectly plastic material.

2.1.1 Neutral Axis of Column in the Column Flange

The lower bound solution commences by assuming as general a stress distribution in the beam and column as is possible. Figures 4 and 5 show the final stress distribution assumed for sections in both the beam and column. All stresses are bounded by the full yield stress, σ_y. In some cases, such as in the web of the column, shear and normal stresses must be added together. In such cases each stress is controlled by a parameter, k or ζ, such that when they are combined a condition of full yield will exist. It is also necessary to establish a parameter, η_o, which will define the location of the neutral axis within a given section.

The section through the column is of prime interest, since it should be the most critical section within the

connection (i.e. the last section to yield). This is why a horizontal section through the column at the extreme top of the connection has been used as the datum for establishing the lower bound presented in this report (see section B-B, Figure 4). Figure 5 gives the stress distributions at this section in the column for the cases when the column has its neutral axis in its flange and in its web, respectively.

Figure 4 shows the section cut in the beam at the face of the column (section A-A). This section is used only to define the magnitude of the concentrated force from the beam couple. This force is combined in the column web as a shear with the shear force already in the column.

The remainder of this section will be used to describe the development of an interaction relationship for the combined axial load-shear-moment interaction for a section in the column at the very top of the connection (see section B-B, Figure 4). The interaction relation will express the maximum moment, M, that can be applied externally to a beam-to-column connection by a column as a function of axial load in the column, beam moment at the column face (M_B), geometry of the frame, and dimensions of the component members. The moment, M, is the column moment which enters a beam-to-column connection at section B-B, Figure 4.

With all the stresses so defined such that their upper limit is the full yield stress, it is possible to write an expression for the external forces interms of the stresses and stress parameters. The column moment, M, can be determined for the case when the neutral axis is in the column flange by using the parameters shown in Figure 5 part (1). Moment is equal to the area of the stress block yielded by moment multiplied by the moment arm and yield stress, σ_y. This relationship for moment is shown in equation (2.1a).

$$M = b [t - \eta_o t] [d_c - (t - \eta_o t)] \sigma_y \quad (2.1a)$$

Equation (2.1a) may be simplified using the parameters d_f, which is equal to the depth of the column between the center lines of its two flanges, and A_f which is equal to double the area of a single column flange. The simplified moment equation is (2.1b).

$$M = \frac{\sigma_y}{2} A_f [d_f - \eta_o d_w - \eta_o^2 t] \quad (2.1b)$$

The expression for the thrust, T, in the column can be gotten using the parameters shown in Figure 5, part (1). The thrust is equal to the area of the stress block yielded by thrust times the yield stress, σ_y. This relationship is shown by equation (2.1c).

$$T = \} \sigma_y A_w + 2 \eta_o tb \sigma_y \quad (2.1c)$$

Remembering that $A_f = 2bt$ and $T_y = (A_f + A_w)\,\sigma_y$ equation (2.1c) may be rearranged to give equation (2.1d).

$$T = \frac{(\zeta A_w + \eta_o A_f)\, T_y}{A_w + A_f} \qquad (2.1d)$$

At this stage, the moment M and the thrust T are defined in terms of the as yet unknown parameters η_o and ζ. Conditions for determining these unknown parameters will be established by considering the shear stress acting along with the normal stress and by considering the forces entering the connection as a result of the loading on the beam and column in a structure.

First the shear stress will be considered. Figures 6a and 7a show longitudinal elements of infinitesimal length just outside the joint for the beam and column respectively. Because there is a moment gradient in both the beam and the column, there are changes $\Delta\sigma_B$ and $\Delta\sigma_C$ in the bending stresses from one end to the other of each infinitesimal length of flange. To maintain equilibrium, the shear force on the element where the web meets the flange must equal the difference in flange forces at the ends of the elements. This is expressed in equations 2.2a and 2.2b.

$$dx_B w_B \tau_B = \frac{a_f}{2}(1 - m_\sigma)\,\Delta\sigma_B \qquad (2.2a)$$

$$dx_C w \tau_C = \frac{A_f}{2}(1 - \eta_o)\,\Delta\sigma_C \qquad (2.2b)$$

The moment diagrams for beam and column is shown in part (b) of Figures 6 and 7. From these figures it is possible to obtain relations for changes in stress, $\Delta\sigma$, for both beam and column in terms of member dimensions. Equations (2.2c) and (2.2d) use the moment gradients to give the expressions for changes of stress in the beam and column, respectively.

$$\frac{\Delta\sigma_B}{dx_B} = \frac{\sigma_y}{L} \qquad (2.2c)$$

$$\frac{\Delta\sigma_C}{dx_C} = \frac{\sigma_y}{\ell} \qquad (2.2d)$$

If equation (2.2c) and (2.2d) are substituted into equations (2.2a) and (2.2b) respectively, expressions for the shear flow in beam and column directly adjacent to the connection are obtained.

$$w_B\tau_B = \frac{a_f}{2}(1 - m_o)\frac{\sigma_y}{L} \qquad (2.3a)$$

$$w\tau_C = \frac{A_f}{2}(1 - \eta_o)\frac{\sigma_y}{\ell} \qquad (2.3b)$$

Equation (2.3a) and (2.3b) express the shear flow in the beam and column, respectively.

Figure 8a shows an exterior beam-to-column connection subjected to a general external loading condition. A beam moment, M_B, is assumed; all other external forces can be calculated using statics. The beam shear force, V_B, and

column shear force, V_c, may be obtained from equations (2.3a) and (2.3b), respectively. The beam and column shear forces are presented in equations (2.4a) and (2.4b).

$$V_B = w_B \tau_B d_B = \frac{a_f}{2} (1 - m_o) \frac{\sigma_y}{L} d_B \qquad (2.4a)$$

$$V_c = w \tau_c d_c = \frac{A_f}{2} (1 - \eta_o) \frac{\sigma_y}{\ell} d_c \qquad (2.4b)$$

By cutting a free body diagram, as shown in Figure 8b, with a section passed through the connection just below the upper horizontal stiffener, the web panel shear stress may be calculated. Figure 8b only contains the effects of the shears, all moments and axial loads are in equilibrium and are removed from the sketch to simplify the presentation. In order to establish vertical equilibrium, a small axial load, ΔP, must be added to the lower column to balance the beam shear (i.e. $\Delta P = V_B$). To establish rotational equilibrium of the free body, moments are taken about the mid-point of the external side of the connection, point 0. It is from this rotational equilibrium that the web panel shear stress, τ, is calculated (see equation 2.5a).

$$V_B d_c - \Delta P \frac{d_c}{2} - V_c \frac{d_B}{2} + \tau w d_w \frac{d_B}{2} = 0 \qquad (2.5a)$$

If equations (2.4a) and (2.4b) are substituted into equation (2.5a), expression (2.5b) presenting a relationship for web panel shear, τ, is obtained.

$$\tau = \frac{1}{2w}\left[A_f(1-\eta_o)\frac{\sigma_y}{\ell} - a_f(1-m_o)\frac{\sigma_y}{L}\right] \qquad (2.5b)$$

Because of the presence of shear stress in the web, the web panel is only able to carry a reduced portion ζ of the full σ_y as is expressed in equation (2.6) and shown in Figure 5, part (1).

$$\sigma = \zeta\sigma_y \qquad (2.6)$$

Equation (2.5b) and (2.6) are the basic stress expressions for the web panel. These expressions must be combined using the von Mises Yield condition for a uniaxial plane stress condition as given in equation (2.7)

$$\sigma^2 + 3\tau^2 = \sigma_y^2 \qquad (2.7)$$

By substituting equations (2.5b) and (2.6) into (2.7) to obtain equation (2.8), an expression is obtained for ζ, the percentage of P_y which can be present along with the given web shear to produce the full yield condition.

$$\zeta = \sqrt{1 - \frac{0.75}{w^2}\left[\frac{(1-\eta_o)}{\ell}A_f - \frac{a_f(1-m_o)}{L}\right]^2} \qquad (2.8)$$

Equation (2.8) can be solved for η_o, the percentage of the column flange not yielded by moment.

$$\eta_o = 1 + \frac{\ell}{A_f}\left[-\frac{a_f(1-m_o)}{L} \mp \frac{2\sqrt{3}}{3}w\sqrt{1-\zeta^2}\right] \qquad (2.9)$$

It should be noted that $\eta_o \leq 1$. Therefore, the last term of equation (2.9) should always be prefaced by a negative sign.

Equation 2.9 may be substituted into equation (2.1d) to obtain an expression for thrust, T.

$$T = \xi \sigma_y A_w + \sigma_y A_f \left[1 + \frac{\ell}{A_f} \left(- \frac{a_f (1-m_o)}{L} \mp \frac{2\sqrt{3}}{3} w \sqrt{1-\xi^2} \right) \right] \quad (2.10)$$

For simplicity m_o is set equal to zero. This is the case when the beam flange is fully yielded by moment. Equation (2.10) is solved for ξ. In order to simplify the equations presented, expression (2.11a) through (2.11d) will be used. Both λ and Φ are functions of the member sizes of the connection. The relative member sizes and the frame geometry are reflected in β. Axial load and column size are reflected by α.

$$\alpha = \frac{A_f}{A_w} - \left[1 + \frac{A_f}{A_w} \right] \frac{T}{T_y} \quad (2.11a)$$

$$\beta = \frac{a_f}{L A_w} \quad (2.11b)$$

$$\lambda = \frac{\ell}{d_w} \quad (2.11c)$$

$$\Phi = 1 + \frac{4}{3} \lambda^2 \quad (2.11d)$$

If the equations of the (2.11) series are substituted in equation (2.10) and it is solved for ζ, the result will be equation (2.12).

$$\zeta = \frac{\frac{2}{\sqrt{3}}\lambda\sqrt{(\Phi - \alpha^2) - 2\beta(\frac{\beta}{2} - \alpha)} - (\alpha - \beta)}{\Phi} \qquad (2.12)$$

Substitution of equation (2.10) into equation (2.7), remembering that m_o is zero, gives:

$$\eta_o = 1 - \frac{A_w}{A_f}\beta - \frac{2\sqrt{3}}{3}\frac{w}{\Phi}\sqrt{\Phi - (\alpha-\beta)^2(1-\frac{4}{3}\lambda^2) + \frac{4}{3}\lambda(\alpha-\beta)\sqrt{\Phi - (\alpha-\beta)^2}} \qquad (2.13)$$

An expression for the plastic moment of a wide-flange section is given in equation (2.14)

$$M_p = \frac{\sigma_y}{2}\left[A_f d_f + \frac{A_w d_w}{2}\right] \qquad (2.14)$$

The interaction relation for the case when the neutral axis of the column is in the column flange can be obtained by substituting expression (2.13) and (2.14) into the moment expression, (2.1b)..

$$\frac{M_{pm}}{M_p} = \frac{2A_f}{A_w}\left[\frac{d_f}{d_w} - \eta_o - \frac{t}{d_w}\eta_o^2\right] \Big/ \left[1 + 2\frac{A_f}{A_w}\left[\frac{d_f}{d_w}\right]\right] \qquad (2.15)$$

The limits of interaction relation (2.15) are from $0 \leq \eta_o \leq 1$ (i,e. when the neutral axis is in the column flange). The moment, M_{pm}, is the column moment which can be applied to an unstiffened connection, with the neutral axis of the column in its flange, in order to cause "shear racking" of the connection.

2.1.2 Neutral Axis of Column in the Column Web

The procedure followed in calculating the moment, shear, and thrust interaction relation when the column has its neutral axis in the web is similar to that described for the case when the neutral axis is in the column flange. The difference in the two cases is the starting stress distributions. For the case under consideration in this section, the stress block used is shown in part (2) of Figure 5.

Equilibrium of the stress blocks resulting from bending moment and the stress blocks resulting from thrust for Figure 4 and case 2 of Figure 5 will give equations (2.16a) and (2.16b) in the same manner as was done for equations (2.1b) and (2.1d). In this instance, an additional parameter y_o gives the distance of the neutral axis in the web from the centerline of the web.

$$M = \frac{\sigma_y}{2} A_f d_f + \zeta \sigma_y w \left(\frac{d_w}{2} - y_o\right)\left(\frac{d_w}{2} + y_o\right) \qquad (2.16a)$$

$$T = 2y_o \sigma_y w \zeta \qquad (2.16b)$$

The shear equation is basically the same as equation (2.5b) with the exception that in this case $\eta_o = 0$. When $\eta_o = 0$ the full column flange takes bending moment, which is the case if the neutral axis is in the column web.

$$\tau = \frac{A_f}{2w\ell}\,\sigma_y - \frac{a_f(1 - m_o)}{2wL}\,\sigma_y \qquad (2.16c)$$

In order to establish the yield condition in the web panel, it is necessary to write expressions for the normal and shear stress, respectively. The normal stress in the web panel is the result of both moment and axial load as is shown in Figure 5, part (2). However, the normal stress is assumed equal to the reduced value $\}\sigma_y$ for the entire width of the web panel as indicated by equation (2.17a).

$$\sigma = \} \sigma_y \qquad (2.17a)$$

The expression for shear in the web panel can be gotten from equation (2.16c) and is restated as equation (2.17b).

$$\tau = \frac{\sigma_y}{2w}\left[\frac{A_f}{\ell} - \frac{a_f\,(1 - m_o)}{L}\right] \qquad (2.17b)$$

The normal and shear stresses are combined to establish the yield condition in the web panel. Von Mises Yield Condition is used for the yield criterion. Using equations (2.17a),

(2.17b), and (2.7) one may obtain equation (2.18) for the percentage ζ of σ_y which can coexist with the web shear to obtain the yield condition.

$$\zeta = \sqrt{1 - \frac{0.75}{w^2}\left[\frac{A_f}{\ell} - \frac{a_f(1 - m_o)}{L}\right]^2} \qquad (2.18)$$

By substituting the value of ζ into the moment equation along with a value of y_o solved from equation (2.16b) a relationship between column moment, section properties, frame dimensions, and thrust is developed. If this relation is non-dimensionalized by dividing by the M_p of the column, the general interaction expression for moment, thrust, and shear is obtained as presented in equation (2.19).

$$\frac{M_{pm}}{M_p} = 1 - \frac{A_w d_w}{4Z}\left\{1 - \sqrt{1 - \frac{0.75}{w^2}\left[\frac{A_f}{\ell} - \frac{a_f(1 - m_o)}{L}\right]}\right\} - \frac{A^2}{4Zw\sqrt{1 - \frac{0.75}{w^2}\left[\frac{A_f}{\ell} - \frac{a_f(1 - m_o)}{L}\right]^2}}\left(\frac{T}{T_y}\right)^2 \qquad (2.19)$$

For the special case when the beam flange is fully yielded, $m_o = 0$, and when the simplifying expressions of equations (2.11) are used, the general interaction relation can be simplified to equation (2.20).

$$\frac{M_{pm}}{M_p} = 1 - \frac{A_w d_w}{4Z}\left[1 - \sqrt{1 - \frac{0.75}{w^2 \ell^2}\left[A_f - \beta A_w\right]^2}\right] - \frac{A^2\left[\frac{T}{T_y}\right]^2}{4Zw\sqrt{1 - \frac{0.75}{w^2 \ell^2}\left[A_f - A_w\right]^2}} \qquad (2.20)$$

The limits of interaction relation (2.20) are from $0 \leq y_o \leq \frac{d_w}{2}$ (i.e. when the neutral axis of the column is in its web).

It should be noted that equations (2.16c) and (2.18) correspond to the similar equations (2.5b), and (2.8), which were developed for the case when the neutral axis of the column is in its flange, if η_o is substituted into the later group of equations.

The interaction curve for a beam-to-column connection is composed of the two solutions just outlined (see Figure 9). At low axial loads, the neutral axis of the column cross-section is within its web. The parabolically shaped curve of Figure 9 corresponds to the case of the neutral axis in the column web. As axial load is increased, the neutral axis shifts out of the column web into the column flange; this corresponds to the almost straight line curve of Figure 9. The two curves should become tangent at the point where the neutral axis shifts from the web to the flange. The curves presented in this report show a slight displacement with respect to each other. It is suspected that this discrepancy is due to the fact that the flanges are really tapered rather than rectangular and each section has fillets at the flanges.

Figure 9 is an interaction curve for a beam-to-column connection made of a 6WF25 column and 12B16.5 beam. The dimensions of the connection subassemblage can be varied and for all practical lengths the interaction curves will be essentially constant and equal to that of Figure 9. The curve shown is one of a family of curves. As the beam moment is changed (i.e. different m_o values), the curves change. However, the family of curves is very similar to the single interaction curve presented. Figure 9 considers the case of a full plastic moment in the beam.

Figure 9 also shows points which represent the ultimate loads reached by certain gaged connections from the braced multi-story frame tests conducted at Lehigh University and described in reference (3). The failure criterion was qualitative. A connection was considered to have failed if large diagonal displacements occurred at the highest load recorded. It should be noted that the interaction curve is in the transition region between the failed and unfailed connections.

If the various component members of a beam-to-column connection are varied, the scatter band for different relative member sizes is small (see Figure 10). In figure 10 interaction curves for a representative light and a heavy connection are plotted. A connection may be designated as light or heavy depending upon the column

size. It can be noticed from this figure that light connections offer greater relative strength at low thrust. However, as thrust increases the interaction curves for light and heavy connections converge, until at about 0.6 P/P_y they coincide.

Tables 1 through 6 present values for the lower bound interaction solution just presented for some selected beam-to-column connections. The connections were selected to illustrate the effect of member geometry, frame dimensions, and beam moment on the beam-to-column interaction curve. The tables are set up for a given member size, frame geometry, and beam moment (i.e. m_o). There are two column moment ratios, M/M_p, given for each axial load ratio, P/P_y. The first M/M_p ratio is for the case of the neutral axis of the column in its flange. The second column moment ratio is for the case when the neutral axis of the column is in its web. If for a given table the lower of the moment ratios for each axial load is plotted against the axial load ratio, a beam-to-column interaction curve is obtained. Also presented in the tables is the parameter shown in Figure 5 as ξ. Xi is the percent of σ_y in the column web which when combined with τ will give a fully yielded condition in the web panel.

Tables 1 to 3 show the effect of the size of the beam moment (Table 1, $m_o = 0$, Table 2, $m_o = 0.5$, and Table 3, $m_o = 1.00$). If Table 1, 2, and 5 are compared, one may

determine the effect of frame dimensions on the interaction curve for a given connection. By the comparison of Table 1 and 6, one may determine the effect of relative member size upon a given frame connection geometry.

If the comparisons described above are made, it can be noted that all the tabulated results would generate interaction curves which would be very similar (i.e. within 5 to 10 percent of each other). Since the results have been non-dimensionalized, it may be anticipated that a simple, workable design formula may be developed for beam-to-column connections by taking advantage of the similarity in the results.

2.2. Upper Bound Approach

The upper bound approach to analysis of a beam-to-column connection was formulated in order to provide a check for the previously described lower bound and to provide a more realistic approach to the problem (i.e. in developing an interaction relationship for an actual failure mechanism as observed from a tested specimen). An upper bound approach could easily be modified to consider the effects of any type of connection stiffening.

The upper bound approach used here is an energy approach. A connection is given a displacement which will cause a mechanism condition to exist within the connection. Using this displacement, the internal and external work expressions are calculated. The following

is a list of assumptions made in this energy formulation:

1. The connection is considered to be made of an elastic perfectly plastic material.
2. The yield surface of the connection is defined by the von Mises Yield Theory.
3. The material is not considered to strain-harden.
4. The connection is analyzed as a plane strain case.
5. The axial load in the beam is neglected.

Equilibrium of the connection is established by equating internal and external work. In order to obtain the best upper bound approach it is necessary to minimize the total energy expression with respect to a moment for a given thrust. This procedure should then give the lowest upper bound answer for a given displacement mode.

The upper bound procedure just described may be illustrated for an exterior beam-to-column connection neglecting the effect of axial load. Consider an exterior connection which is deformed causing a shear displacement rate, $\dot{\delta}$, (see Figure 11). The shear displacement is a lateral displacement of one edge of the connection with respect to the other edge. This displacement will be called shear racking.

Four discrete yielding points in the column flanges at the four corners of the connection are shown in Figure 11. A detailed view of the flange yield concentration is shown as an inset. This yield concentration is the major difference between the solution presently recommended for the plastic design of beam-to-column connections[1] and the solution outlined in this report. The relation presently used to predict shear failure of a connection was developed originally for a portal frame. In portal frames the members adjacent to the connection usually are subjected to a moment in the range of a full plastic moment. Therefore, the beam flanges would be fully yielded and offer no stiffness to the web panel. However, in a multistory frame with large axial loads in the columns, less of the overall column strength is being taken by the bending moment. Therefore, the column flange will offer some additional stiffeness to resist column bending.

To calculate the bound solution for a mechanism such as those shown in Figures 11 or 12, it is necessary to have some expressions to compute the internal and external work done by the assumed mechanism as it goes through a given displacement.

Computation of the external work done by mechanism motion is the most direct and easiest to visualize. The external work, W_E, is equal to the algebraic sum of all external forces times their respective displacements in the direction of the forces.

The expression for internal work done by a mechanism motion is more complex and difficult to visualize. However, if certain basic theorems of the theory of plasticity and tensor notation are used, simple expressions for the internal energy dissipated may be developed. Before any energy dissipation will be expressed, certain plasticity concepts should be realized. The energy dissipated by an element will be expressed as a function of the strains, ϵ_{ij}, in the element. The subscripts i and j vary from 1 to 3. These strains may be directly related to the displacement to which the given element is subjected. The strains, ϵ_{ij}, in an element may be broken down into elastic strains, ϵ^e_{ij}, and plastic strains, ϵ^P_{ij}, as is shown in Equation (2.21).

$$\epsilon_{ij} = \epsilon^e_{ij} + \epsilon^p_{ij} \qquad (2.21)$$

Since elastic strains are determined uniquely by stress, there is no change in stress and correspondingly no elastic change in strain at the limit load (i.e. ϵ^e_{ij} = constant, at the limit load). If the first partial derivative of equation (2.21) is taken with respect to time, an expression for strain rate, $\dot{\epsilon}_{ij}$, is obtained. Since ϵ^e_{ij} is a constant, $\dot{\epsilon}^e_{ij}$ equals zero. Equation (2.22) is in an equation for the strain rate.

$$\dot{\epsilon}_{ij} = \frac{\partial(\epsilon_{ij})}{\partial t} = \dot{\epsilon}^p_{ij} \qquad (2.22)$$

Since an expression for strain rate $\dot{\epsilon}_{ij}$ is much simpler than an expression for strain, ϵ_{ij}, at ultimate load, the internal energy will be expressed as a function of a strain rate. By definition, the energy dissipation per unit volume of the given element will be expressed as D. D will then be expressed as a function of strain rate (i.e. $D(\dot{\epsilon}_{ij}) \equiv D(\dot{\epsilon}^P_{ij})$).

Figures 11 and 12 show all displacements as displacement rates. This procedure makes the calculation of the unit energy dissipation, $D(\dot{\epsilon}^P_{ij})$, possible by calculating the plastic strain rates, $\dot{\epsilon}^P_{ij}$, directly from the displacement rates assumed (i.e, $\dot{\sigma}$ in Figure 11).

If the von Mises Yield Criterion is assumed to govern yielding, an expression for the unit internal energy dissipation can be derived using tensor manipulation and various properties of the strain tensor. The resulting unit internal work expression is given as equation (2.23).

$$D(\dot{\epsilon}^P_{ij}) = k_o \sqrt{2\, \dot{\epsilon}^P_{ij}\, \dot{\epsilon}^P_{ij}} \qquad (2.23)$$

A complete derivation of equation (2.23) is given in Chapter 8 of reference 10. The quantity k_o, is an invariant of the stress tensor.

If for the case of plane strain, two normal principal strains ϵ_1 and ϵ_2 are given, it can be proved that there

is no volume change during plastic deformation. Therefore,

$$\dot{\epsilon}^p_1 + \dot{\epsilon}^p_2 = 0$$

Using this fact and substituting $\dot{\epsilon}^p_1$ and $\dot{\epsilon}^p_2$ into equation (2.33) one obtains equation (2.24).

$$D(\dot{\epsilon}^p_{ij}) = k_o\sqrt{2(\dot{\epsilon}^p_1)^2 + 2(\dot{\epsilon}^p_2)^2} = 2k_o\left|\dot{\epsilon}^p_1\right| \qquad (2.24)$$

From a Mohr's Circle of strains it can be proved that the absolute value of the maximum shear strain rate is twice the absolute value of the maximum normal strain rate.

$$\left|\dot{\gamma}_{max}\right| = \left|\dot{\epsilon}^p_1 - \dot{\epsilon}^p_2\right| = 2\left|\dot{\epsilon}^p_1\right|$$

Therefore, equation (2.25) relating unit energy dissipation to shear strain rate may be directly obtained from this relationship and equation (2.24).

$$D(\dot{\epsilon}^p_{ij}) = k_o\dot{\gamma}_{max} \qquad (2.25)$$

Equations (2.24) and (2.25) are the basic relations used to calculate the internal energy dissipation per unit volume of a structural element strained inelastically by

normal strains and shear strains, respectively. To obtain the total internal work of an element, W_I, the unit energy dissipation, $D(\dot{\epsilon}^p_{ij})$, must be multiplied by the volume of the element.

With equations (2.24) and (2.25) in mind, it is now possible to attempt an upper bound solution for a beam-to-column mechanism such as is shown in Figure 11. When the joint is subjected to a displacement rate, $\dot{\delta}$, the web of the column is subjected to a shear strain rate $\dot{\gamma} = \dot{\delta}/d_B$ which deforms a volume $wd_w d_B$. Four stations on the flanges at the corners of the web panel are bent in pie-shape sectors through normal strain rates averaging $\dot{\epsilon}_1 = 1.0$. The volumes of the deformed material for the four sectors total $2bt^2\dot{\delta}/d_B$. Substituting the strain rates into equation (2.25) and (2.24) and multiplying each energy term by the volume affected gives equation (2.26) for the total internal energy due to the shear racking shown in Figure 11.

$$W_{I_s} = k_o \dot{\delta} \left[\frac{4t^2 b}{d_B} + wd_w \right] \qquad (2.26)$$

The first term in the brackets of equation (2.26) is the additional strength of the connection contributed by the yielding concentrations in the column flange. If the quantities which make up this additional strength term are noted, one may observe that this additional

strength is directly proportional to the area of a single column flange, tb, and the column flange thickness, t, and inversely proportional to the depth of the beam, d_B. The constant k_o is an invariant of the stress tensor and is defined by the von Mises Yield Condition to equal the shear yield stress as shown by equation (2.27).

$$k_o = \frac{\sigma_y}{\sqrt{3}} \tag{2.27}$$

The calculation of the external work done by the forces shown in Figure 11 is given in equation (2.28). The external work, W_E, is equal to the sum of all external forces times their respective displacement rates (i.e. in Figure 11, the shear force V has a displacement rate $\dot{\delta}$ opposite in sense to its own direction and the moment M_B has a rotation rate $\dot{\delta}/d_B$.)

$$W_{E_s} = \dot{\delta}\left[\frac{M_B}{d_B} - V\right] \tag{2.28}$$

Equating the internal and external energy expressions, assuming the columns are bent in symmetric double curvature and the beam moment is distributed equally to the upper and lower column at a connection, will yield equation (2.29).

$$M = \frac{\frac{\sigma_y}{2\sqrt{3}}\left[wd_w + \frac{4t^2_b}{d_B}\right]}{\left[\frac{1}{d_B} - \frac{1}{2\ell}\right]} \tag{2.29}$$

It is important to note that this expression is the same as the relation presently used in the plastic design of connections for multi-story frames with the exception of the column flange bending term, $\frac{4t^2b}{d_B}$. If expression (2.29) were plotted on an interaction curve with moment and axial load the variables, it would be a straight line of zero slope.

In order to include axial load in the upper bound solution another independent displacement mode must be used which includes the thrust in at least one of its work expressions. An axial load failure mode is shown in Figure 12. Equations (2.30) and (2.31) give the internal and external work, respectively, for the axial shortening mode of Figure 12. Equation (2.30) is gotten by applying equation (2.24) to the displacement mode of Figure 12. The rate ϵ_1 averages to $\dot{\rho}/d_B$. This rate and a deformed volume of Ad_B results in an internal energy rate given by equation (2.30).

$$W_{I_A} = 2k_o A\dot{\rho} \qquad (2.30)$$

Since the only work done by the external forces of the axial displacement mode of Figure 12 is done by the axial loads, they must be determined as accurately as possible. The lower column axial load contains the upper column thrust, P, and the beam shear, S.

The beam shear, S, can be calculated by statics as equal to the relationship given in equation (2.31).

$$S = \frac{2M}{L} + \frac{3\omega L}{2} \qquad (2.31)$$

The uniform beam load is given by the element ω. The beam length, L, is the distance from the column face to the beam inflection point.

To calculate the external work of the axial displacement mode of Figure 12, each column thrust is multiplied by the average displacement rate ($\dot{\rho}/2$) through which it moves. Equation (2.32) is the resulting expression for the external work for the axial displacement mode of Figure 12.

$$W_{E_A} = (P + \frac{M}{L} + \frac{3\omega L}{4})\dot{\rho} \qquad (2.32)$$

By equating internal and external work of the axial load displacement mode the governing interaction relation given in equation (2.33) can be found.

$$M = \frac{2\sigma_y}{\sqrt{3}} AL - PL - \frac{3\omega L^2}{4} \qquad (2.33)$$

A non-dimensionalized revision of equation (2.33) is presented as equation (2.34).

$$\frac{M}{M_p} = \frac{AL}{Z}\left[\frac{2}{\sqrt{3}} - \left(\frac{P}{P_y}\right)\right] \qquad (2.34)$$

It should be recalled that A and Z are the area and plastic modulus, respectively, of the column, with L equal to the distance from the inflection point of the beam to the column face.

By adding the work expressions developed for the two independent displacement modes, it is possible to obtain a total work expression which considers both shear deformations and axial shortening. Equation (2.35) has been derived in such a manner.

$$k_o\left\{\dot{\delta}\left[\frac{4t^2b}{d_B} + wd_w\right] + 2A\dot{\rho}\right\} = 2M\dot{\delta}\left[\frac{1}{d_B} - \frac{1}{2\ell}\right] + \frac{M\dot{\rho}}{L} + \left[\frac{\omega L}{4} + P\right]\dot{\rho} \qquad (2.35)$$

Dividing equation (2.36) by $\dot{\delta}$ and letting $\mu = \dot{\rho}/\dot{\delta}$.

$$k_o\left\{\left[\frac{4t^2b}{d_B} + wd_w\right] + 2A\mu\right\} = 2M\left\{\left[\frac{1}{d_B} - \frac{1}{2\ell}\right] + \frac{\mu}{2L}\right\} + \left[\frac{\omega L}{4} + P\right]\mu \qquad (2.36)$$

Using equation (2.27), equation (2.36) is solved for the ultimate moment in one column, M.

$$M = \frac{\frac{\sigma_y}{\sqrt{3}}\left\{\left[\frac{4t^2b}{d_B} + wd_w\right] + 2A\mu\right\} - \left[\frac{\omega L}{4} + P\right]\mu}{2\left[\frac{1}{d_B} - \frac{1}{2\ell} + \frac{\mu}{2L}\right]} \qquad (2.37)$$

Equation (2.37) is the general upper bound solution for an exterior beam-to-column connection. In order to obtain the lowest upper bound, it is necessary to optimize the column moment in equation (2.37) with respect to μ for a given thrust, P.

If equation (2.37) is non-dimensionalized by dividing by the M_p of the column, equation (2.38) is obtained.

$$\frac{M}{M_p} = \frac{\sqrt{3}\left[\left(\frac{4t^2b}{d_B} + wd_w\right) + 2A\mu\right] - 3\mu\left[\frac{\omega\ell}{4\sigma_y} + A\left(\frac{P}{P_y}\right)\right]}{6Z\left[\frac{1}{d_B} - \frac{1}{2\ell} + \frac{\mu}{2L}\right]} \qquad (2.38)$$

Attempts have been made to optimize equation (2.38). However, all attempts thus far have been unsuccessful. It is possible that the quantity M/M_p is not a minimum with respect to any of the displacement modes used to calculate equation (2.38). Therefore, equation (2.38) should be used as an indicator of the important parameters and how they affect beam-to-column connection behavior problems.

3. TEST PROGRAM

The remainder of this paper is the presentation of a preliminary experimental study of welded beam-to-column connections. The final objective of the test series was a better understanding of the shear, axial-load, moment interaction in a beam-to-column connection which is loaded beyond first yield.

3.1 Connection Subassemblage

The connection subassemblages tested in this series were exterior connections of a frame as is shown in Figure 14. The test specimens were all cut from the frames of Fritz Laboratory Project 273, Plastic Design of Multi-Story Frames. Seven connection subassemblages were saved. Figure 13A and 13B show the connection sub-assemblage test setups. The connection subassemblages will be classified here according to the stiffening treat-ment of the shear panel in the column web. Some of the connections had no web stiffening and some had diagonal stiffening. Figure 14 shows the types of connections tested along with their identifying test number.

Specimens with diagonal stiffening were tested in such a manner that the web stiffening was subjected to either tension or compression. Two of the five diagon-ally stiffened connections were tested with the stiffener

acting in tension. Three tests on subassemblages with tension diagonal stiffeners were chosen in order that the third test, 333.A7, could be used as a supplement to an earlier tension diagonal test, 333.A4, in which some data may have been subjected to an instrumental error which could not be traced to its source.

Two of the diagonally stiffened test subassemblages were tested using columns with pinned ends. This type of setup forced the connection to be subjected to the most critical shear, moment, and thrust interaction condition. However, it made ths subassemblage so flexible that the failure mode was forced outside the connection at a relatively low external load. Since all of the diagonally stiffened connections were overdesigned (i.e. stronger than the members they join), the connections never reached a condition near their ultimate strength. Therefore, the remaining diagonally stiffened subassemblages were tested with columns having fixed ends. This increased the subassemblage stiffness, which allowed a higher external load to be applied. The stiffening of the connection was then subjected to higher loads, which were closer to the ultimate condition, while the connection was less critically stressed with the combined shear, moment, and axial-load interaction.

The diagonally stiffened subassemblages all were the same size. The columns were 8 feet 4 inches in height

(base to base). The beams were about 2 feet 6 inches long and were loaded vertically 2 feet from the inside column face. This simulated a beam-to-column connection for a multi-story frame in the inverted position. The sub-assemblage dimensions simulate the dimensions of a frame with columns spaced every 12 feet and a story height of 8 feet 4 inches. The dimensions of the subassemblage were chosen in order to prevent instability in any of its members. Columns were made from either a 6WF20. (L/r_y = 66.6) or a 6WF25 (L/r_y = 65.8) depending upon the portion of the original frame from which they were taken. All beams were made from 12B16.5 (L/r_y = 32) sections.

The remaining two subassemblages contain unstiffened connections. However, due to salvage operations on the multi-story frame from which they were obtained, the columns of these subassemblages were very short. Both unstiffened subassemblages were tested with the columns having fixed ends. Both specimens of the unstiffened group were of the same size. The columns were 5 feet in height (base to base). The beams were about 2 feet 6 inches long and were loaded vertically 2 feet from the inside column face. The columns were made of a 6WF25 (L/r_y = 40) and beams of a 12B16.5 (L/r_y = 32). ASTM - A36 steel was used in all members of the seven tests.

The unstiffened test specimens were tested to determine the force description in a web panel of a connection as yielding progressed throughout the section. These unstiffened test specimens also supplied valuable test data which could be used to determine if the present plastic design connection criterion can be applied not only to connections of low axial load values but to those with relatively high values of thrust in the column.

The unstiffened connections were loaded in such a manner that the present plastic design method would predict that a shear failure would not occur in the connection web panel. However, theory indicates that the combined effect of high axial load and high shear will reduce the carrying capacity of such a connection under high axial load.

The general purpose of the test series presented is three fold:

1. To help determine the stress distribution on a connection web panel loaded into the plastic range.
2. To determine the effect of various types of web stiffening on both the strength and stress distribution of a connection.
3. To determine if the method presently used in plastic-design for designing beam-to-column connections can be applied to cases of high axial load and beam moment.

3.2 Test Setup

The test setups used are shown in Figure 13. Column loads were applied by an 800 kip screw-type universal testing machine with a poise-and-lever-type weighing system.

Two types of end connections for the columns had been considered. Both pinned and fixed-end columns were studied. The most desirable end condition would be pinned, because this simulates the actual behavior of a column in a real frame. However, due to the high axial load and end shear in the column a very large pin is required. The cost of a machined end fixture which would supply the required pin action was considered to be excessive for the pilot tests.

Fixing the column end against rotation can be accomplished by a much simpler test setup. End fixity is developed by bolting the column base plates directly to the load applicator. A setup of this type no longer simulates usual column behavior in a frame, because the shear force resulting from the column bending causes too great a reduction in the shear entering the connection from the beam flange. However, for tests whose principal goal is to determine the behavior of a connection under a given set of force boundary conditions, a fixed end condition for the columns would be satisfactory.

As was discussed in the previous section, five of the test specimens were tested with the column ends in a fixed condition. This was because either the columns were very short or higher loads were desired in the stiffeners of a connection. The remaining specimens were tested in a manner which more closely simulates frame action. The action was simulated by inserting pins at the top and bottom of the specimen column. The pins would correspond to the inflection points in the columns above and below a floor level of an actual structure. In order to obtain a inexpensive pin-end condition, use was made of the 2,000 kip capacity column pin-end fixtures available at Fritz Laboratory.(9)

Columns of the subassemblage were welded to reusable base plates. The base plates were bolted to the fixture plate of the 2,000 kip capacity column end fixtures. A slight modification was made to the column end fixture described by Huber in Reference 9. A shear plate was designed which could be bolted to the fixed base of the fixture. The shear plate provided significant horizontal restraint to the column and still allowed pin-end rotation. The shear plate had a hole in it large enough to pass a 1 inch diameter bolt through it. The bolt was bolted to the rotating pin, sandwiching the shear plate between the pin and the bolt head. Two shear plates were used on each end fixture (see Figure 15), which converted the fixtures from a roller resisting only vertical motion to

a pin resisting vertical and horizontal motion, but still allowing rotation.

Beam loads were manually applied to a point on the beam 2 feet from the column face, using a 35 ton mechanical jack. The beam loads were measured using a calibrated aluminum dynamometer placed under the jack.

3.3 Instrumentation

Each connection was instrumented with electrical strain gages at selected locations on the column flanges, stiffeners, and web panel (see Figure 16). The gages on the web panel were rosettes. These gages indicated quantitatively the stress distribution around the connection in the elastic range. A preliminary study on a gaged beam-to-column connection has indicated that it is possible to get strain readings from relatively inexpensive gages well into the plastic range. Despite the fact that gage readings were obtained in the plastic range, it is doubtful that any more than a qualitative value should be placed on the high strains due to the localized effect of a yield line passing through a gage or the change in gage resistance at such a high strain. However, using a plot of strain versus load and knowing the yield strain of the material in question, it is certainly possible to

obtain a very good idea of the manner in which a connection progresses from the elastic range toward failure.

The beam and columns of each test were instrumented with electrical strain gages, as is shown in Figure 16, in such a manner that moments and axial loads could be calculated for each load increment.

Attached to all connections were rotation gages which gave the relative rotation of the top and bottom columns with respect to each other and the relative rotation of the beam with respect to the column. Figure 17 shows in detail how the rotation gage was mounted on the web of the connection. The gage was clamped to rods which were spot welded to the member web a short distance from the joint. The rotation gage was made of a series of clamped rods whose relative movements were measured by dial gages. The rotation gage was modified in tests 333.A4, 333.A5, and 333.A6. In the modified system, the rigid rods were replaced by five wires stretched between the rods which were spot welded to the web and the measuring gage. The basic principal of the modified gage is the same as that shown in Figure 17. Its advantage was that it was easy to assemble and easy to adjust when the gages had to be reset. Comparable results were gotten using both systems.

Deformations were measured along both the tension and compression diagonal of each connection. In tests

A2, A3, and A6 a modified Whittemore type gage was used for the measurements. However, data taken with this instrument had a wide scatter band. Therefore, in the remaining tests one Ames Dial Gage was anchored at one end of each diagonal of the connection. A wire was anchored at the other end of the diagonal. The wire was stretched taut and fastened to the dial gage. This provides an accurate measuring system which will give diagonal deformations with a very narrow scatter band.

Also checked, in test 333.A2, were out-of-plane web movements. These measurements were taken to determine if web buckling was significant and should be considered when the ultimate strength of a connection is calculated. It was found that for the seven tests conducted, out-of-plane web movement was insignificant and therefore, not an important factor in the ultimate strength of the connections tested.

Rotations of the beam and column ends were measured using 20 inch level bars. These measurements gave an absolute value for all end rotations. The pedestal was also gaged in order to determine its absolute rotation.

Beam deflection was measured using a mechanical dial gage which was fixed to the base of the testing machine at one end and the beam on the other end. This measurement served as a criterion measurement by which it was

possible to determine if the connection was in an equilibrium state in the plastic range. This measurement was chosen to be the criterion measurement because it was the most direct deformation reading obtainable and reflected the entire behavior of the subassemblage.

3.4 Testing Procedure

Figures 13A and 13B show a subassemblage ready to test. Testing was begun by aligning the subassemblage column until strain gages on the top and bottom column located at the four corners of the column read within about 10% of each other at a given cross section during the application of a modest thrust on the column. When the column was aligned a zero datum set of readings was taken.

The actual subassemblage test was begun by incrementally building up the column axial load to the predetermined axial load for the test. Beam load was then applied incrementally using a mechanical jack and calibrated dynamometer. After an incremental beam load had been applied, the column load was finely adjusted back to the desired axial load for the test. The beam deflection was now observed and when it became steady all gages were read. This procedure was repeated for each beam load increment.

Each subassemblage was tested in the same manner. The only variable (with the exception of stiffening) was the magnitude of the column working load. Table 7 gives a summary of the loads for the test series.

4. TEST RESULTS

This section of the report is a summary of the results found from the pilot tests described in the previous section. Since the test specimens were designed to remain elastic in a frame and not to be tested as connections, the test results should only be considered as a guide as to the actual behavior of similar beam-to-column connections subjected to high column axial load.

4.1 Subassemblage Behavior

Beam jacking load, V, was plotted versus the beam end deflection, Δ, giving a general overall deformation pattern for each subassemblage. Figures 18 and 19 show the load-deflection curves of all the tests conducted. These curves are characterized by an initial straight line elastic region followed by a curving transition zone which changes to a gently sloping curve which eventually will be terminated by a local failure. In none of the tests conducted in this pilot study were the tests terminated due to a local failure in any of the connections. All tests were terminated due to a local failure in either the beam or column of the test subassemblage. Whenever yielding occurred in the connection, the stresses were shifted to the beam or column to such an extent that when the actual ultimate

load of the subassemblage was achieved, it was the result of a local failure outside the connection zone.

The most typical type of failure in the subassemblages with 6WF20 columns was a local buckle in the compression flange of the upper column just above the connection (see Figure 20a). This portion of the flange was the most highly stressed region of the upper column. The upper column received the beam shear as axial load causing it to be the most highly stressed of the two columns. The local buckle in the column was always preceded by the formation of plastic hinges in both the upper and lower column just above and below the connection, respectively. Extremely large rotations were noticed at these hinges. The rotations were high enough to put tension in the column's tension flange when the column had a P/P_y of as high as 80 percent. A column plastic hinge never progressed through the entire cross section in any of the tests conducted. This was due to the fact that a local buckle occurred in the column compressive flange before the full hinge could form. It should be noted that the local buckle was only noticed in the 6WF20 columns (b/t = 16.4).

The heavier 6WF25 columns (b/t = 13.3) did not show any signs of a local buckle in either column. This is due to the smaller b/t ratio of the 6WF25 column as compared to a 6WF20 column. The most typical failure mode

in the heavier column (6WF25) subassemblages was one in which a localized failure occurred in the beam. There were three of the 6WF25 column subassemblages tested. Of these three specimens, two failed with a local buckle in the beam flange (one of these two tests had a tension beam flange weld failure at the column face, which precipitated the local buckle in the beam compression flange). The third test was terminated because it was considered unsafe to continue the test due to the fact that the high angle of deformation of the beam might cause the mechanical jack and the pin, through which load was applied, to slip. Figure 20b shows a test which has its ultimate strength limited by a local buckle in the beam flange. It should be noted that in all tests where a local failure occurred in the beam, at least some portion of a plastic hinge had formed in the beam.

Table 8 gives a summary of the failure modes and ultimate loads for all tests conducted. Also given in the table is the beam shear which will cause a plastic moment and a reduced plastic moment in the beam and column, respectively.

If Figure 18 is examined, one may observe that the two unstiffened test subassemblages behave similarly in the elastic range up to a point where the subassemblage with the higher stressed column begins to deflect at a higher rate. This is due to the earlier formation of

column hinges in the higher stressed column. However, as beam load increases the load-deflection curves tend to become asymptotic at the ultimate load. This is caused by the nature of the failure which causes the ultimate load. In both cases the ultimate load is the result of a local beam failure. The beam failure load is independent of the axial load in the column. However, these two curves will never become equal because the column with the higher axial load goes through a greater hinge rotation causing more beam rotation. As a result of the additional beam rotation a slightly lower beam load is required to cause a local beam failure.

Figures 19 and 21 give a comparison of the load-deflection curves for diagonally stiffened test specimens. Since all of the ultimate failures in this group of tests were the result of a local buckle in the column flange, the ultimate load of each specimen is independent of the direction of the diagonal stiffening. This is shown by Figure 21. Figure 19 shows that the ultimate load for this group of tests is indirectly proportional to the axial load or in some manner related to the reduced plastic moment of the column.

If only the overall subassemblage behavior is examined, one may conclude that all specimens tested performed satisfactorily (i.e. all failures occurred in regions outside the connection zone).

4.2 Connection Behavior

Connection behavior may be observed by plotting beam load, V, versus the diagonal deformation of the connection. Figure 22 shows a photograph and a sketch of the system used to measure the diagonal deformations. This is the most localized and direct measurement found which could give an indication when shear racking occurs in the connection. The shear racking load is defined in this report as the load at which the beam load-diagonal deflection curve becomes nearly horizontal.

Figures 23 to 26 are the beam load-diagonal deformation curves for the pilot tests conducted. The curves are characterized by an initial straight line elastic region followed by a transition zone in which the connection changes from elastic to plastic behavior. In most tests, the diagonal deformations reach a plastic or shear racking state in which the curve becomes horizontal.

Figure 23 is a beam load-diagonal deformation curve for test 333.A2, an unstiffened connection subjected to an axial load of $P/P_y = 0.8$. The curve has both the tension and compression diagonal deformation curves superimposed upon each other. The abscissa of this figure is positive for the tension diagonal and negative for the compression diagonal. As was described in Chapter 2 of this report, the diagonal deformations were measured in the first four tests with a modified Whittemore type

gage. This type gage gave a wide scatter band of results, with the general trend being shown in Figure 23. The initial regions of the two curves shown in this figure tend to be a straight line elastic loading curve. Both curves begin to decrease slope at about the 19 kip ordinate, this is an indication of initial shear racking or initial plastic deformation of the connection. It should be noted that an unstiffened connection shows about 30 percent greater deformation along the compression diagonal than the tension diagonal. If in Figure 23 the transition zones (i.e. V = 19 K and greater) of both diagonals are compared, the compression diagonal curve seems to flatten out much faster than the tension diagonal. This evidence tends to indicate that yielding tends to progress along the compressive diagonal of an unstiffened connection before it spreads to the tension diagonal.

Figure 24 gives a comparison of the compressive diagonal deformations for two subassemblages tested which contain diagonal stiffeners acting in compression. For both tests of Figure 24 the tension diagonal deformation is not shown but the trend is similar to Figure 23. In all tests performed the compressive diagonal deformation recorded was greater than the tension diagonal deformation. Figure 24 compares the deformations of two identically stiffened connections subjected to different axial loads ($P = 0.6P_y$ and $P = 0.8P_y$). The lower of the two curves presented shows a great increase in ductility over the upper curve which was

subjected to a 20 percent lower axial load. This indicates that, even for an "overdesigned" connection, much more shear deformation occurs for connections subjected to very high axial loads in the column.

Figure 25 is a comparison of the diagonal deformations of two identical subassemblages with diagonal connection stiffening acting in tension. It should be noted that the data obtained for test 333.A4 is questionable due to the possible influence of untraceable instrumental errors. If the two curves of Figures 24 and 25 with P/P_y = 0.6 are compared, the connection with a compression diagonal stiffener seems to reduce the shear racking. This finding would seem consistent with the connection behavior already presented in this report. It was noted earlier that the maximum deformation occurs along the compressive diagonal. If a stiffener is placed along the compressive diagonal, one would expect correctly that the shear racking would be reduced.

Figure 26 shows the load-diagonal deformation curves for both tension and compression diagonals of test 333.A7. This is a subassemblage made from a 6WF25 column section. The connection itself is diagonally stiffened with the stiffener acting in tension. It should again be noted that the compression diagonal shows the maximum deformation. The failure of the connection shown in Figure 26 was recorded and will be discussed later in this report.

The first yield, beam shear load given in Table 8 was calculated from Figures 23 to 26. The first yield load was taken as that load at which shean racking first started in a given connection. Initial shear racking was previously described as the first deviation from a fully elastic condition.

By placing rosette gages at specific locations on the web panel of the connection, it is possible to obtain the stress distribution within a connection for any given load. Figures 27 through 30 are the principal stress distributions for an unstiffened connection and for two diagonally stiffened connections for selected loads.

Figure 27 gives the principal stress distribution for an unstiffened test connection for two selected loads. An elastic stress distribution is shown in Figure 27. In this figure, all the principal compressive stresses are lined up parallel and in the direction of the compression diagonal of the connection. The effect of the column moment can be seen by the magnitudes of the principal compressive stresses in the upper and lower row of gages in the connection.

The remainder of this report will use the terms upper and lower compressive triangles. An upper compressive triangle for this test series will be defined as that portion of a connection web panel which is above the compression diagonal. If the connection has a tension stiffener

diagonal, the upper compressive triangle will be everything above the tension diagonal. The remainder of the web panel will be defined as the lower compressive triangle.

In an unstiffened connection first yielding occurs along the compressive diagonal of the connection. Reference should be made to Figure 28, which shows the principal stresses at a load causing some yielding in the web panel. As yielding spreads in an unstiffened connection, it progresses into the upper compressive triangle. The lower compressive triangle has a lower compression stress due to the tension effect of the beam moment. At the lowest corner of the lower compressive triangle a state of pure shear exists for a certain beam load. If this shear state is great enough in magnitude, yielding will occur. As loading increases in an unstiffened connection, it spreads in a band along the compressive diagonal into the upper compressive triangle, and then into the lower compressive triangle with the initial yield in the lower compressive triangle being at the bottom, column face corner of the triangle.

For diagonally stiffend connections the principal compressive stresses align themselves along the compressive diagonal of the connection (see Figures 29 and 30). Initial yielding of diagonally stiffened test connections occurs along the welds used to fasten the diagonal stiffener to the web panel. In tests performed on connections with

diagonal stiffeners acting in tension, after the initial yielding along the diagonal stiffener welds, the first web panel yielding occurred along the compression diagonal. As beam load was increased the yielding spread into both the upper and lower compressive triangles. Figure 31 is a photograph taken of a diagonally tension stiffened connection. It is evident from this photograph that the major deformation and yielding occurs along the compressive diagonal. Tests performed on connections with diagonal stiffeners acting in compression did not exhibit such wide spread web panel yielding as that described for tension diagonal stiffeners. Compression diagonally stiffened connections did show initial yielding along the diagonal welds. It should be noted that all tests on connections with diagonal stiffeners acting in compression were on subassemblages with light columns. Therefore, the web panels of the connections tested were never subjected to extremely large loads due to the tests being terminated as a result of local failures in the column flange.

Observations indicate that as the web panel of a connection yields and finally reaches a mechanism state, it shifts load to the stiffening system. The connection then appears to increase slightly in stiffness until a complete mechanism has been reached for the entire system.

It should again be mentioned that in all tests performed, yielding was encountered in the web panels of the test connections. However, in no case were any of the connection's ultimate strengths the direct result of a failure within any connection. Therefore, it must be concluded that strain-hardening within the connection plays an important role in shifting the ultimate failure zone outside the connection.

5. TEST CONCLUSIONS

The results of the tests conducted as described in this report can be listed as follows:

1. All the connections tested showed a great deal of post initial yield strength. None of the subassemblages tested failied due to a localized connection failure.

2. Strain-hardening is a very important factor in the overall ultimate strength of a test connection.

3. The principal compressive stresses of all connections tested were parallel and in the direction of the compressive diagonal of the connection.

4. As yielding progresses in a test connection it spreads out into the web panel from an initial yield band along the compressive diagonal.

5. When a web panel of a diagonally stiffened connection reaches a mechanism condition, load is shifted to the stiffening system.

6. Axial load plays an important role in the behavior of beam-to-column connections. It was noted that even for connections which

were "over designed" the shear racking deflections are proportional to the magnitude of the axial load in the column of the connection.

6. TEST RECOMMENDATIONS

This section presents a list of suggestions which are intended to serve as an aid to any researchers planning tests on beam-to-column connections. The list was assembled from the experience gained in the testing of the seven connections described in this report. The following is the list assembled:

1. If the ultimate strength of a connection is to be studied, the connection must be designed as the weakest region of the subassemblage to be tested.

2. If a stiffened connection is to be tested, stiffeners should be designed so that they will fail causing the ultimate load of the connection to be reached.

3. A much higher shear condition will be introduced into the connection if the columns of the subassemblage are long. Therefore, tests with columns as long as possible are desirable.

4. It is necessary to gage the column with enough electrical strain gages so that the shape of the column moment diagram is always defined.

5. When the diagonal deformations and relative rotations of a connection are measured, a direct reading system such as an Ames dial gage under tension from a wire gives fastest and most accurate results.

6. When instruments are chosen to read the electrical strain gages in the region of the connection, it is best to have an instrument which will record a wide range of strains.

7. Avoid excessive grinding or welding in the area of the web panel, in order to prevent any localized disturbance of the residual stress distribution in the connection.

8. Initial alignment of a test specimen to closer than a 10 percent difference in strains at a cross section seems to be impractical and unnecessary.

9. The test procedure of first building up a working axial load then adding the beam load incrementally, seems to be a simple and satisfactory test method.

As a result of the pilot study presented in this report, the following list of additional beam-to-column connection problems has been assembled. These topics

are presented in order to aid in the planning of future beam-to-column test programs.

1. Tests should be conducted on connections specifically designed to determine the ultimate strength of a web panel. These tests could be used to check the relationships presented in this report.

2. A specific test series should be designed to determine the effect the column flange has on the ultimate strength of a beam-to-column connection.

3. A study should be started on the behavior of interior connections.

4. A study could be started to determine the behavior of a three-dimensional beam-to-column connection under the influence of high axial load in the column.

5. An investigation could be conducted in order to determine the most efficient method of attaching the beam to the column.

6. Better methods of designing web stiffening should be examined. It is important to know how much of the column web functions with the transverse stiffeners so that the stiffener size can be determined more accurately.

7. Tests on larger subassemblages could be designed in order to determine the effect of a "failed" connection on the rest of the subassemblage. From these tests, possibly a method could be developed to use the "under strength" of the connection as a reduced plastic hinge moment rather than the nominal M_p of the beam or column. The method would then take into account the effect of this plastic hinge behavior on the rest of the structure. If this method requires a small increase in member sizes, but saves the fabrication cost of details and permits easy framing of perpendicular floor members into the column web, designers might be able to provide substantial savings in material. These savings could be achieved under the condition that this new form of plastic hinge would give the required rotation capacity to permit the necessary redistribution of moment in the structure.

7. DESIGN SUGGESTIONS

A design formula should be as simple but yet as accurate as is possible. The results of the theoretical derivations of part 2 are somewhat complex in form. Therefore, the interaction relations of formula (2.15) and (2.20) should be simplified, if at all possible, to improve their usefulness as design formulas.

By plotting the lower bound interaction calculations for many connections, it is possible to obtain a composite interaction diagram which contains the lowest points of all the connections examined. Figure 32 is a plot of the lowest composite interaction curve obtainable from the connections examined. It should be noted that all the connections examined were within about 5 percent of this curve. Therefore, it should be possible to develop a design equation for beam-to-column connections by obtaining the equation of the lowest composite interaction curve. Design equation (7.1) is obtained by fitting a parabola to the data of Figure 32.

$$M/M_p = 0.992 - 0.736 \left(\frac{P}{P_y}\right) - 0.253 \left(\frac{P}{P_y}\right)^2 \qquad (7.1)$$

Equation (7.1) is an exact least squares fit to the curve of Figure 32. A parabola was chosen for the design curve

because both equation (2.15) and (2.20) are parabolas. If a straight line design formula would have been chosen, too much of the strength of the connection would be wasted.

It is possible to approximate equation (7.1) conservatively with equation (7.2).

$$\frac{M}{M_p} = 0.95 - 0.75 \left(\frac{P}{P_y}\right) - 0.25 \left(\frac{P}{P_y}\right)^2 \qquad (7.2)$$

Figure 33 is a comparison of design equation (7.2) to the lowest composite interaction curve obtained. Equation (7.2) is about 5 percent conservative for low values of column axial load (i.e. P/P_y). As axial load increases, equation (7.2) and (7.1) become almost equal.

If equation (7.2) is compared to the interaction curves obtained from equations (2.15) and (2.20), it is possible to note that as axial load increases the interaction curves become more similar (see Figure 34). The two upper curves of Figure 34 are typical interaction curves obtained from the equations of part 2 of this report for two given connections.

Table 8 gives a summary of the test results as predicted by the various interaction relationships. The analysis and design relations can only be applied to the unstiffened test connections. Therefore, there are some

blank columns in this table. The difference between the lower bound prediction of part 2 and the design formula (7.2) is less than 1 kip for both tests. These two prediction values should be compared to the first yield value in the table. The first yield value is that load at which shear racking begins.

Since the present formula limiting the shear deformation of beam-to-column connections is being used successfully on columns with low thrust, it would seen appropriate to make use of the present design method for low axial load conditions.

A possible design method would be as follows:

For a given size of beam and column, substitute the member dimensions into the formula presently used for the design of beam-to-column connections, equation (7.3).

$$\frac{M}{M_p} = \frac{\sqrt{3}}{6Z} \frac{(wd_c)}{\left(\frac{1}{d_b} - \frac{1}{2\ell}\right)} \qquad (7.3)$$

Also substitute the relative axial load in the column into equation (7.2).

$$\frac{M}{M_p} = 0.95 - 0.75 \left(\frac{P}{P_y}\right) - 1.25 \left(\frac{P}{P_y}\right)^2 \qquad (7.2)$$

The smaller of these two M/M_p values should be used as the design value for column moment. The moment, M, calculated is the column end moment at one side of the connection. To check if the connection is sufficiently strong to carry the external loads, one must double the column moment, M, and if this value is greater than the applied beam moment the connection will carry the applied load. This procedure is summarized in relation (7.4).

$$2M \geq \text{Applied Beam Moment} \qquad (7.4)$$

If relation (7.4) is not satisfied the connection must be stiffened.

The design procedure outlined results in the design interaction curve of Figure 35. The horizontal line is the present ultimate strength prediction of a beam-to-column connection. The remainder of the curve is equation (7.2), a modified design curve based upon the analysis of part 2 of this report.

8. NOMENCLATURE

A = Area of column

A_f = Area of column flanges (2)

A_w = Area of column web

a = Area of beam

a_f = Area of beam flanges (2)

a_w = Area of beam web

d_f = Depth of column from $\mathbb{C}_L$ Flange to $\mathbb{C}_L$ Flange

d_B = Depth of beam

d_{Bw} = Depth of beam web

d_c = Depth of column

d_w = Depth of column web

L = Length of beam to point of zero moment

ℓ = Length of column to point of zero moment

t_f = Thickness of column flange

w = Thickness of column web

w_B = Thickness of beam web

y_o = Distance from column web $\mathbb{C}_L$ to yield interface

Z = Plastic section modulus

m_o = Percent of beam flange <u>not</u> yielded by moment

n_o = Percent of column flange <u>not</u> yielded by moment

k = Percent of full yield load in beam web which is given by axial load

ξ = Percent of full yield load in column web which is given by axial load

M = Column moment entering the connection

M_B = Moment in the beam at the column face

M_{pm} = Plastic moment due to shear, bending, and thrust

S = Beam shear

T = Thrust in column

V = Column shear

τ = Shear in column web

$\dot{\delta}$ = Shear displacement rate

$\dot{\rho}$ = Axial displacement rate

ω = Uniform beam load

W_E = Total external work

W_I = Total internal work

9. TABLES

TABLE 1. BEAM-TO-COLUMN CONNECTION - INTERACTION CURVES

6WF20 COLUMN - LENGTH = 60.00
12B16.5 BEAM - LENGTH = 45.00
RATIO OF BEAM FLANGE YIELDED = 0.0000

P/PY	M/MP	WEB AXIAL LOAD PARAMETER [N.A. IN COL. FLANGE]	M/MP	WEB AXIAL LOAD PARAMETER [N.A. IN COL. WEB]
0.00000	1.09579	0.98370	0.99921	0.99419
0.05000	1.04700	0.98639	0.99352	0.99419
0.10000	0.99773	0.98884	0.97644	0.99419
0.15000	0.94799	0.99105	0.94798	0.99419
0.20000	0.89771	0.99301	0.90814	0.99419
0.25000	0.84710	0.99473	0.85691	0.99419
0.30000	0.79597	0.99620	0.79431	0.99419
0.35000	0.74443	0.99743	0.72031	0.99419
0.40000	0.69253	0.99842	0.63494	0.99419
0.45000	0.64041	0.99917	0.53818	0.99419
0.50000	0.58863	0.99967	0.43004	0.99419
0.55000	0.54053	0.99993	0.31051	0.99419
0.60000	0.53563	0.99995	0.17960	0.99419
0.65000	0.58231	0.99972	0.03731	0.99419
0.70000	0.63421	0.99924	-0.11637	0.99410
0.75000	0.68670	0.99852	-0.28143	0.99419
0.80000	0.73915	0.99755	-0.45787	0.99419
0.85000	0.79137	0.99632	-0.64570	0.99419
0.90000	0.84329	0.99484	-0.84491	0.99419
0.95000	0.89488	0.99311	-1.05551	0.99419
1.00000	0.94613	0.99112	-1.27748	0.99419

TABLE 2. BEAM-TO-COLUMN CONNECTION - INTERACTION CURVES

6WF20 COLUMN - LENGTH = 60.00
12B16.5 BEAM - LENGTH = 45.00
RATIO OF BEAM FLANGE YIELDED = 0.5000

P/PY	M/MP [N.A. IN COL. FLANGE]	WEB AXIAL LOAD PARAMETER	M/MP [N.A. IN COL. WEB]	WEB AXIAL LOAD PARAMETER
0.00000	1.08084	0.96960	0.99784	0.98417
0.05000	1.03210	0.97335	0.99209	0.98417
0.10000	0.98300	0.97684	0.97484	0.98417
0.15000	0.93335	0.98008	0.94609	0.98417
0.20000	0.88323	0.98308	0.90585	0.98417
0.25000	0.83263	0.98582	0.85410	0.98417
0.30000	0.78154	0.98833	0.79085	0.98417
0.35000	0.72998	0.99059	0.71610	0.98417
0.40000	0.67795	0.99260	0.62986	0.98417
0.45000	0.62545	0.99437	0.53211	0.98417
0.50000	0.57250	0.99590	0.42287	0.98417
0.55000	0.51913	0.99718	0.30213	0.98417
0.00000	0.46537	0.99823	0.16988	0.98417
0.65000	0.41137	0.99903	0.02614	0.98417
0.70000	0.35752	0.99958	-0.12910	0.98417
0.75000	0.30596	0.99990	-0.29584	0.98417
0.80000	0.28416	0.99997	-0.47408	0.98417
0.85000	0.32790	0.99979	-0.66382	0.98417
0.90000	0.38129	0.99937	-0.86506	0.98417
0.95000	0.43566	0.99870	-1.07780	0.98417
1.00000	0.49007	0.99778	-1.30204	0.98417

TABLE 3. BEAM-TO-COLUMN CONNECTION - INTERACTION CURVES

6WF20 COLUMN - LENGTH = 60.00
12B16.5 BEAM - LENGTH = 45.00
RATIO OF BEAM FLANGE YIELDED = 1.0000

P/PY	M/MP [N.A. IN COL. FLANGE]	WEB AXIAL LOAD PARAMETER [N.A. IN COL. FLANGE]	M/MP [N.A. IN COL. WEB]	WEB AXIAL LOAD PARAMETER [N.A. IN COL. WEB]
0.00000	1.06476	0.95099	0.99578	0.96905
0.05000	1.01622	0.95582	0.98994	0.96905
0.10000	0.96718	0.96039	0.97242	0.96905
0.15000	0.91760	0.96470	0.94322	0.96905
0.20000	0.86766	0.96875	0.90235	0.96905
0.25000	0.81718	0.97255	0.84979	0.96905
0.30000	0.76621	0.97610	0.78556	0.96905
0.35000	0.71477	0.97939	0.70965	0.96905
0.40000	0.66284	0.98244	0.62206	0.96905
0.45000	0.61042	0.98525	0.52279	0.96905
0.50000	0.55753	0.98780	0.41184	0.96905
0.55000	0.50415	0.99011	0.28921	0.96905
0.60000	0.45031	0.99218	0.15490	0.96905
0.65000	0.39599	0.99401	0.00892	0.96905
0.70000	0.34121	0.99559	-0.14874	0.96905
0.75000	0.28600	0.99692	-0.31809	0.96905
0.80000	0.23040	0.99802	-0.49911	0.96905
0.85000	0.17452	0.99887	-0.69181	0.96905
0.90000	0.11860	0.99948	-0.89619	0.96905
0.95000	0.06427	0.99985	-1.11225	0.96905
1.00000	0.02790	0.99997	-1.33998	0.96905

TABLE 4. BEAM-TO-COLUMN CONNECTION - INTERACTION CURVES

6WF20 COLUMN - LENGTH = 19.80
12B16.5 BEAM - LENGTH = 27.00
RATIO OF BEAM FLANGE YIELDED = 0.0000

P/PY	M/MP	WEB AXIAL LOAD PARAMETER	M/MP	WEB AXIAL LOAD PARAMETER
	[N.A. IN COL. FLANGE]		[N.A. IN COL. WEB]	
0.00000	1.02535	0.74470	0.98044	0.85657
0.05000	0.98370	0.77822	0.97383	0.85657
0.10000	0.94105	0.80892	0.95401	0.85657
0.15000	0.89741	0.83699	0.92098	0.85657
0.20000	0.85281	0.86258	0.87474	0.85657
0.25000	0.80726	0.88581	0.81528	0.85657
0.30000	0.76077	0.90676	0.74262	0.85657
0.35000	0.71335	0.92552	0.65674	0.85657
0.40000	0.66500	0.94212	0.55764	0.85657
0.45000	0.61572	0.95662	0.44534	0.85657
0.50000	0.56551	0.96904	0.31982	0.85657
0.55000	0.51435	0.97939	0.18109	0.85657
0.60000	0.46225	0.98767	0.02915	0.85657
0.65000	0.40921	0.99386	-0.13601	0.85657
0.70000	0.35529	0.99792	-0.31438	0.85657
0.75000	0.30142	0.99983	-0.50596	0.85657
0.80000	0.31649	0.99951	-0.71075	0.85657
0.85000	0.37216	0.99689	-0.92875	0.85657
0.90000	0.42853	0.99186	-1.15997	0.85657
0.95000	0.48521	0.98430	-1.40440	0.85657
1.00000	0.54218	0.97404	-1.66204	0.85657

TABLE 5. BEAM-TO-COLUMN CONNECTION - INTERACTION CURVES

6WF20 COLUMN - LENGTH = 60.00
12B16.5 BEAM - LENGTH = 60.00
RATIO OF BEAM FLANGE YIELDED = 0.0000

P/PY	M/MP	WEB AXIAL LOAD PARAMETER	M/MP	WEB AXIAL LOAD PARAMETER
	(N.A. IN COL. FLANGE)		(N.A. IN COL. WEB)	
0.00000	1.08277	0.97161	0.99805	0.98569
0.05000	1.03407	0.97522	0.99231	0.98569
0.10000	0.98490	0.97858	0.97509	0.98569
0.15000	0.93524	0.98169	0.94638	0.98569
0.20000	0.88510	0.98456	0.90620	0.98569
0.25000	0.83448	0.98718	0.85453	0.98569
0.30000	0.78339	0.98955	0.79138	0.98569
0.35000	0.73182	0.99168	0.71675	0.98569
0.40000	0.67978	0.99356	0.63064	0.98569
0.45000	0.62728	0.99521	0.53304	0.98569
0.50000	0.57434	0.99661	0.42397	0.98569
0.55000	0.52100	0.99776	0.30341	0.98569
0.60000	0.46733	0.99868	0.17137	0.98569
0.65000	0.41355	0.99935	0.02785	0.98569
0.70000	0.86056	0.99978	-0.12715	0.98569
0.75000	0.31613	0.99996	-0.29363	0.98569
0.80000	0.33529	0.99990	-0.47159	0.98569
0.85000	0.38657	0.99960	-0.66104	0.98569
0.90000	0.44046	0.99905	-0.86197	0.98569
0.95000	0.49466	0.99824	-1.07438	0.98569
1.00000	0.54874	0.99719	-1.29827	0.98569

TABLE 6. BEAM-TO-COLUMN CONNECTION - INTERACTION CURVES.

14WF426 COLUMN - LENGTH = 60.00
21WF142 BEAM - LENGTH = 45.00
RATIO OF BEAM FLANGE YIELDED = 0.0000

P/PY	M/MP	WEB AXIAL LOAD PARAMETER	M/MP	WEB AXIAL LOAD PARAMETER
	[N.A. IN COL. FLANGE]		[N.A. IN COL. WEB]	
0.00000	0.98987	0.50731	0.96761	0.62778
0.05000	0.95630	0.56553	0.95802	0.62778
0.10000	0.92087	0.61751	0.92925	0.62778
0.15000	0.88368	0.66432	0.88131	0.62778
0.20000	0.84481	0.70669	0.81418	0.62778
0.25000	0.80429	0.74516	0.72787	0.62778
0.30000	0.76215	0.78013	0.62239	0.62778
0.35000	0.71841	0.81192	0.49772	0.62778
0.40000	0.67307	0.84078	0.35388	0.62778
0.45000	0.62614	0.86689	0.19086	0.62778
0.50000	0.57760	0.89042	0.00866	0.62778
0.55000	0.52745	0.91148	-0.19272	0.62778
0.60000	0.47567	0.93017	-0.41328	0.62778
0.65000	0.42226	0.94658	-0.65302	0.62778
0.70000	0.36718	0.96075	-0.91193	0.62778
0.75000	0.31043	0.97272	-1.19003	0.62778
0.80000	0.25197	0.98252	-1.48730	0.62778
0.85000	0.19181	0.99016	-1.80376	0.62778
0.90000	0.12993	0.99563	-2.13939	0.62778
0.95000	0.06652	0.99891	-2.49420	0.62778
1.00000	0.01252	0.99997	-2.86819	0.62778

TABLE 7. CONNECTIONS TESTED

Test	Col. Size	Stiffening	L/r_y	P/P_y	End Fixture
333.A1	6WF25	None	40*	0.60	Fixed
333.A2	6WF25	HC	40*	0.80	Fixed
333.A3	6WF20	HCT DT	67	0.60	Pinned
333.A4	6WF20	HCT DT	67	0.80	Fixed
333.A5	6WF20	HCT DC	67	0.80	Fixed
333.A6	6WF20	HCT DC	67	0.60	Pinned
333.A7	6WF25	HCT DT	66	0.80	Fixed

HC = Horizontal stiffening in compression
HCT = Horizontal stiffening in both compression and tension
DT = Diagonal stiffening in tension
DC = Diagonal stiffening in compression
* Due to salvage operations these columns are 5 feet in length

Test	333.A1	333.A2	333.A3	333.A4	333.A5	333.A6	333.A7
Beam Shear Causing:							
Ult. Load	38.60	35.60	29.10	22.75	17.40	27.10	35.00
First Yield (Shear Racking)	25.50	19.00	21.20	13.70	15.30	25.40	15.60
Beam M_p	28.30	30.90	32.00	31.45	31.00	31.90	31.45
Column M_{pc}	19.80	13.74	16.35	16.85	17.40	16.73	13.98
Present Ult. Load	41.00	42.00	---	---	---	---	---
Lower Bound Ult. Load	24.50	13.10	---	---	---	---	---
Design Eq. (7.2)	23.80	12.85	---	---	---	---	---
Failure Mode	Local Buckle Beam Flange	Local Buckle Due to Weld Failure	Local Buckle Top Column	Local Buckle Top Column	Local Buckle Top Column	Local Buckle Top Column	Local Buckle Beam Flange

NOTE: All loads listed in this table are beam loads (V) in kips.

Table 8 Summary of Test Results

10. FIGURES

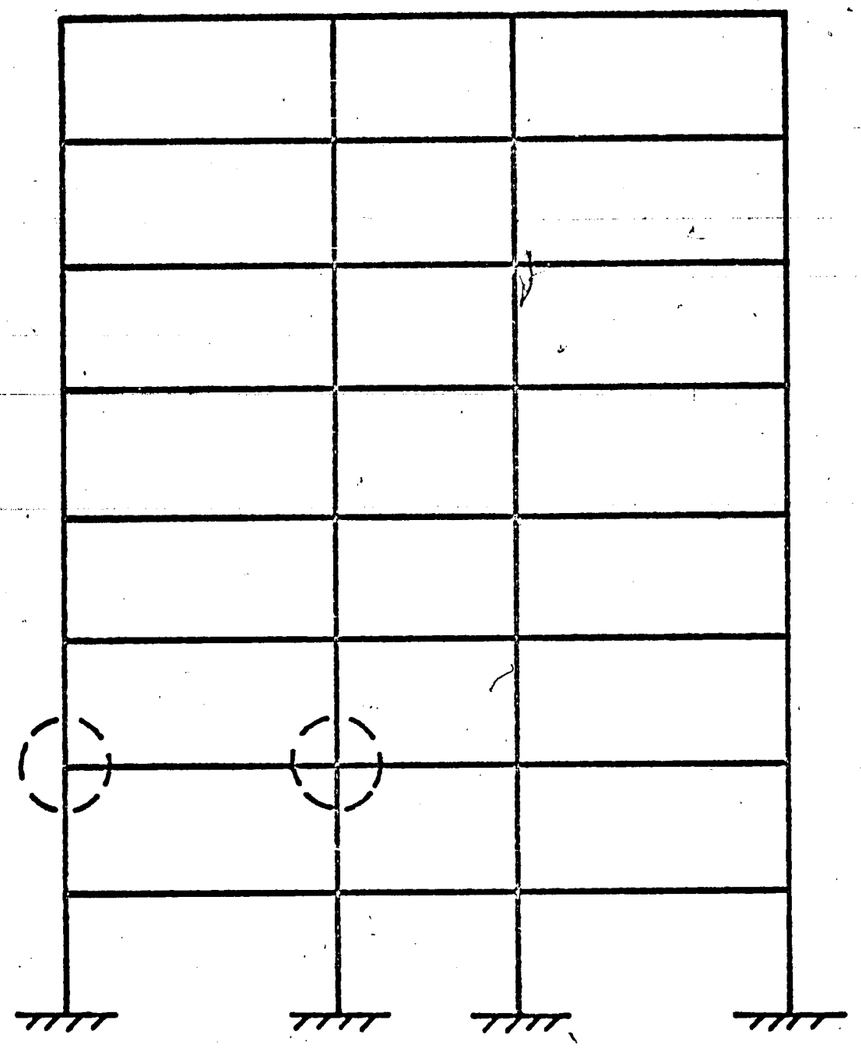

Typical Multi-Story Frame

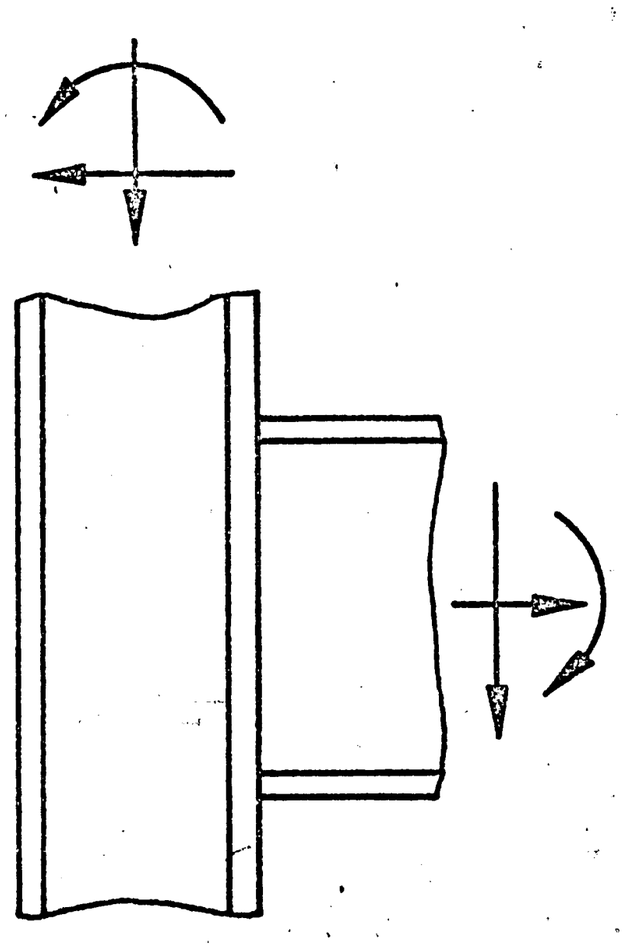

Exterior
Beam-to-Column
Connection

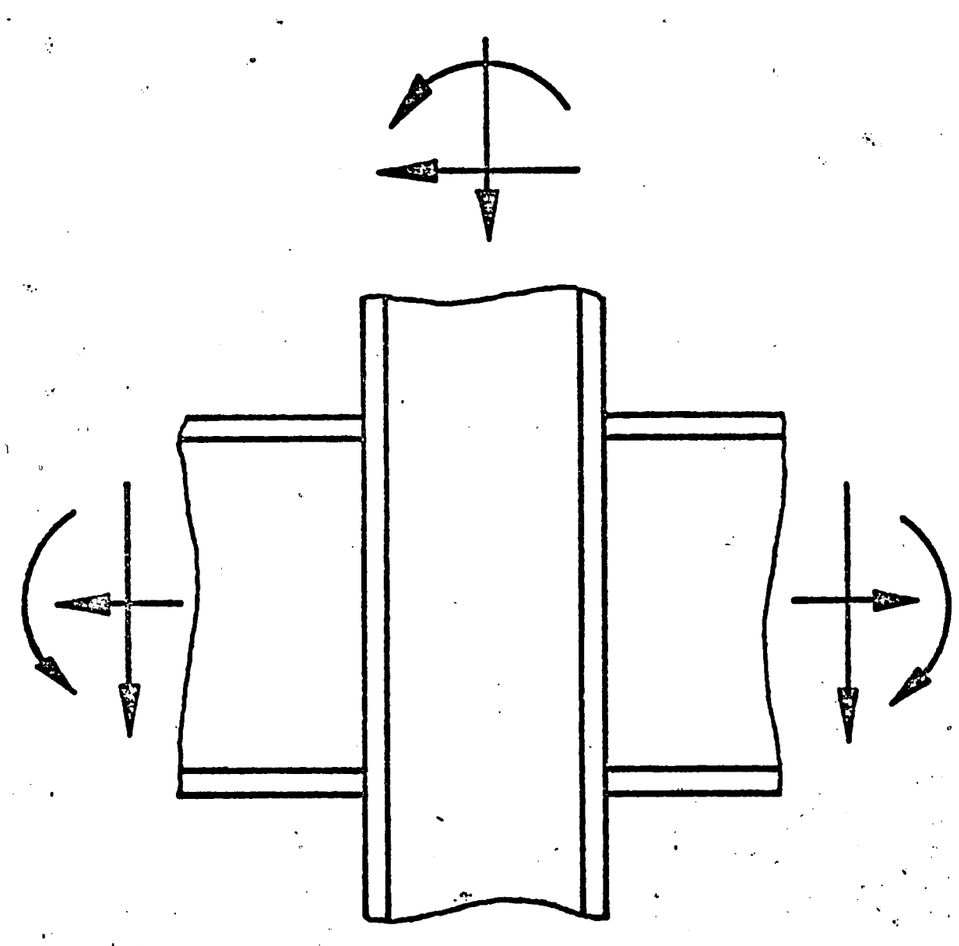

Interior
Beam-to-Column
Connection

FIGURE 1. Types of Beam-to-Column Connections and Their Relative Position Within a Frame

$$F = \frac{2M}{d_B}$$

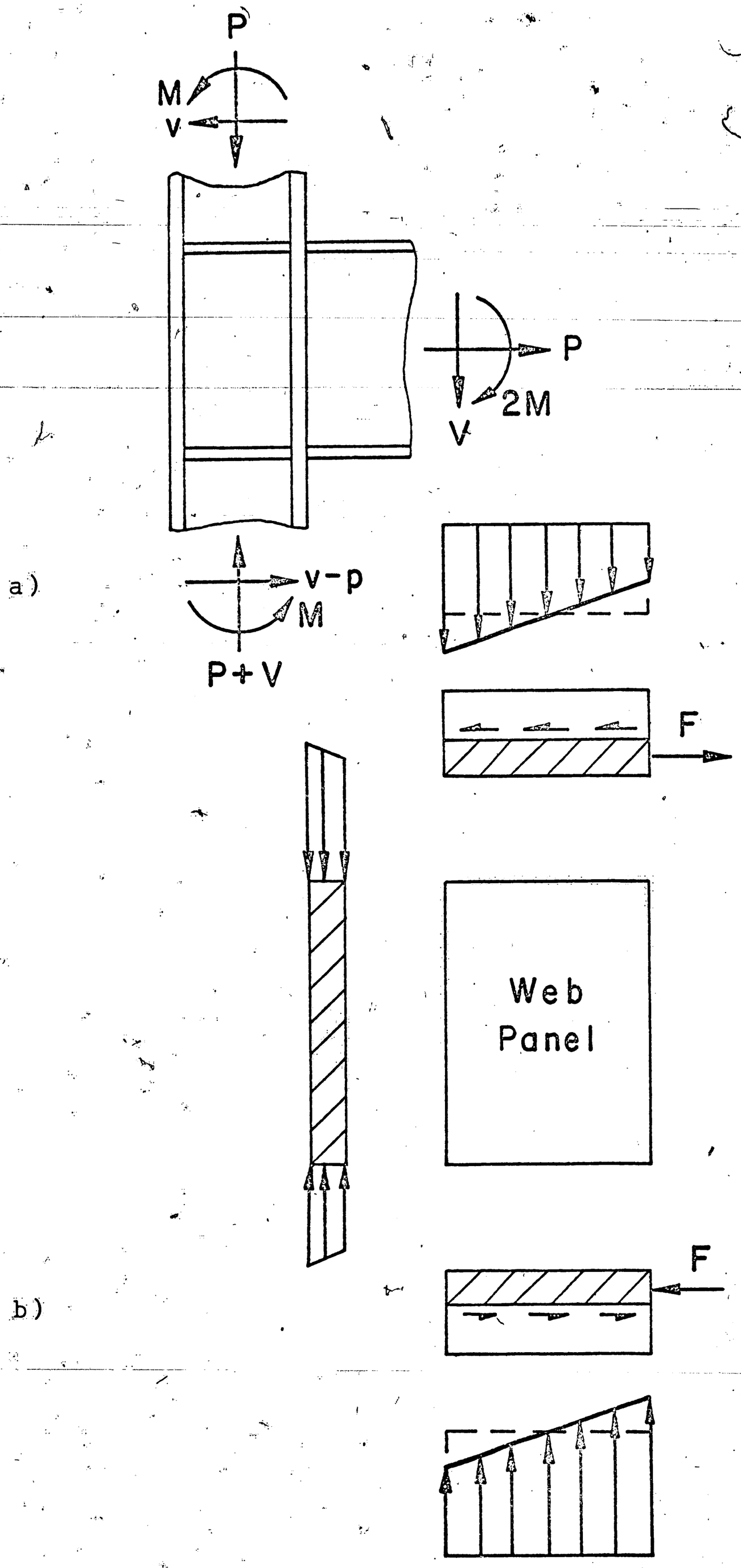

FIGURE 2. An Exploded View of an Exterior Beam-to-Column Connection Subjected to a General Loading

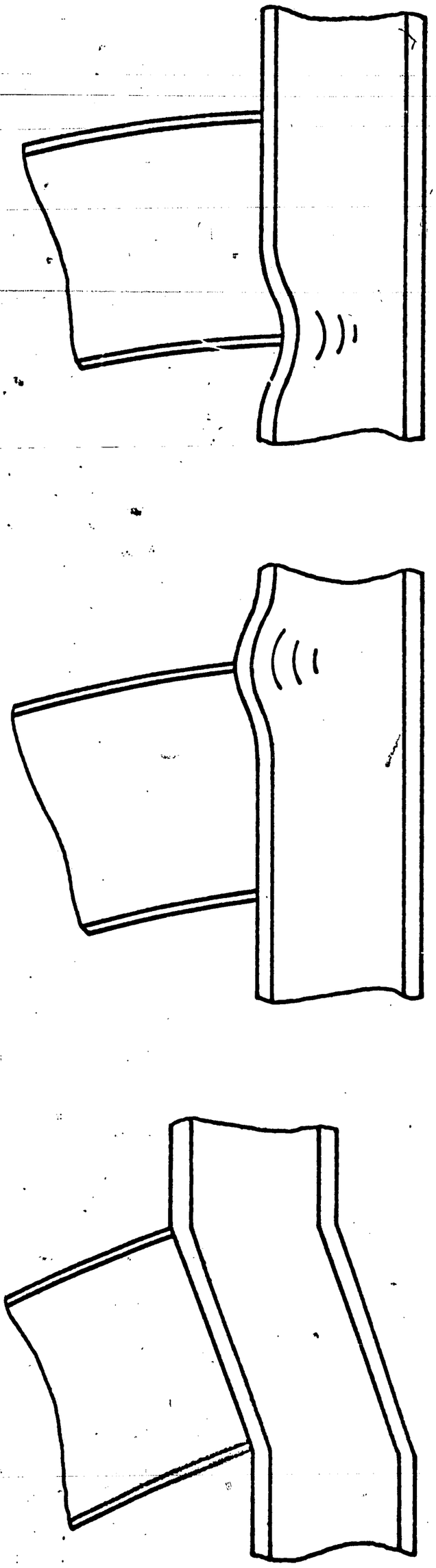

(a) Compressive Failure

$$w_c = \frac{b_b\, t_h}{t_b + 5k_c}$$

(b) Tension Failure

$$t_c = 0.4\sqrt{b_b\, t_b}$$

(c) Shear Failure

$$w_c = \frac{\sqrt{3}}{\sigma_y\, d_c}\left[\frac{\Delta M_B}{d_b} - V_c\right]$$

FIGURE 3. The Three Most Common Types of Connection Failure Modes are Presented Along With the Relationship Presently Being Used for Design

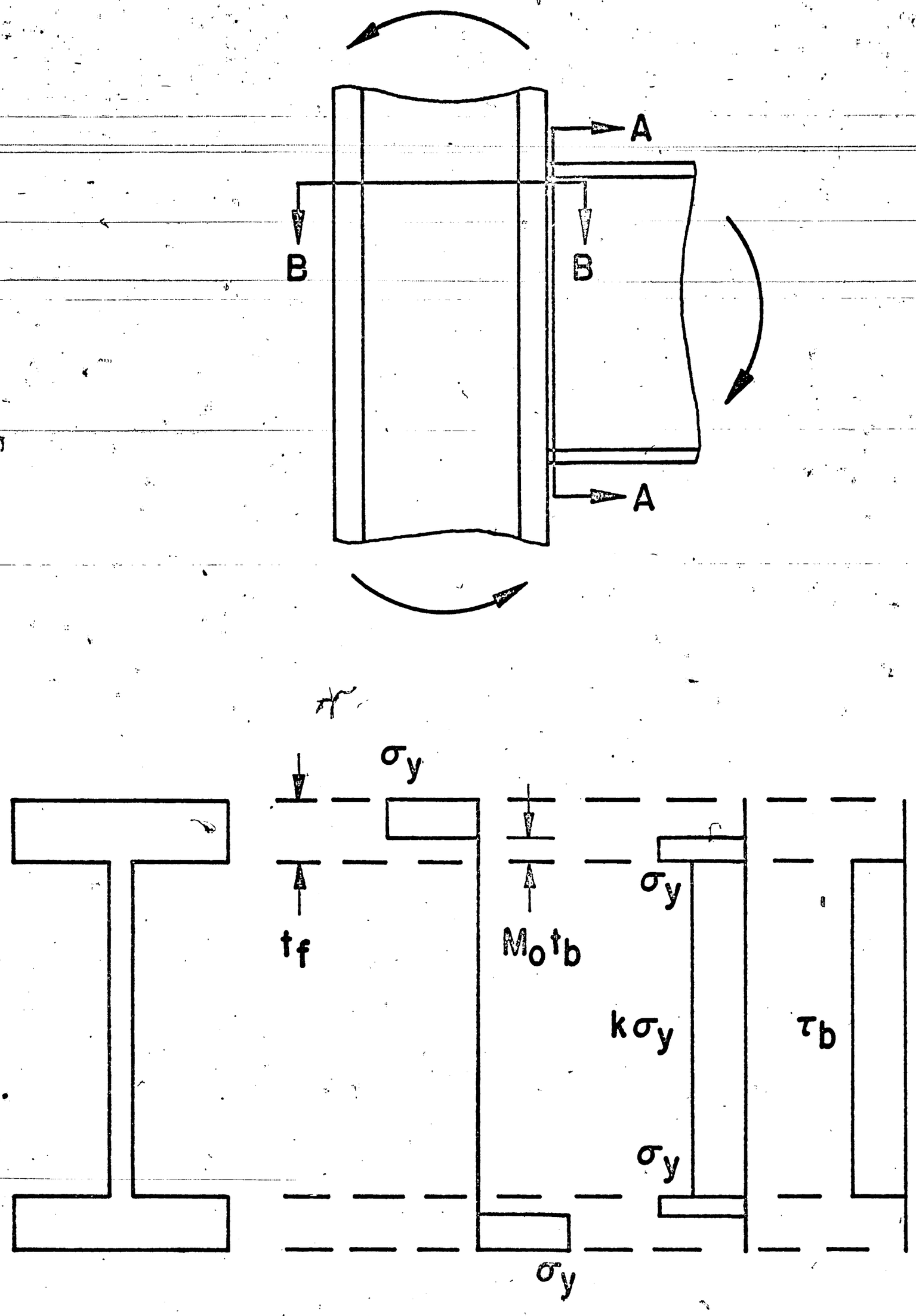

FIGURE 4. Stress Distribution in Beam of an Exterior Connection (See Section A-A).

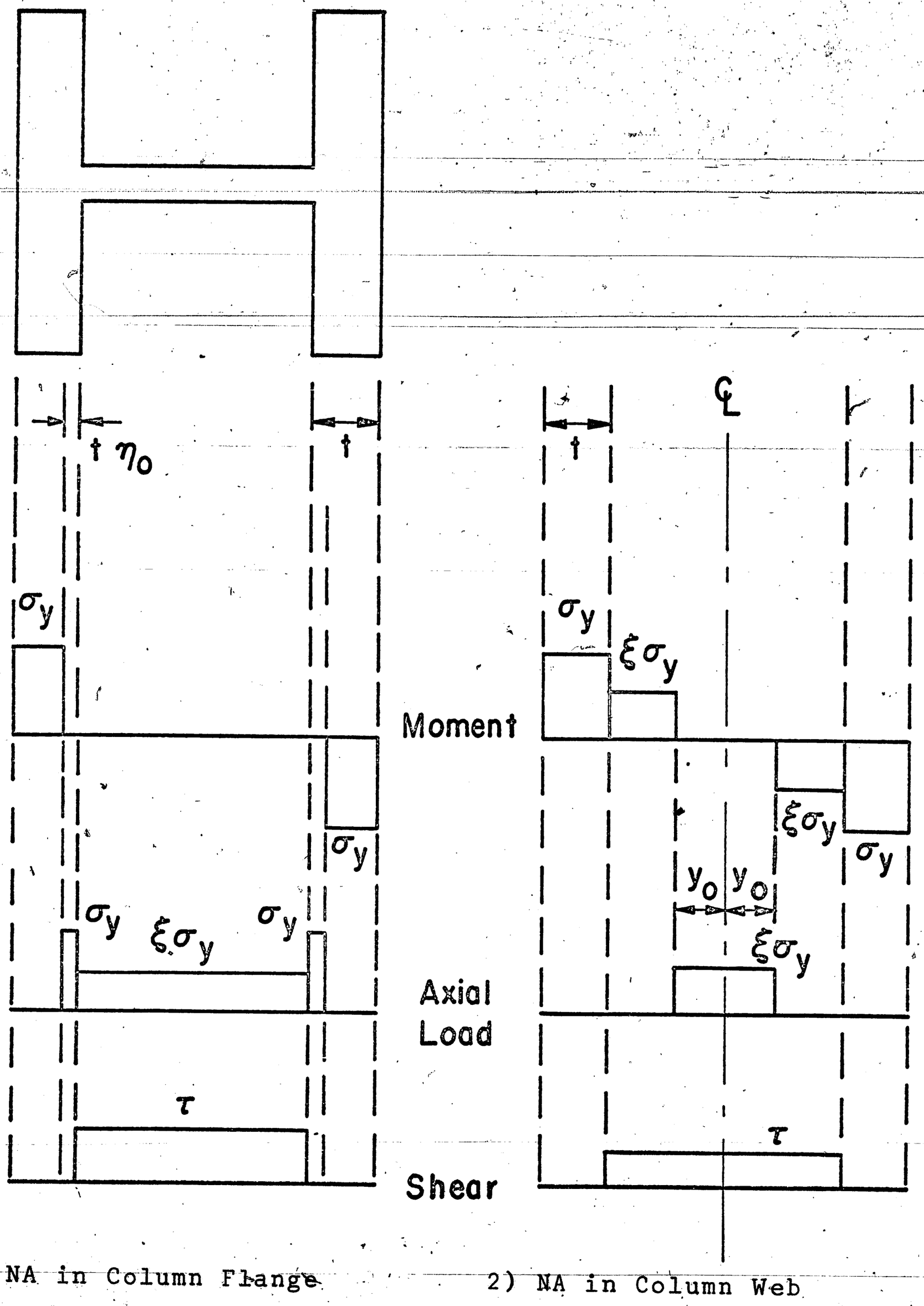

1) NA in Column Flange

2) NA in Column Web

FIGURE 5. Stress Distribution in Column of an Exterior Connection (See Section B-B).

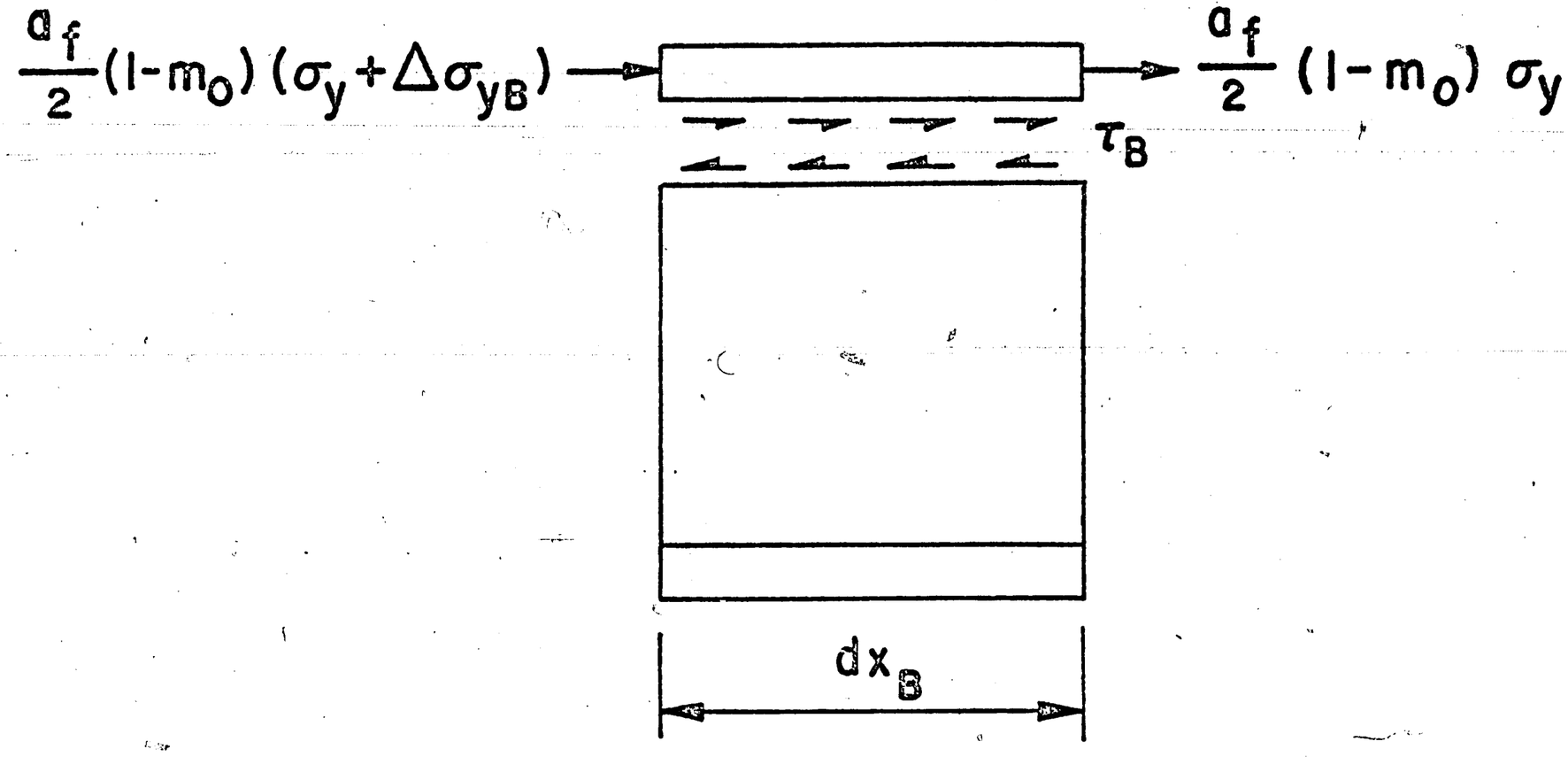

$$dx_B\, w\, \tau_B = \frac{a_f}{2}(1-m_o)\Delta\sigma_{yB}$$

a) An Infinitely Short Element Cut From the Beam

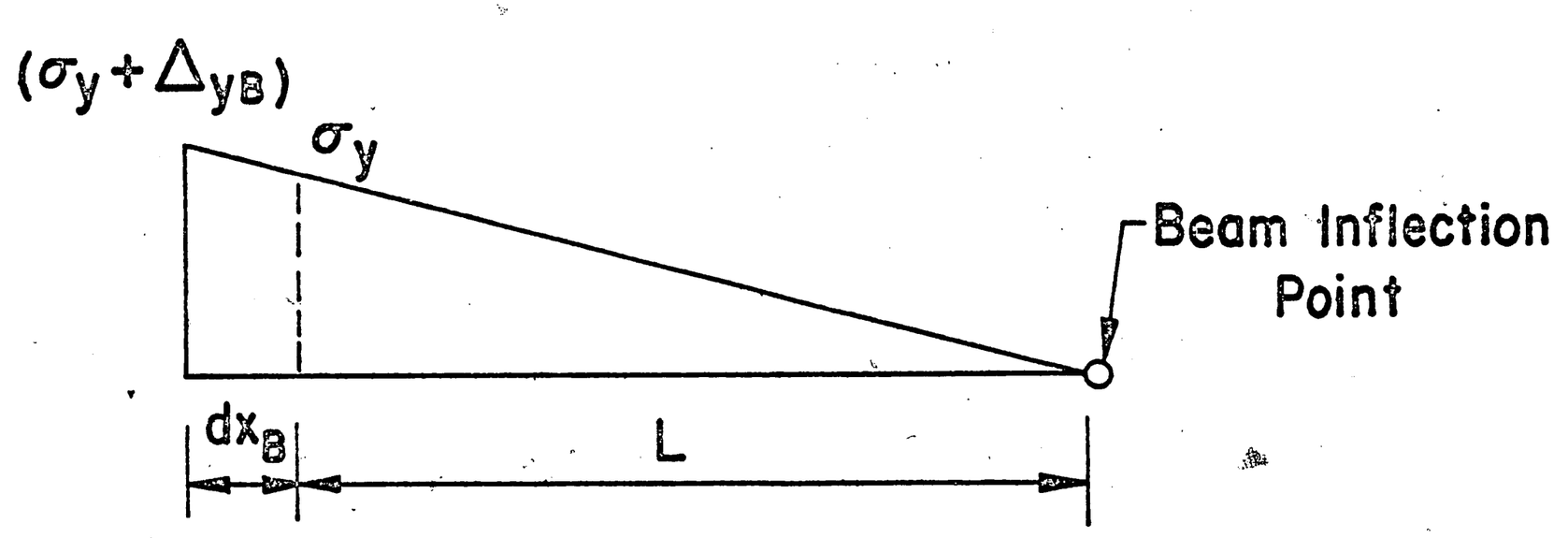

$$\Delta\sigma_{yB} = \frac{\sigma_y\, dx_B}{L}$$

b) Moment Diagram of the Beam

FIGURE 6. Shear Expression for the Beam

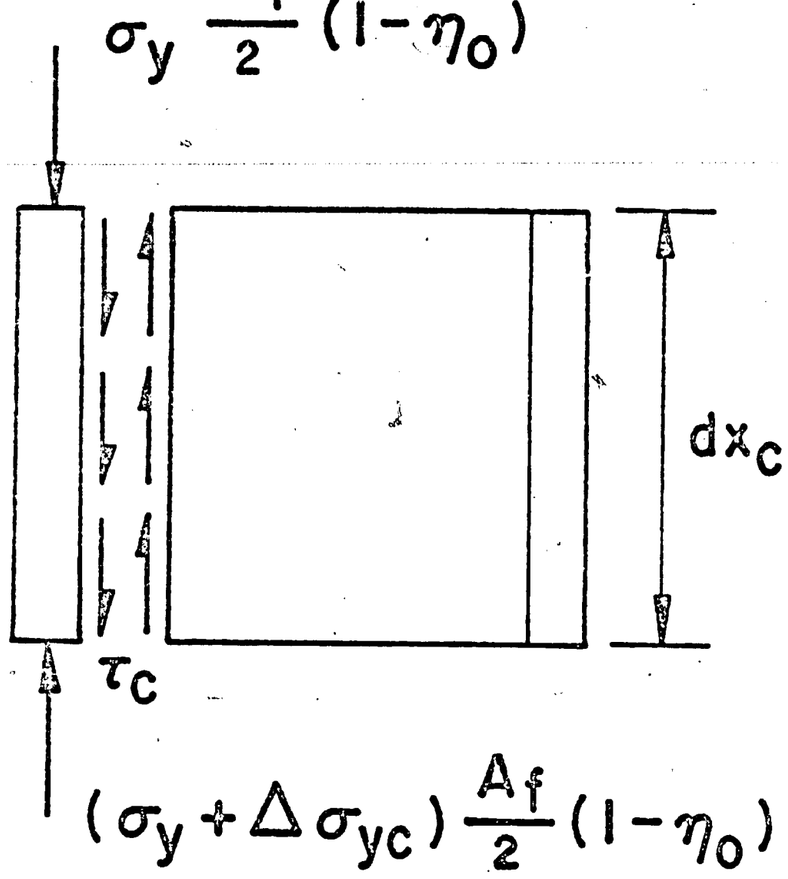

$$dx_c \; w \; \tau_c = \frac{A_f}{2}(1-\eta_o)\,\Delta\sigma_{yc}$$

a) An Infinitely Short Element Cut From the Column

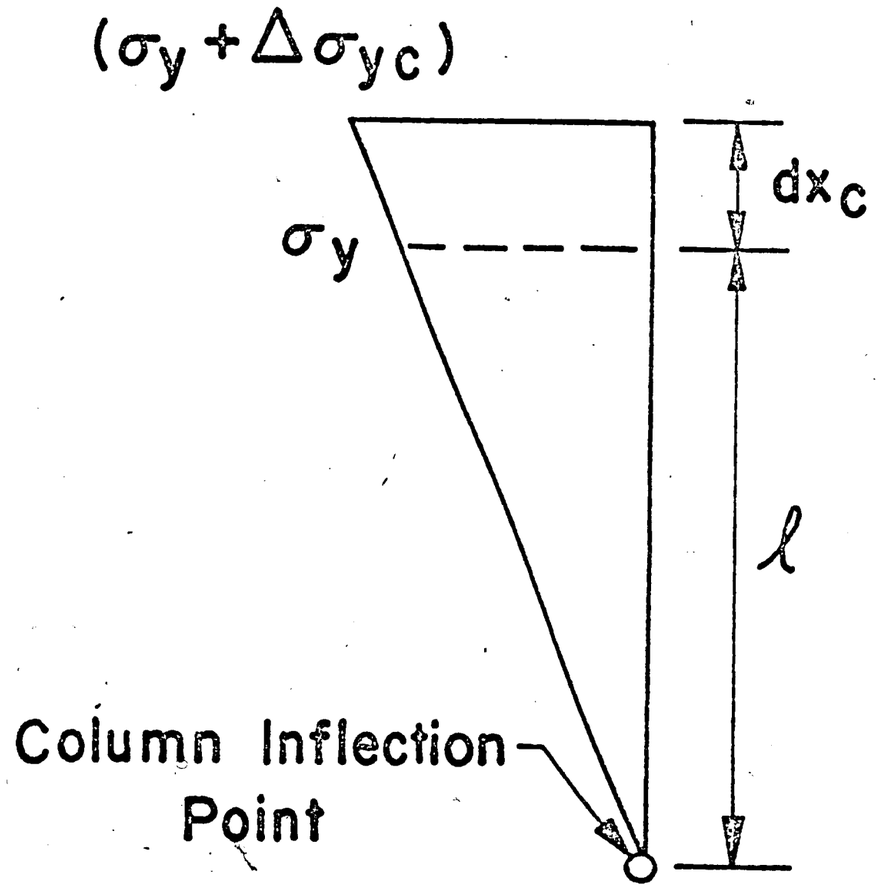

$$\Delta\sigma_{yc} = \frac{\sigma_y\, dx_c}{\ell}$$

b) Moment Diagram of the Column

FIGURE 7. Shear Expressions for the Column

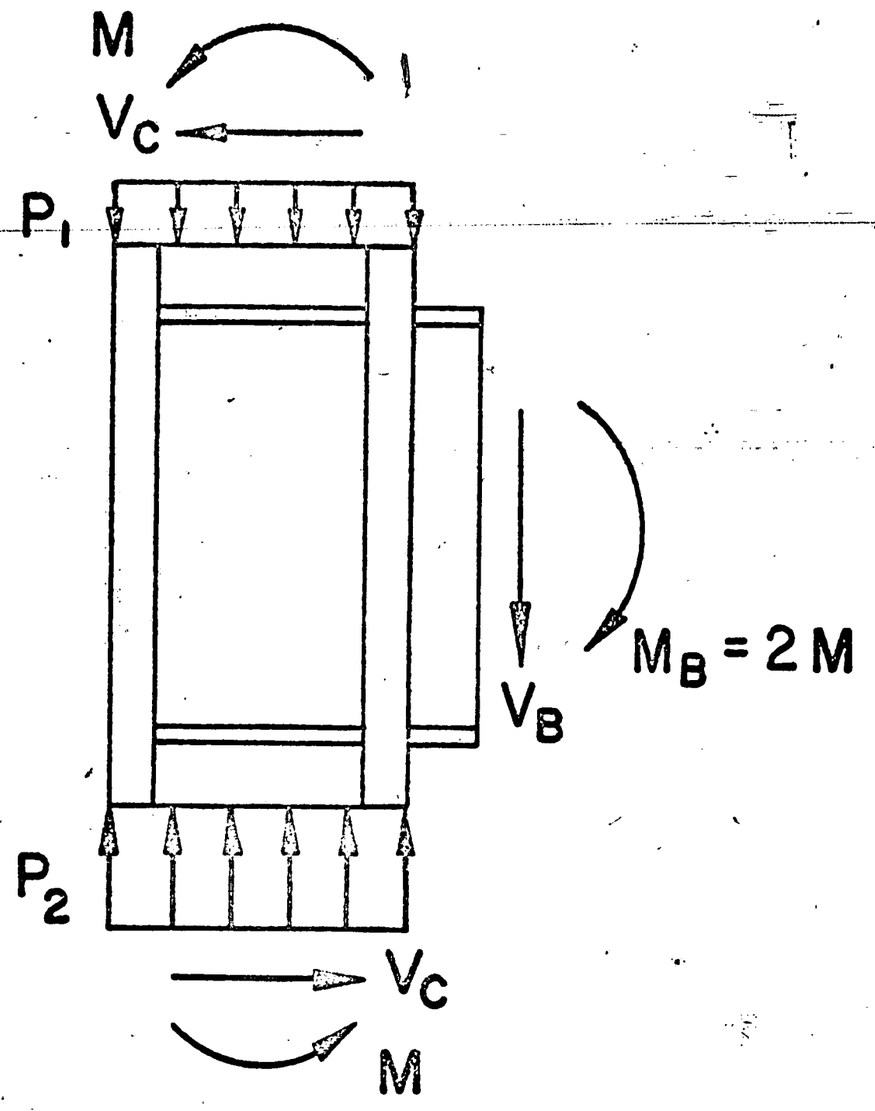

a) General Diagram of Forces on an External Connection

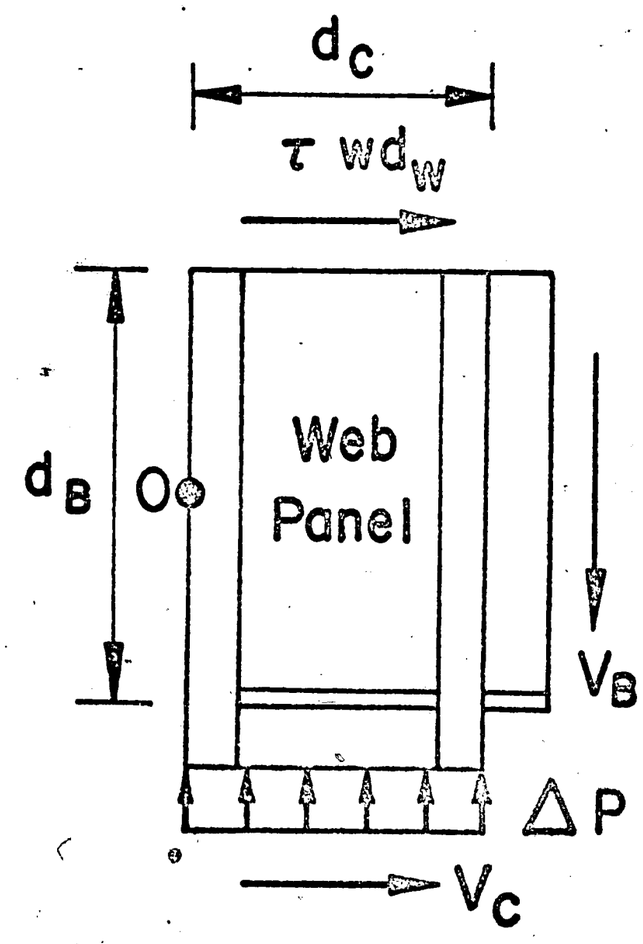

$$\Delta P = V_B$$

b) Free Body Diagram Used to Calculate the Shear Stress in the Web Panel

FIGURE 8. Free Body Diagrams Used for the Calculation of the Shear in the Web Panel

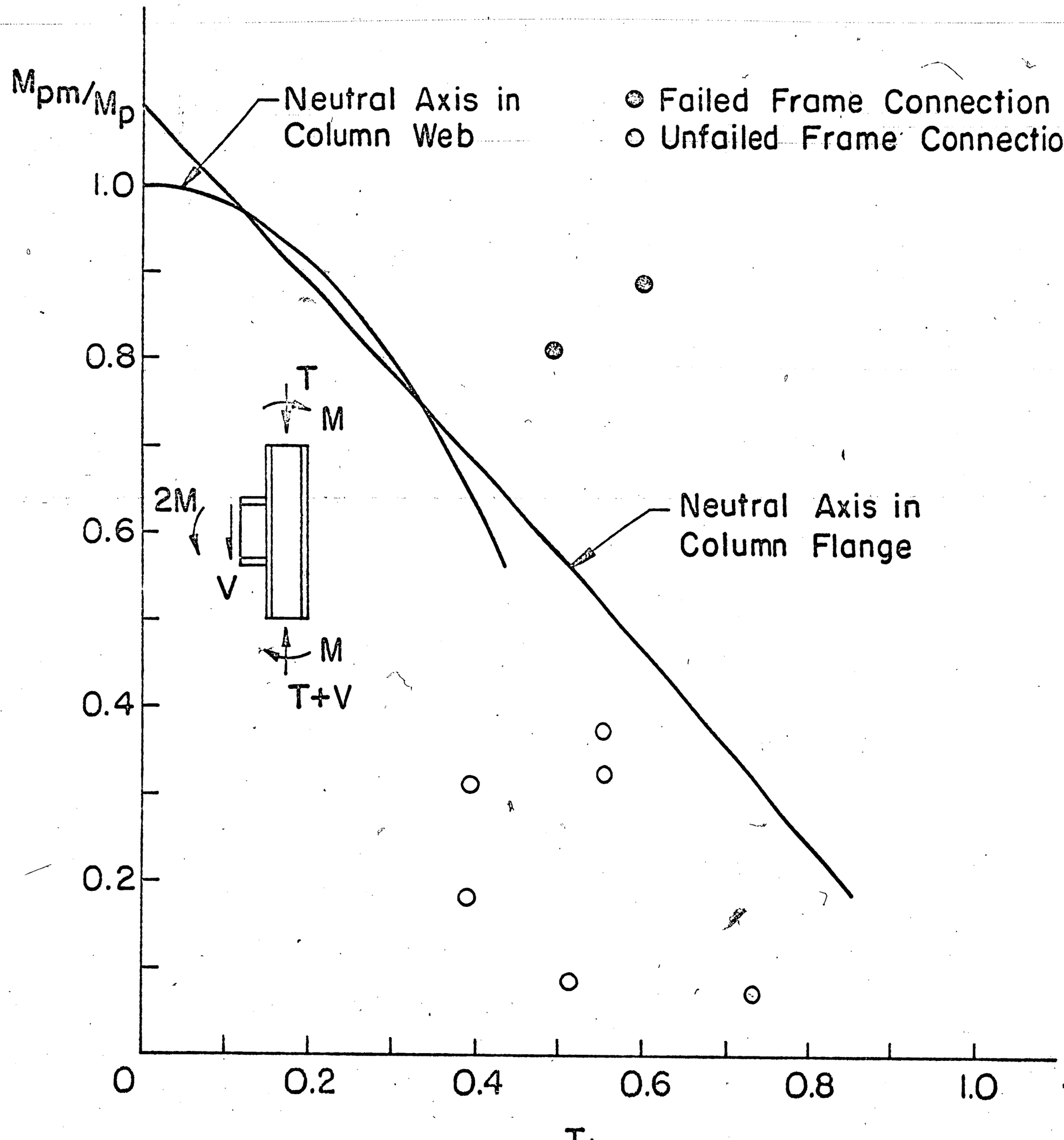

FIGURE 9. Shear-Moment-Axial Load Interaction Curve Developed from the preliminary lower bound investigation. Data from previous frame tests is also shown.

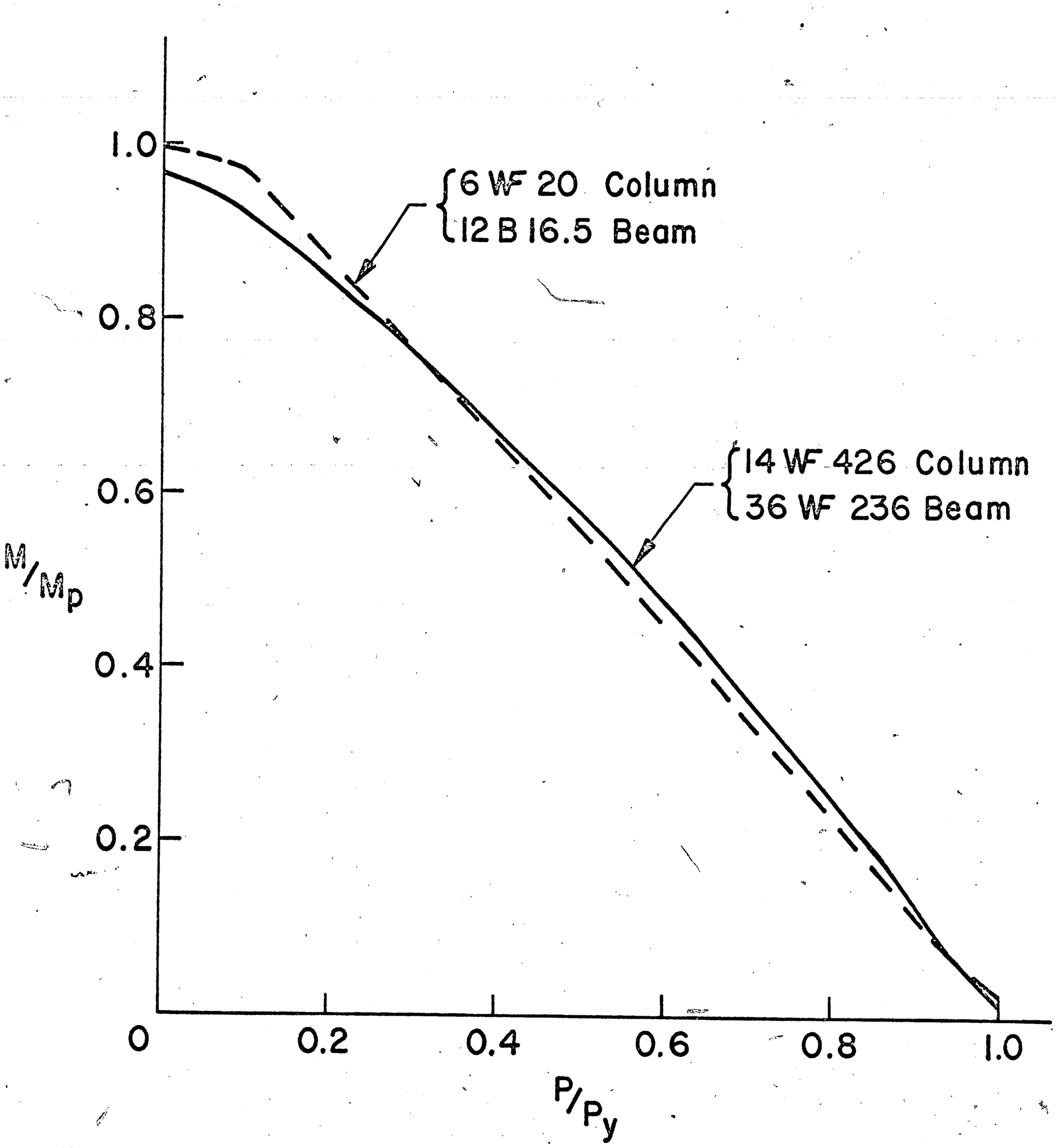

FIGURE 10. Shear-Moment-Axial Load Interaction Curve for Beam-to-Column Connections Made from Different Member Dimensions
(Column Length = 60", Beam Length = 30")

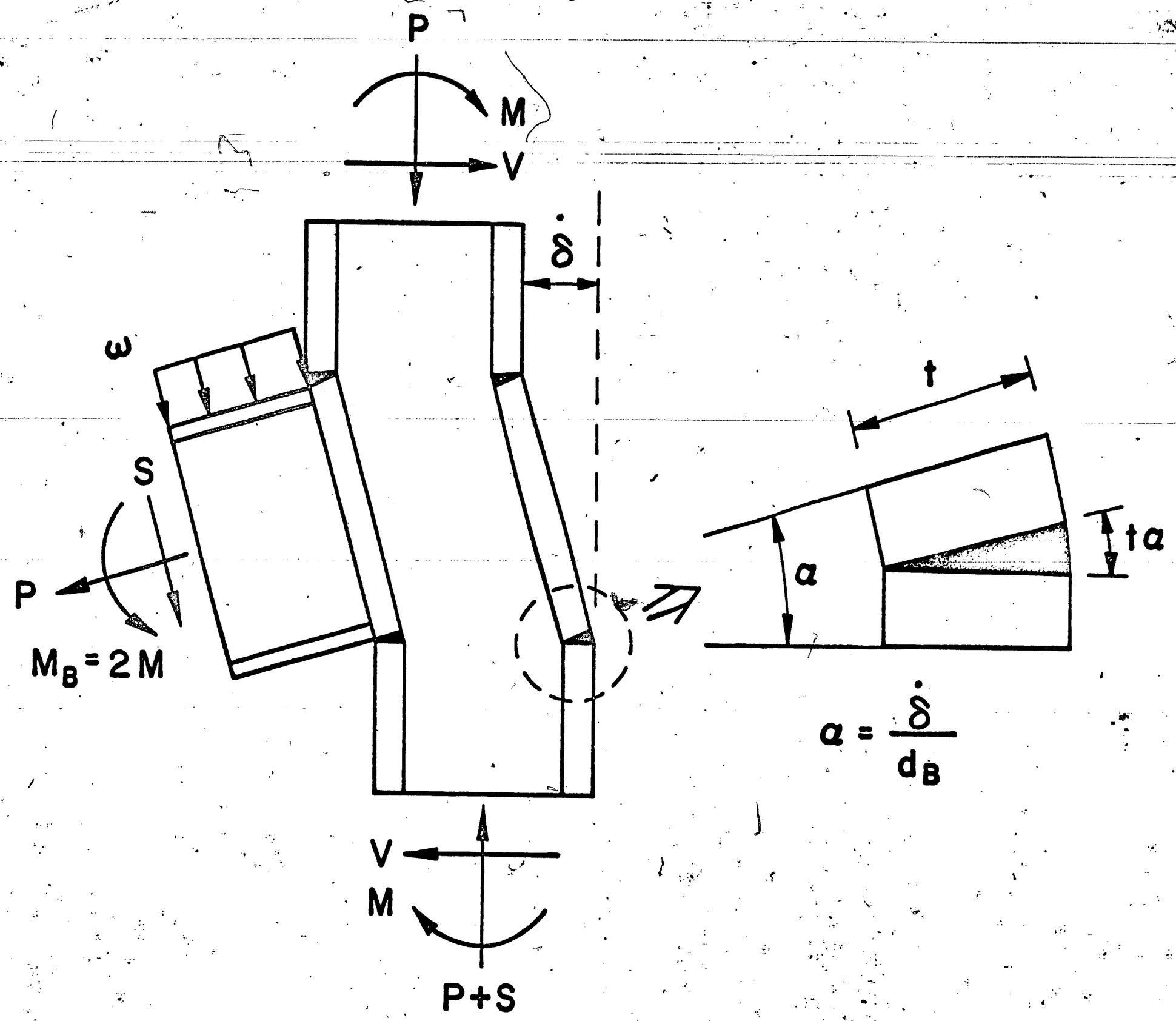

FIGURE 11. Upper Bound Displacement Mode Neglecting Axial Shortening

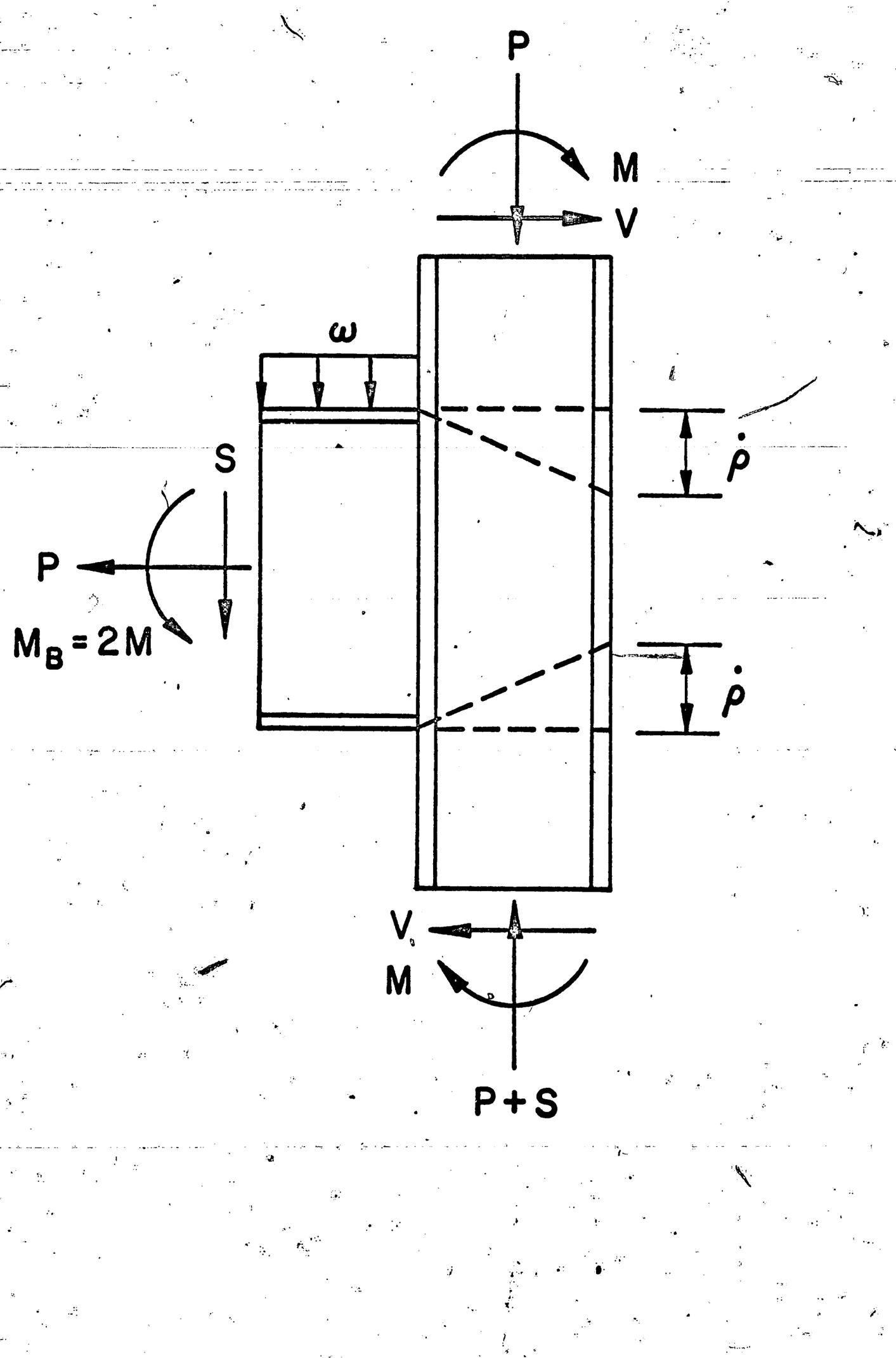

FIGURE 12. Upper Bound Displacement Mode Considering the Effect of Axial Load

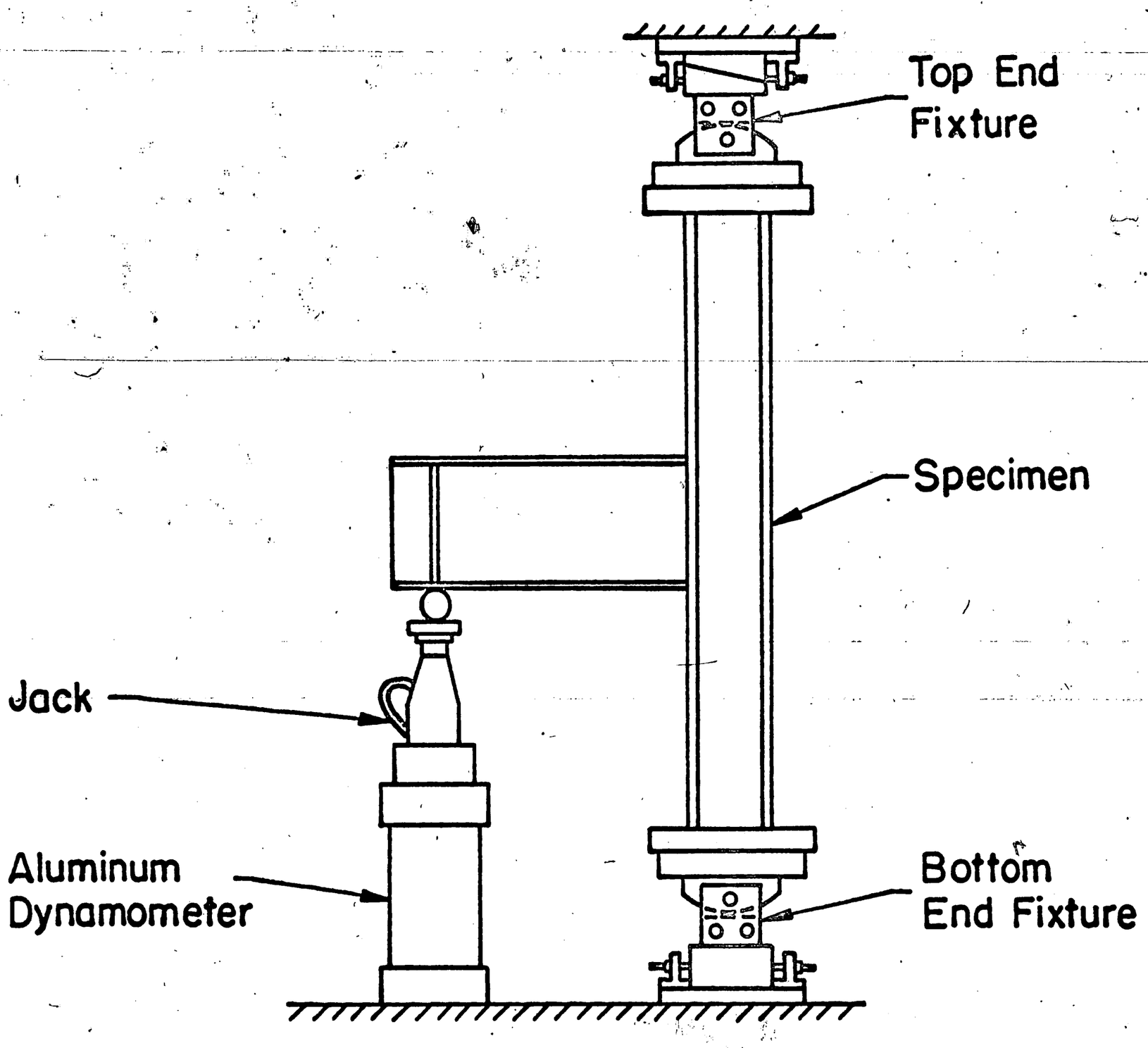

FIGURE 13A. Test Setup with Pinned-End Column Fixtures

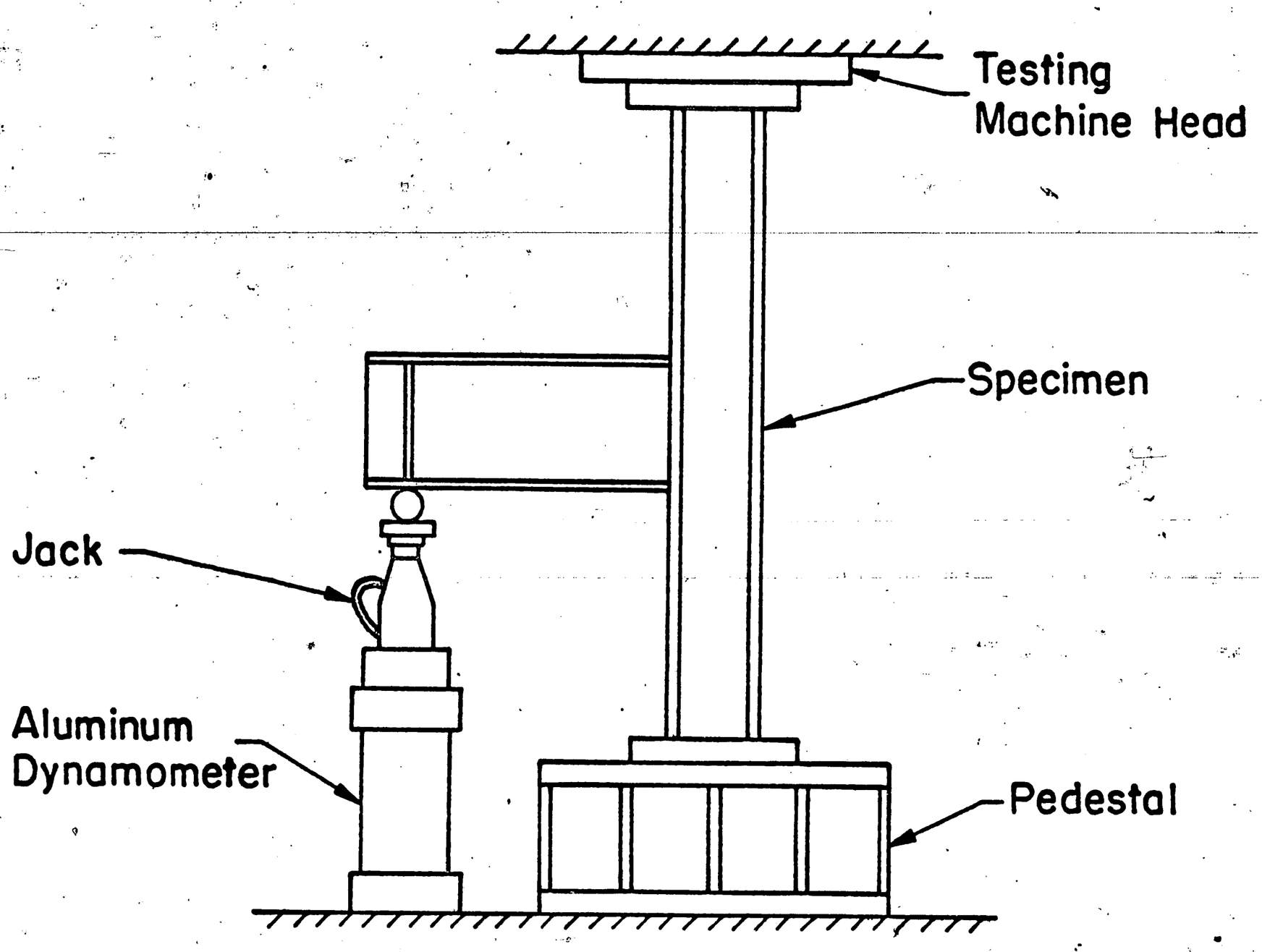

FIGURE 13B. Test Setup with Fixed-End Columns

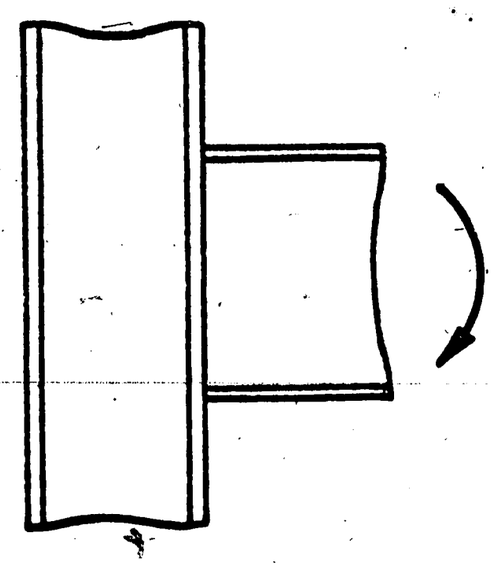

a) Exterior Connection, No Stiffening -- Test A1, A2

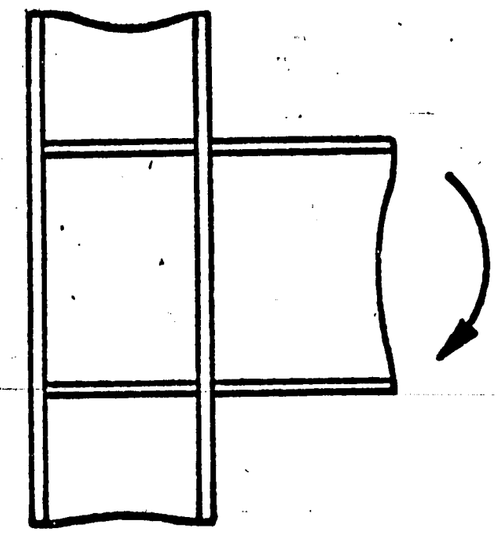

b) Exterior Connection, Horizontal Stiffening

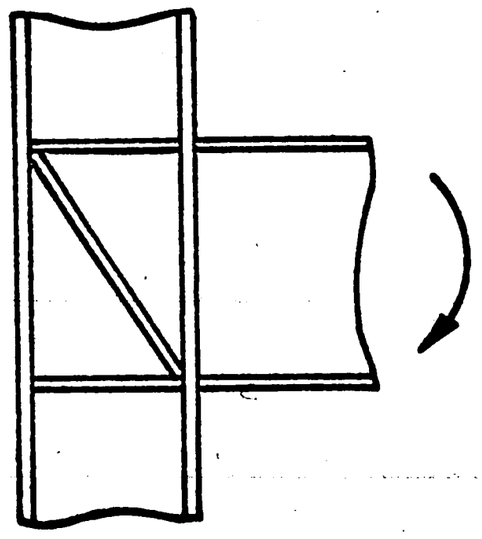

c) Exterior Connection, Diagonal Stiffening in Compression -- Test A5, A6

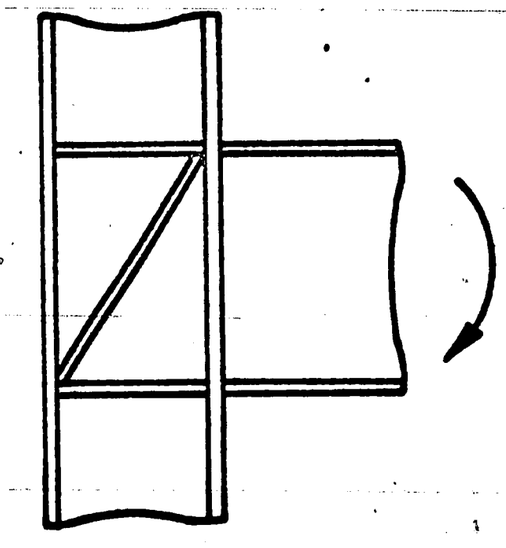

d) Exterior Connection, Diagonal Stiffening in Tension -- Test A3, A4, A7

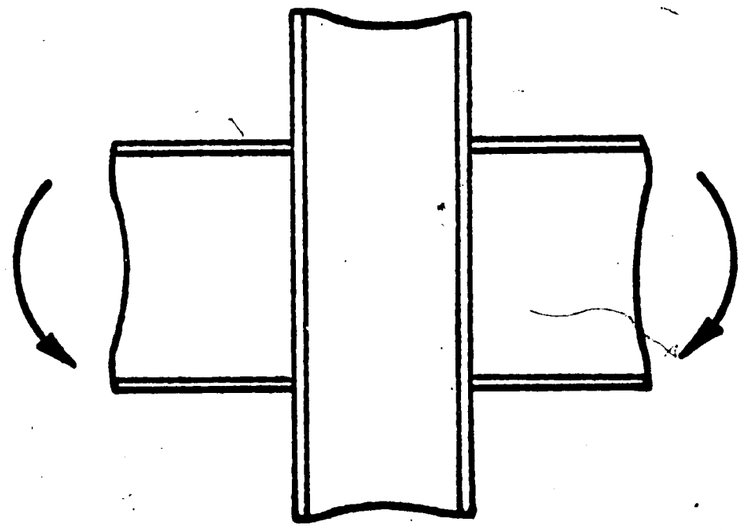

e) Interior Connection

FIGURE 14: Types of Beam-to-Column Connections

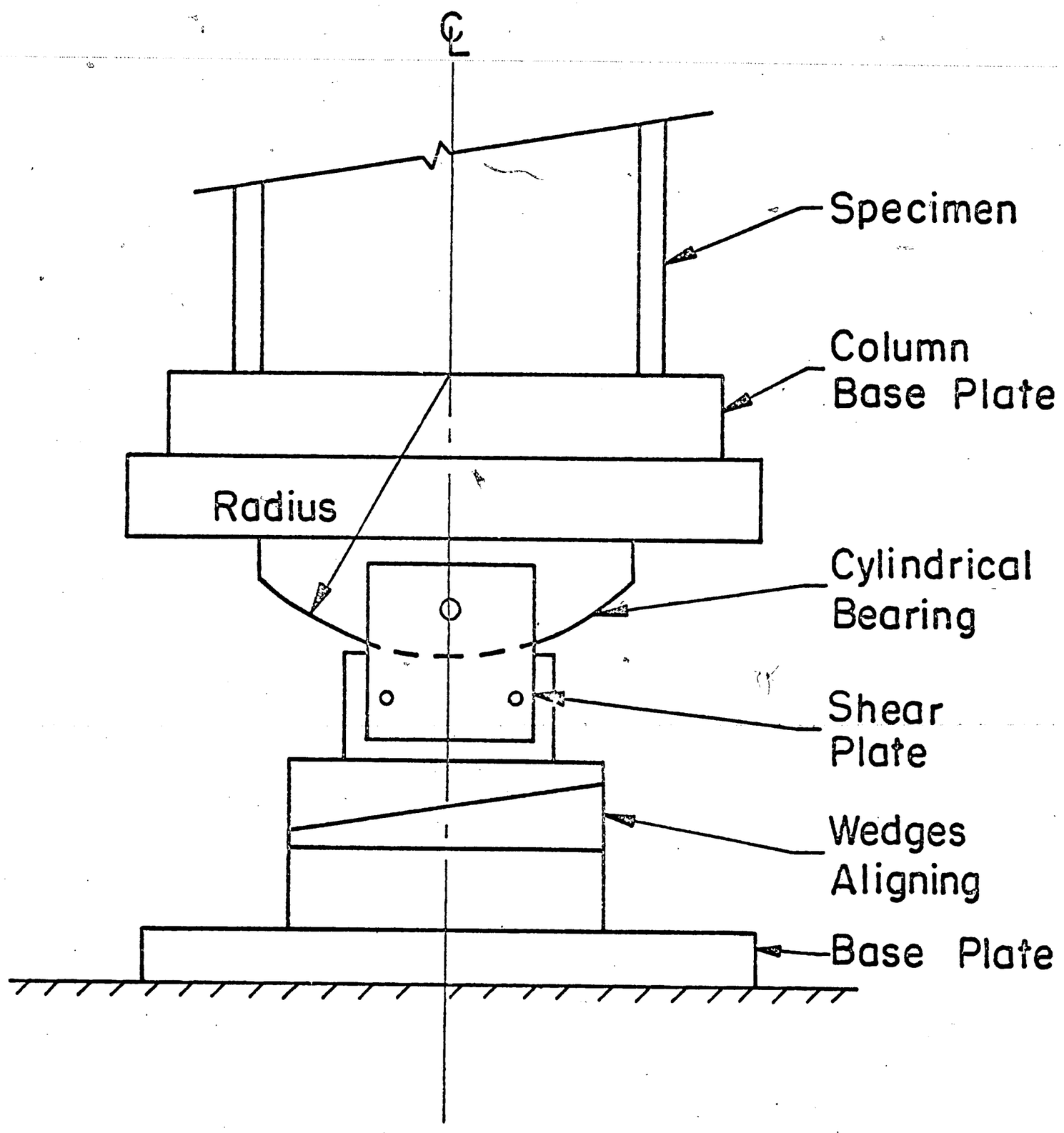

SCHEMATIC VIEW

FIGURE 15. View of End Fixtures

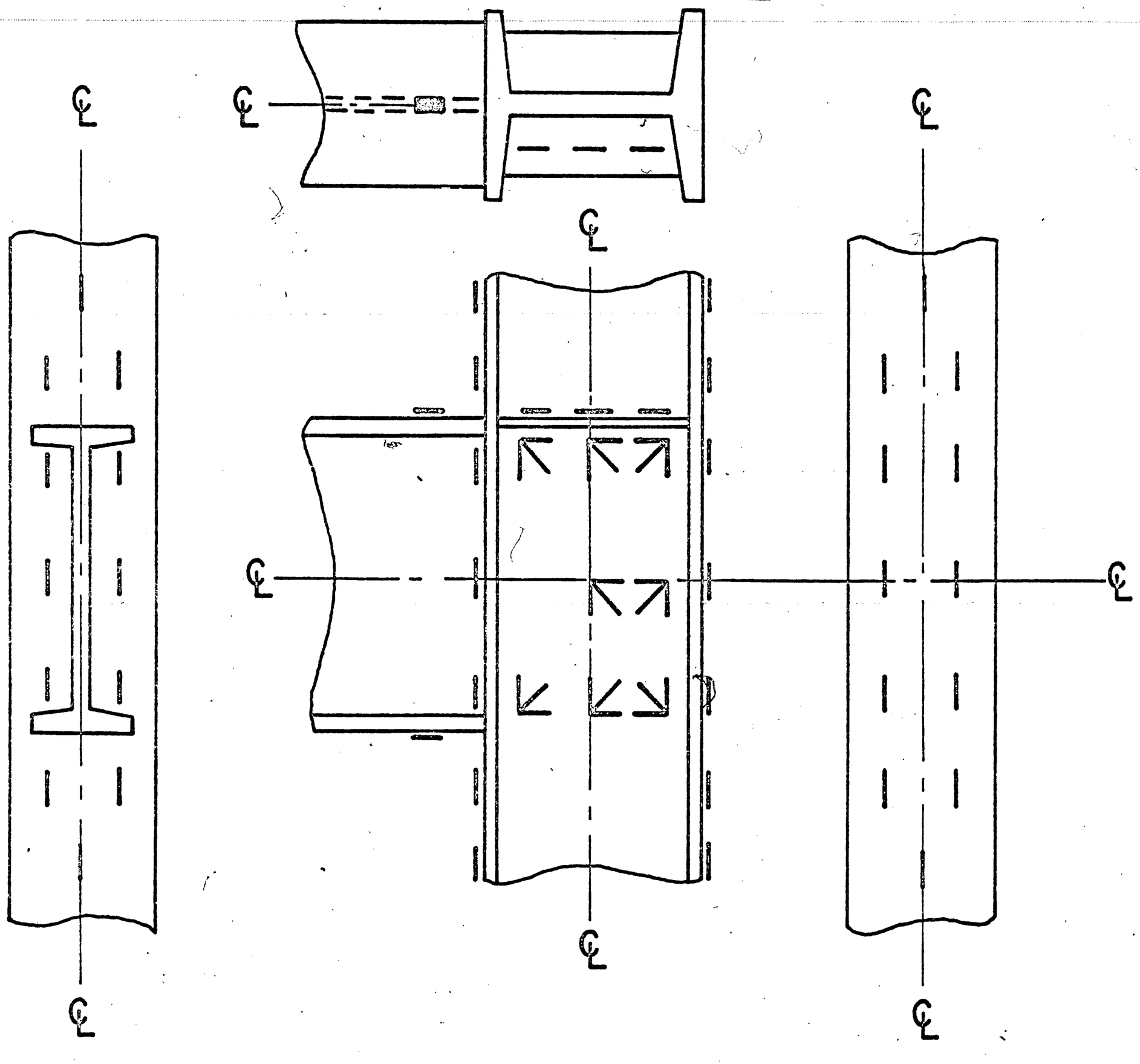

FIGURE 16. Electrical Strain Gage Locations

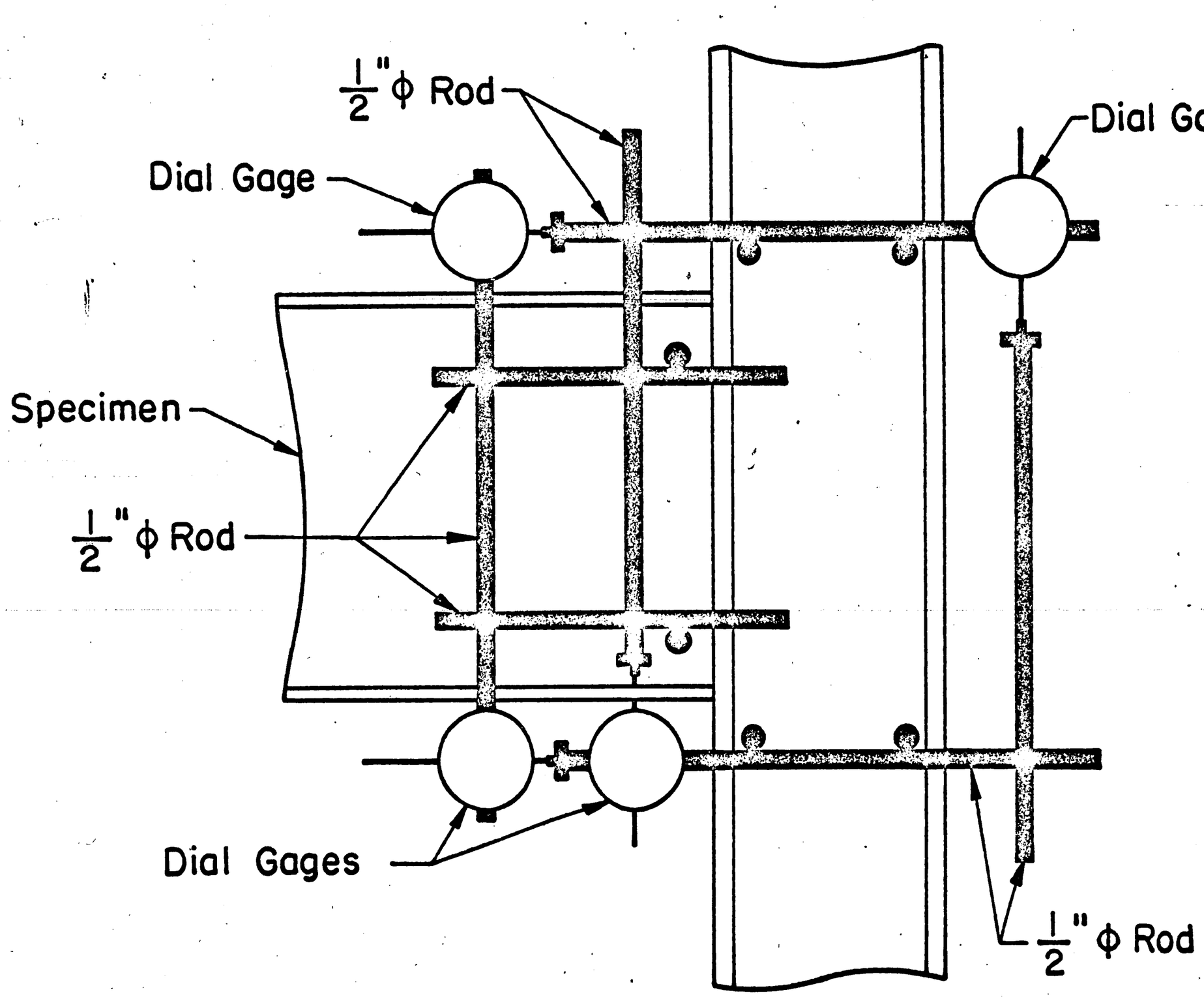

FIGURE 17. Web Panel Rotation Gage

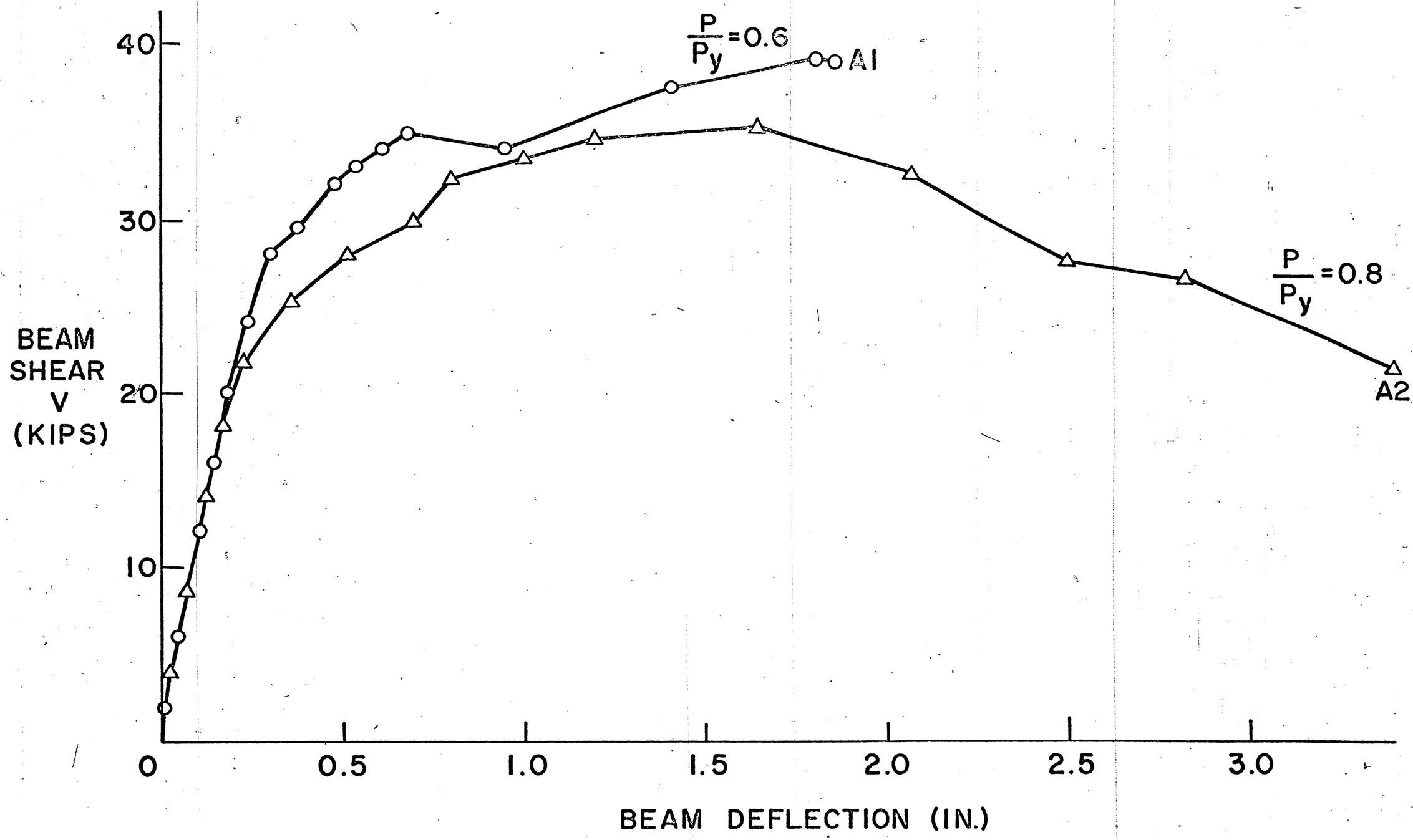

FIGURE 18. Beam Load-Deflection Curve for the Unstiffened Test Connections

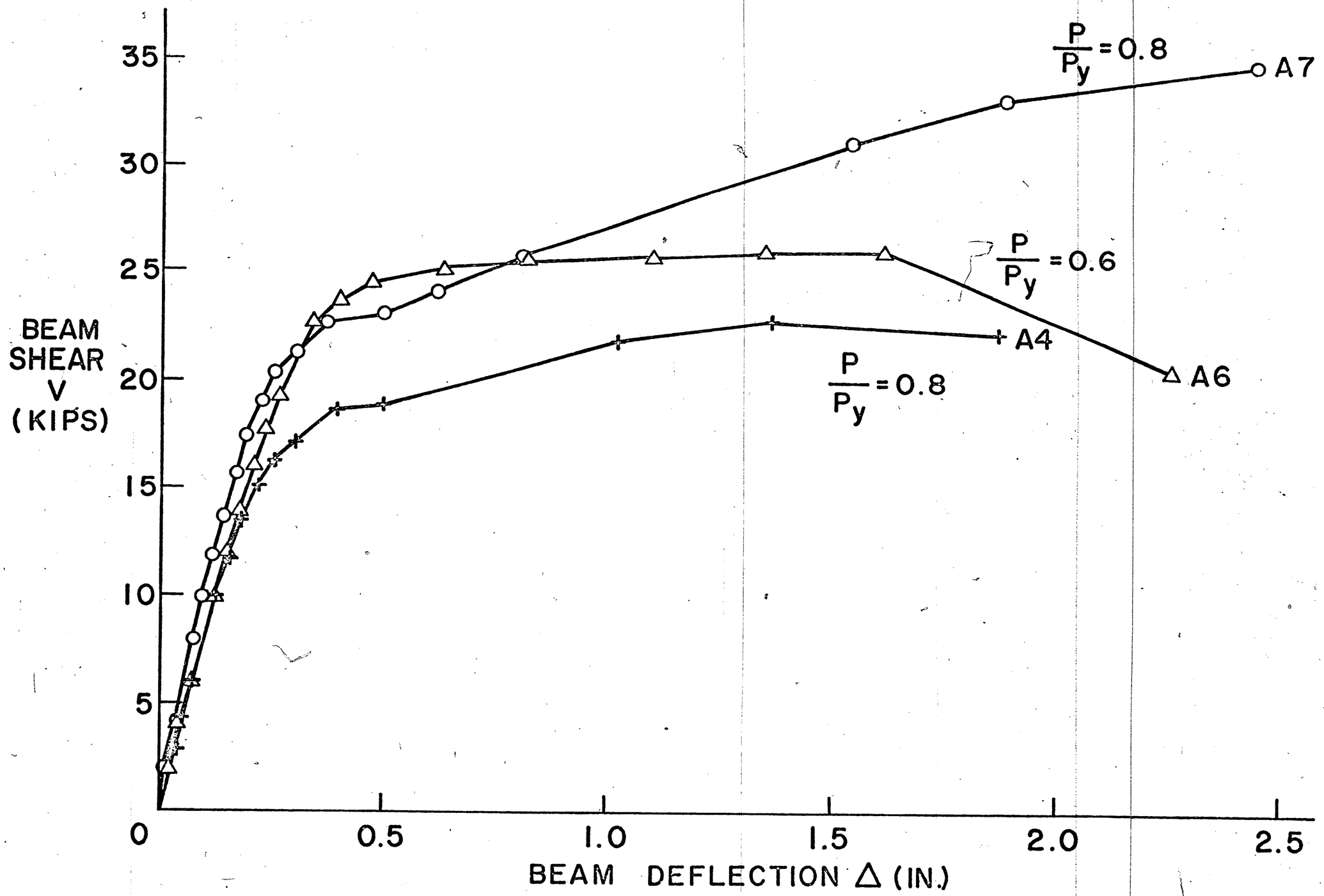

FIGURE 19A. Beam Load-Deflection Curves for Test Connections with Diagonal Stiffeners Acting in Tension

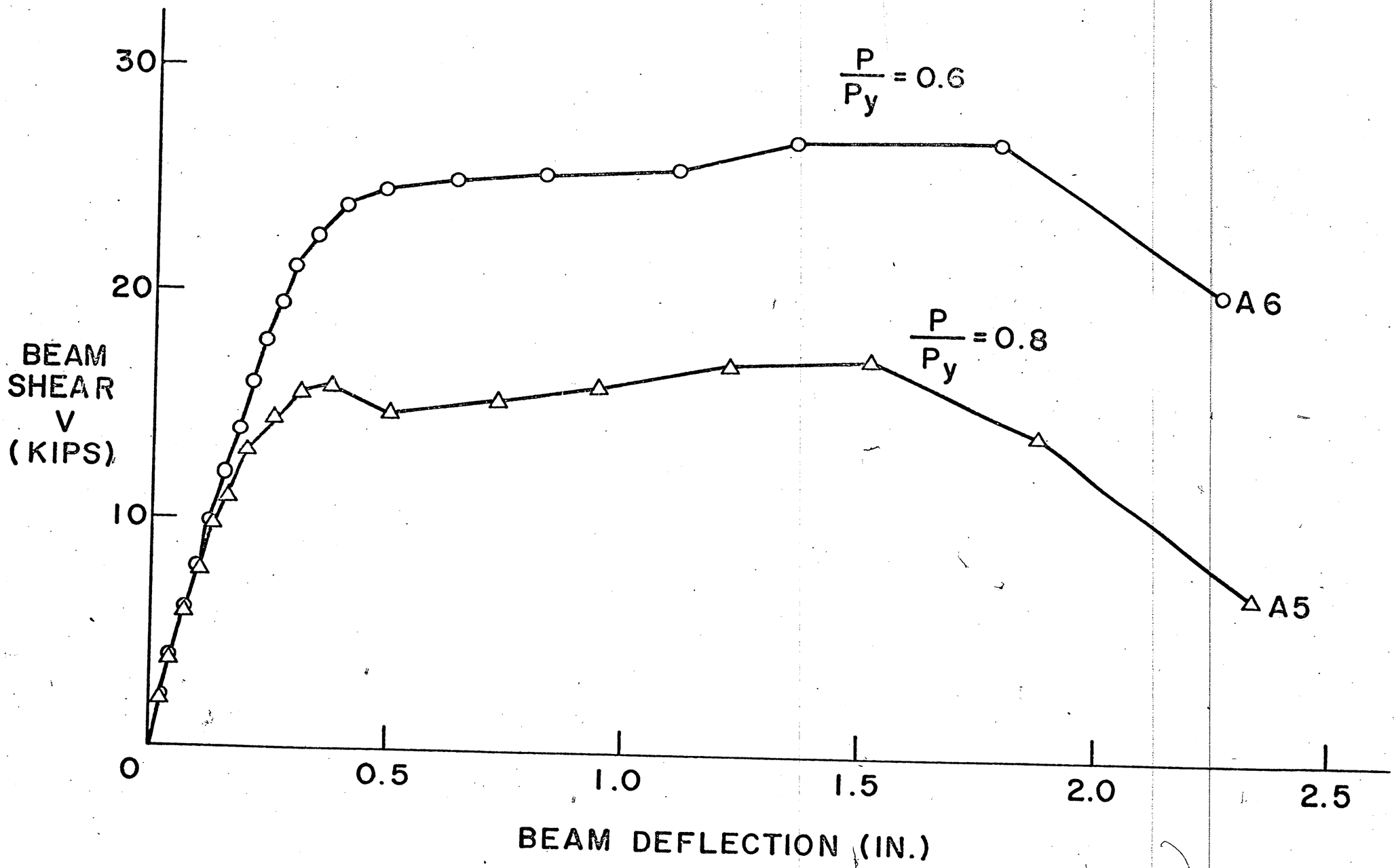

FIGURE 19B. Beam Load-Deflection Curves for Test Connections with Diagonal Stiffeners Acting in Compression

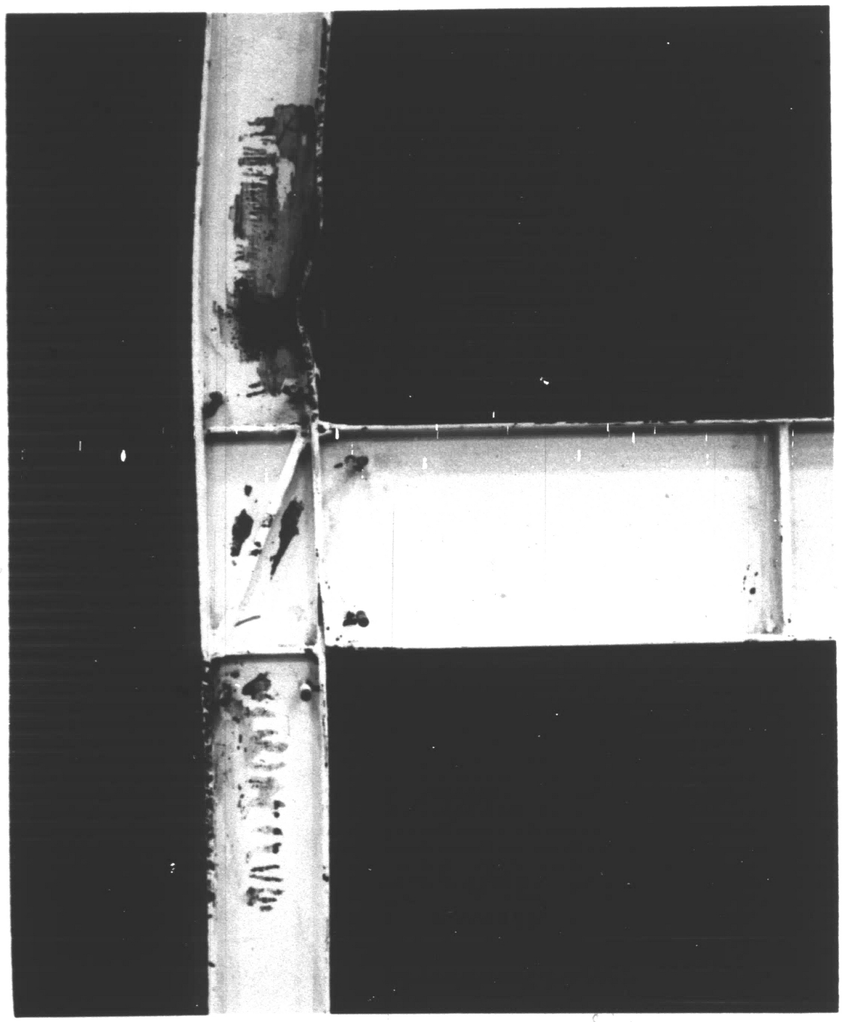

a) Failure Mode of a Diagonally Stiffened Connection

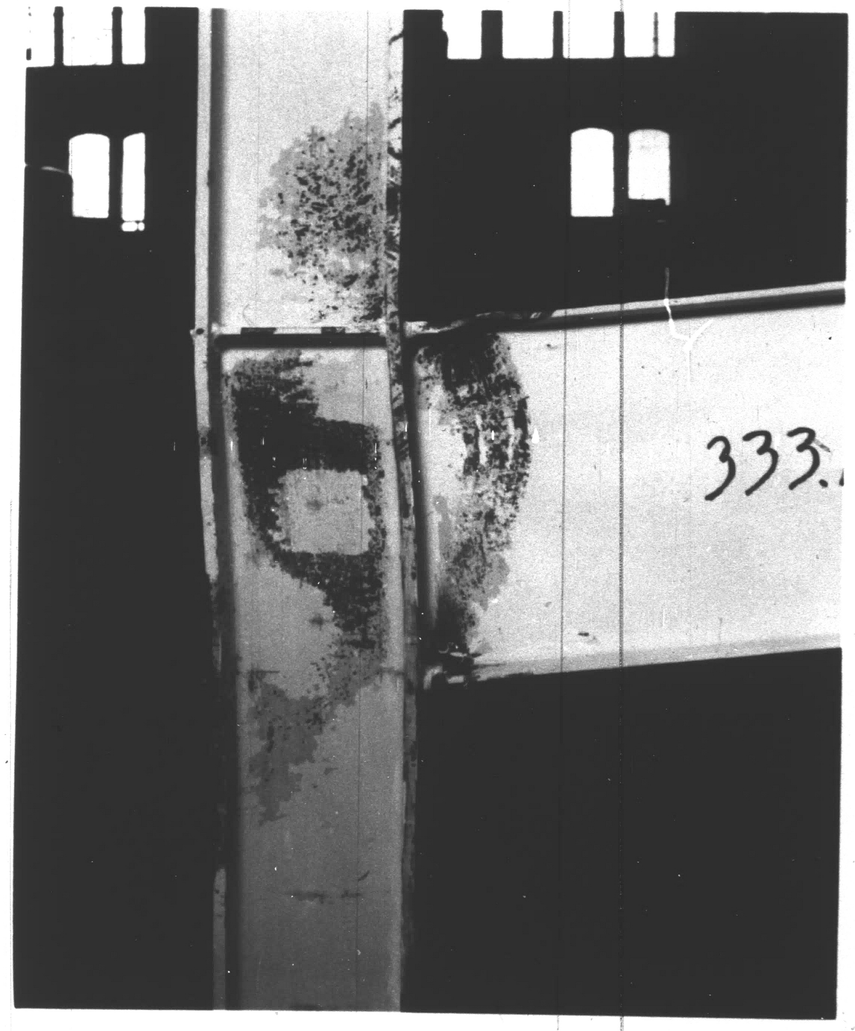

b) Local Buckle in the Beam Flange

FIGURE 20. Failure Modes of the Test Specimens

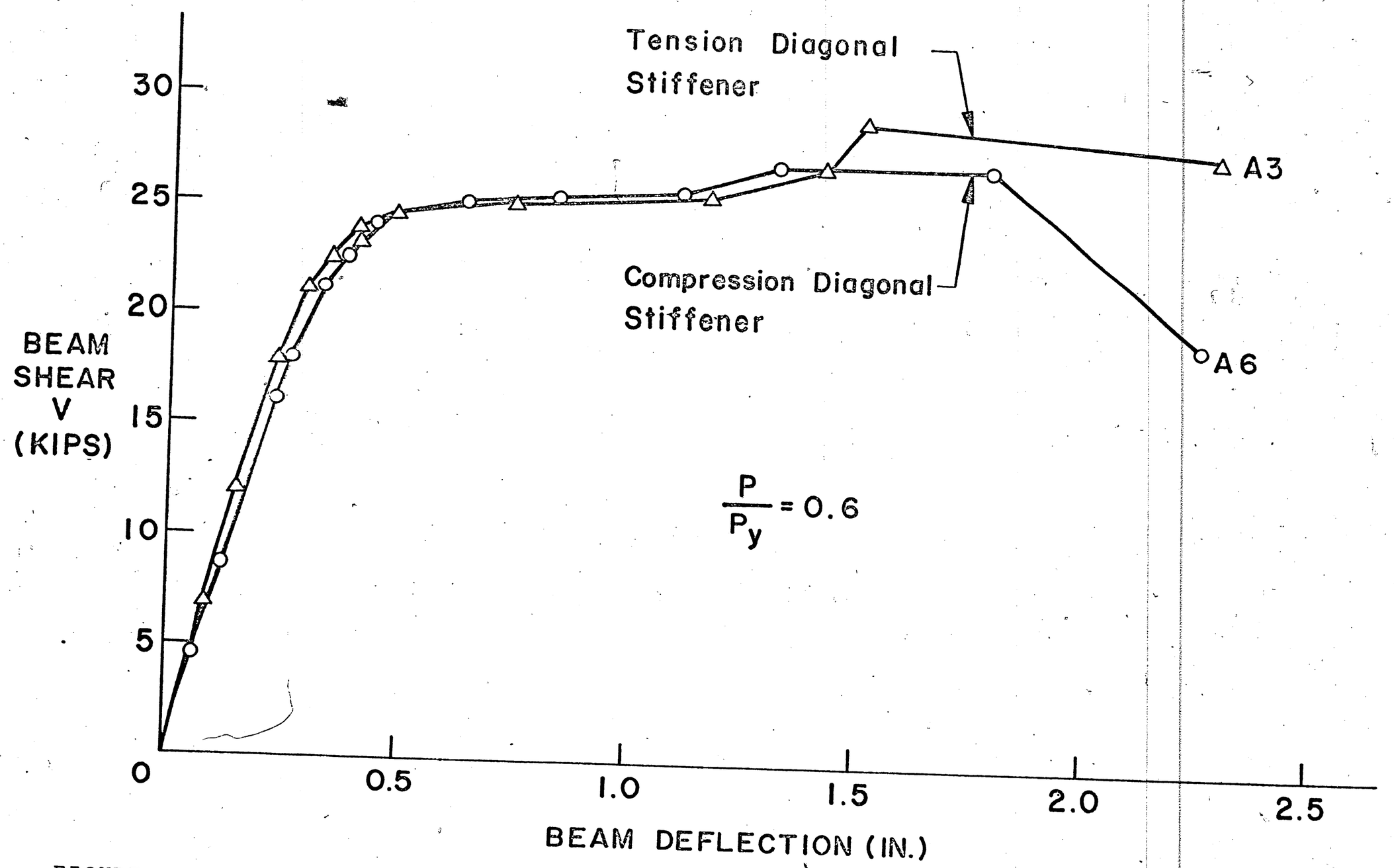

FIGURE 21. Beam Load-Deflection Curve Comparing the Results for the Test Connections with Diagonal Stiffeners in Tension and Compression

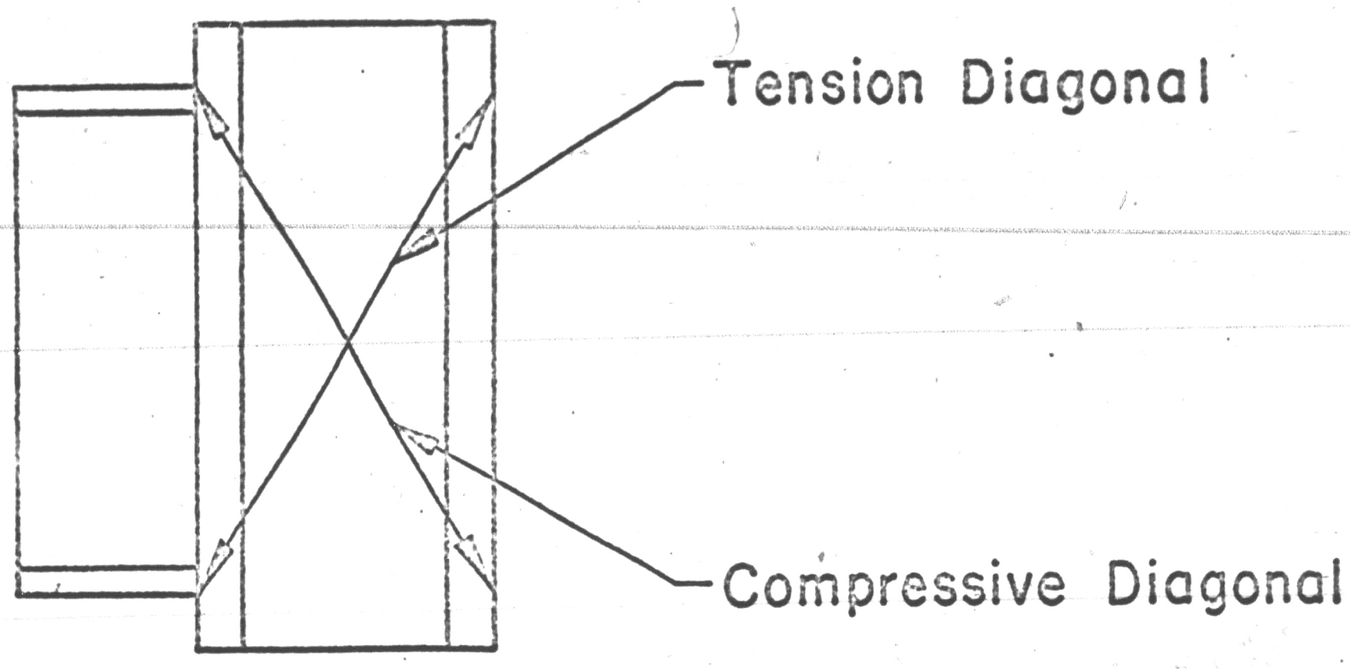

a) Diagonal Deformations Measured on Test Specimens

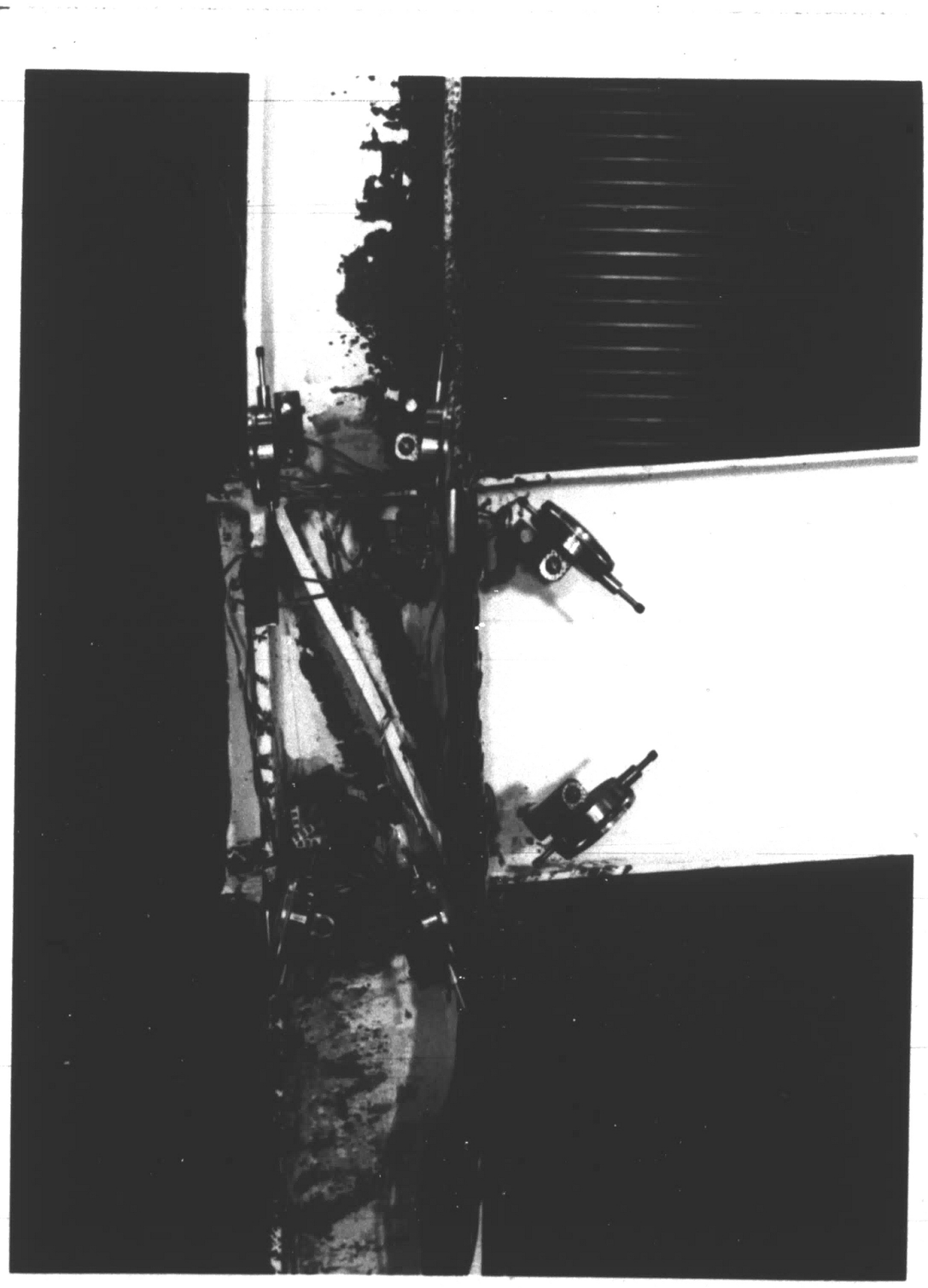

b) Photo of Equipment Used to Measure Relative Rotations and Diagonal Deformations of a Connection

FIGURE 22. Equipment to Measure Connection Behavior

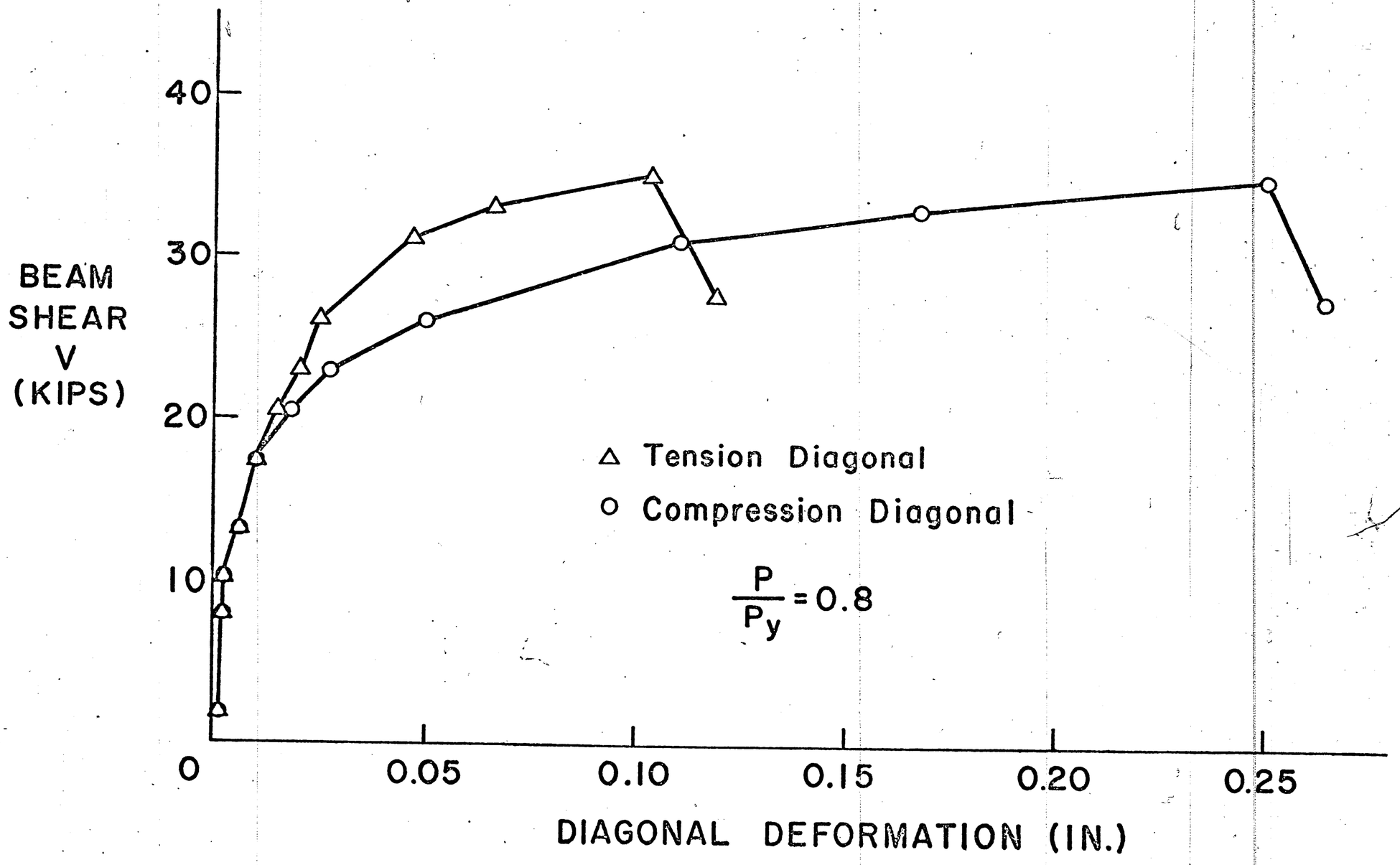

FIGURE 23. Diagonal Deformations of Test 333.A2 an Unstiffened Connection

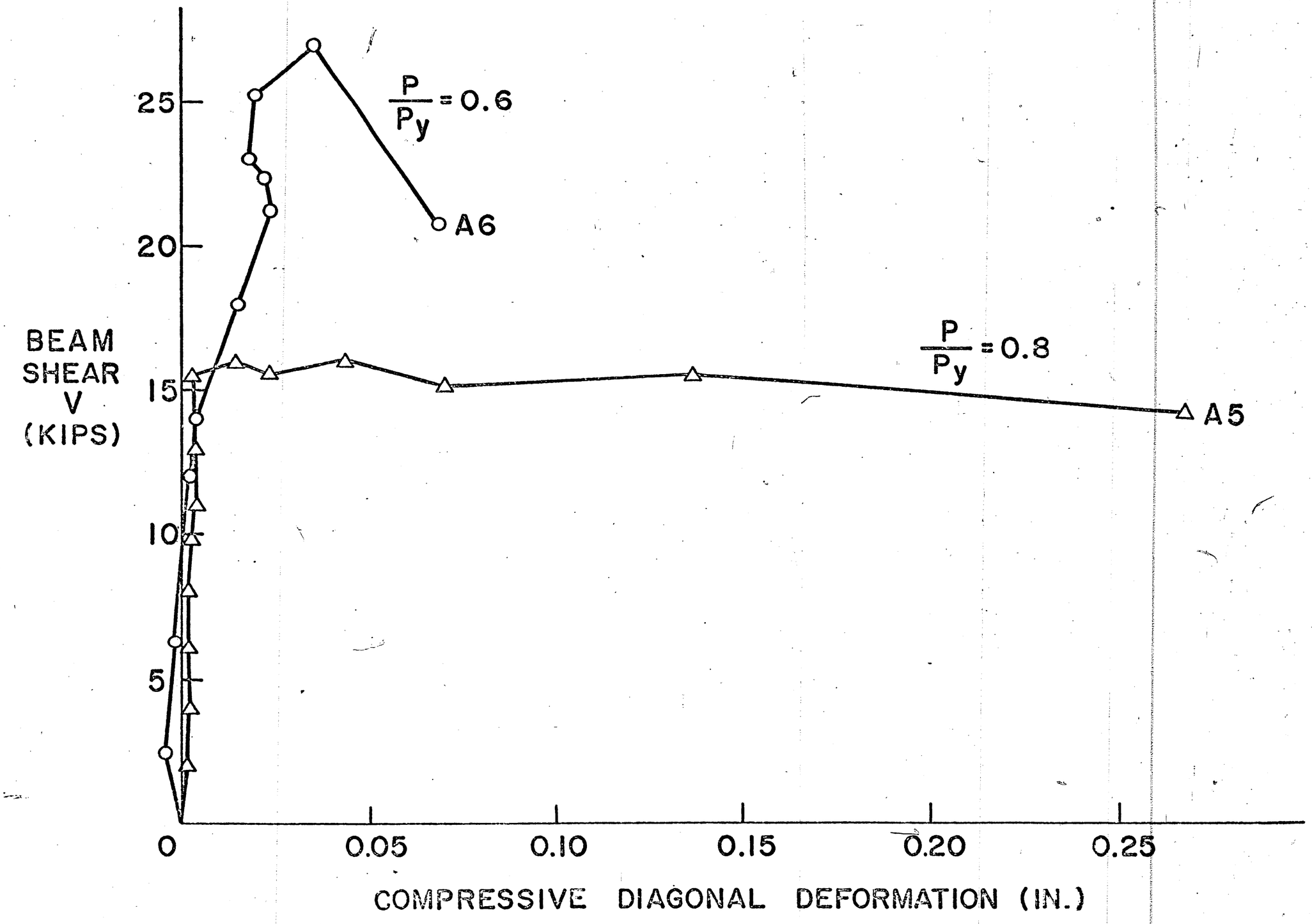

FIGURE 24. Diagonal Deformations of the Test Specimens with Diagonal Stiffeners Acting in Compression

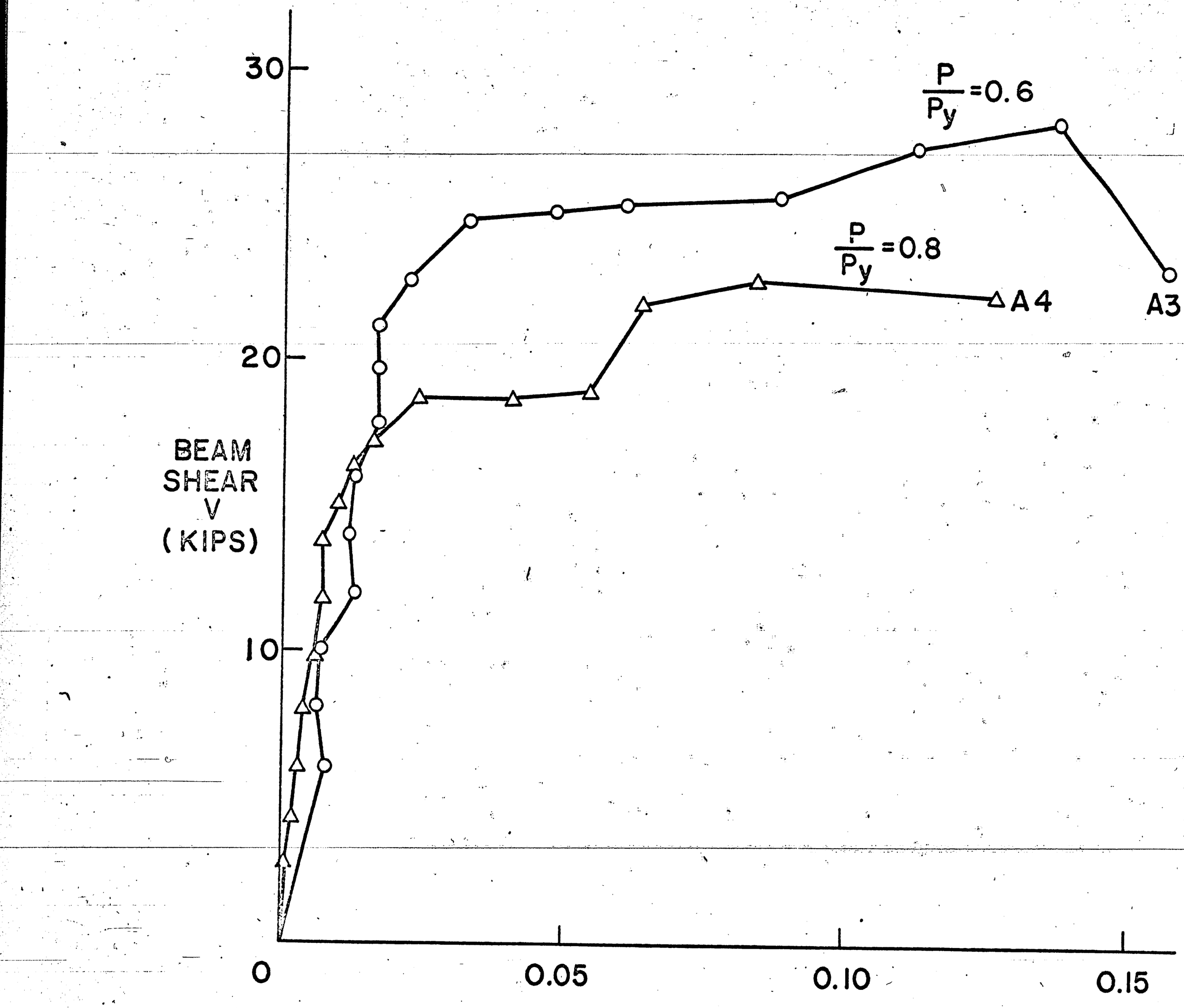

FIGURE 25. Diagonal Deformations of the Test Specimens with Diagonal Stiffeners Acting in Tension

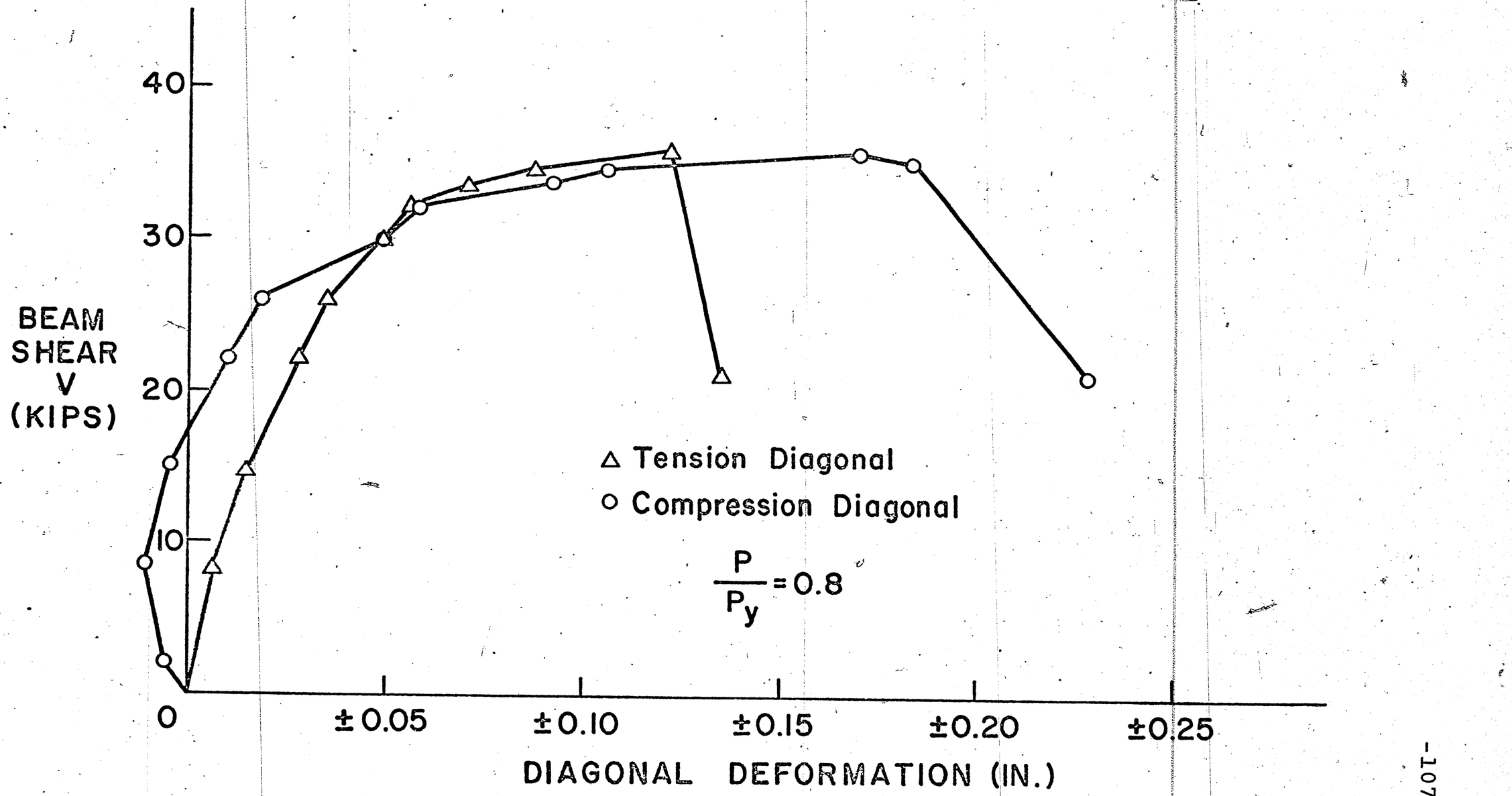

FIGURE 26. Typical Load-Diagonal Deformation Curve for Both Diagonals of a Diagonally Stiffened Connection (Test 333.A7)

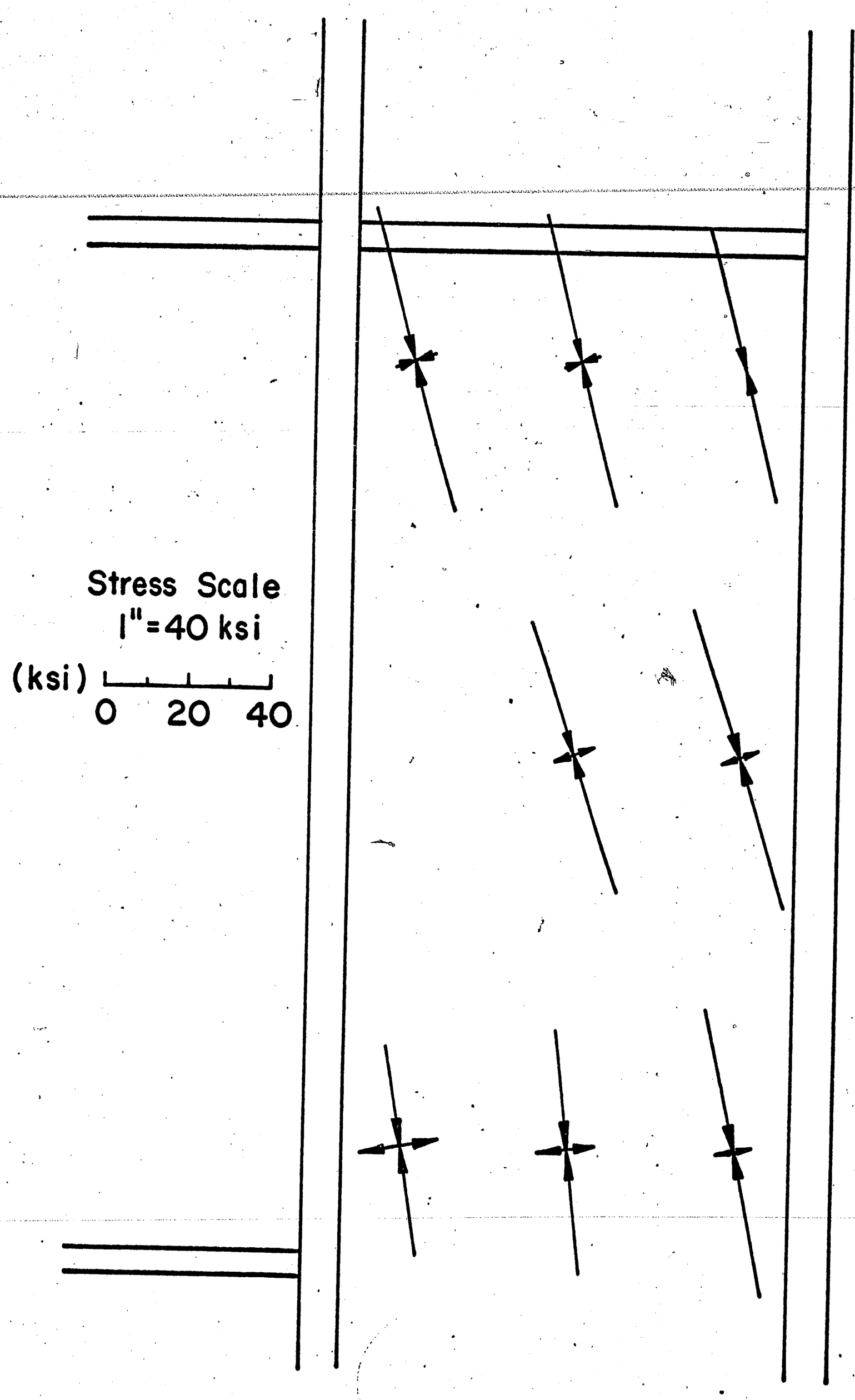

FIGURE 27. Principal Stresses in the Web Panel of an Unstiffened Connection Subjected to an Elastic Loading Condition

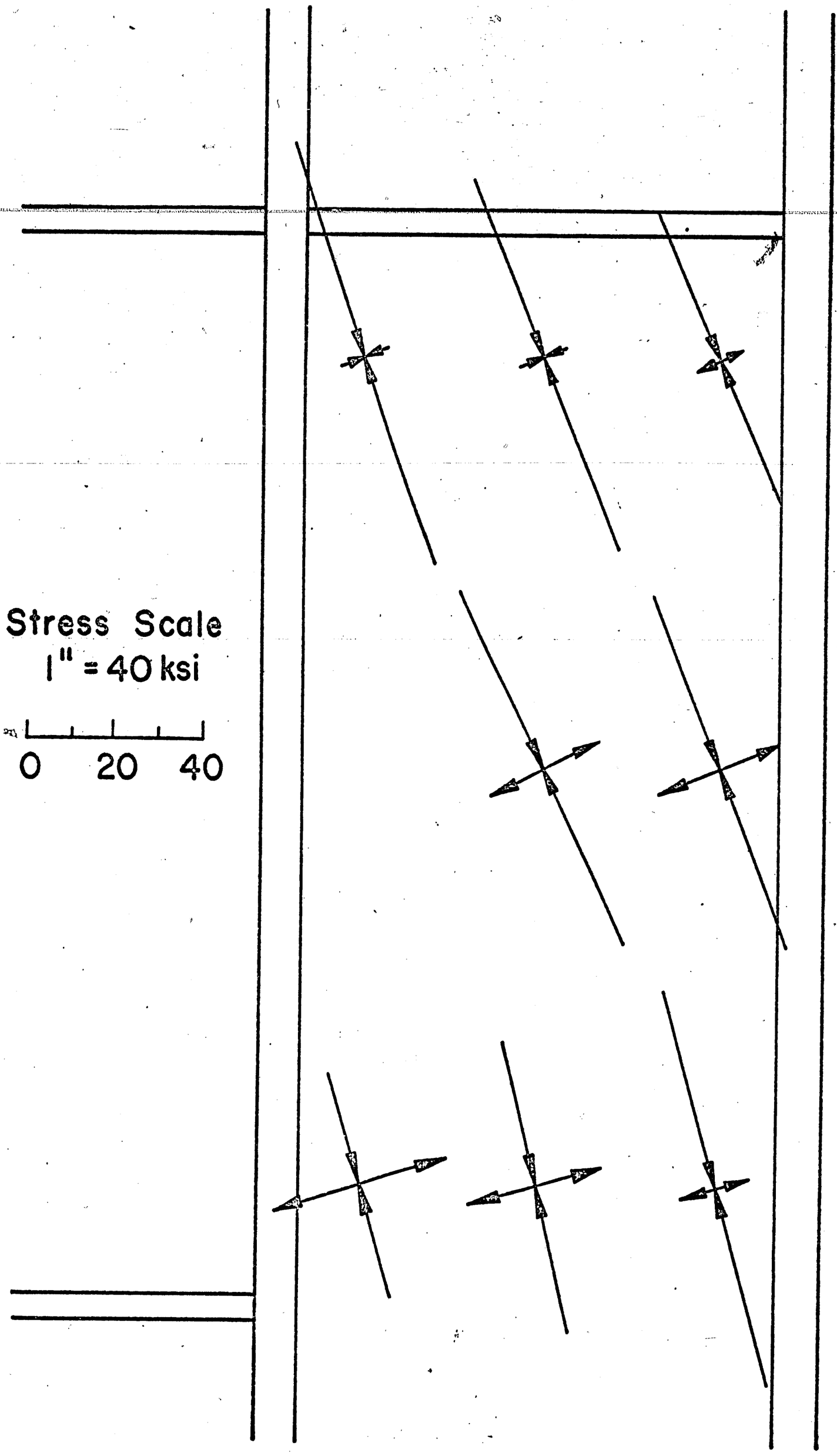

FIGURE 28. Principal Stresses in the Web Panel of an Unstiffened Connection Subjected to an Inelastic Loading Condition

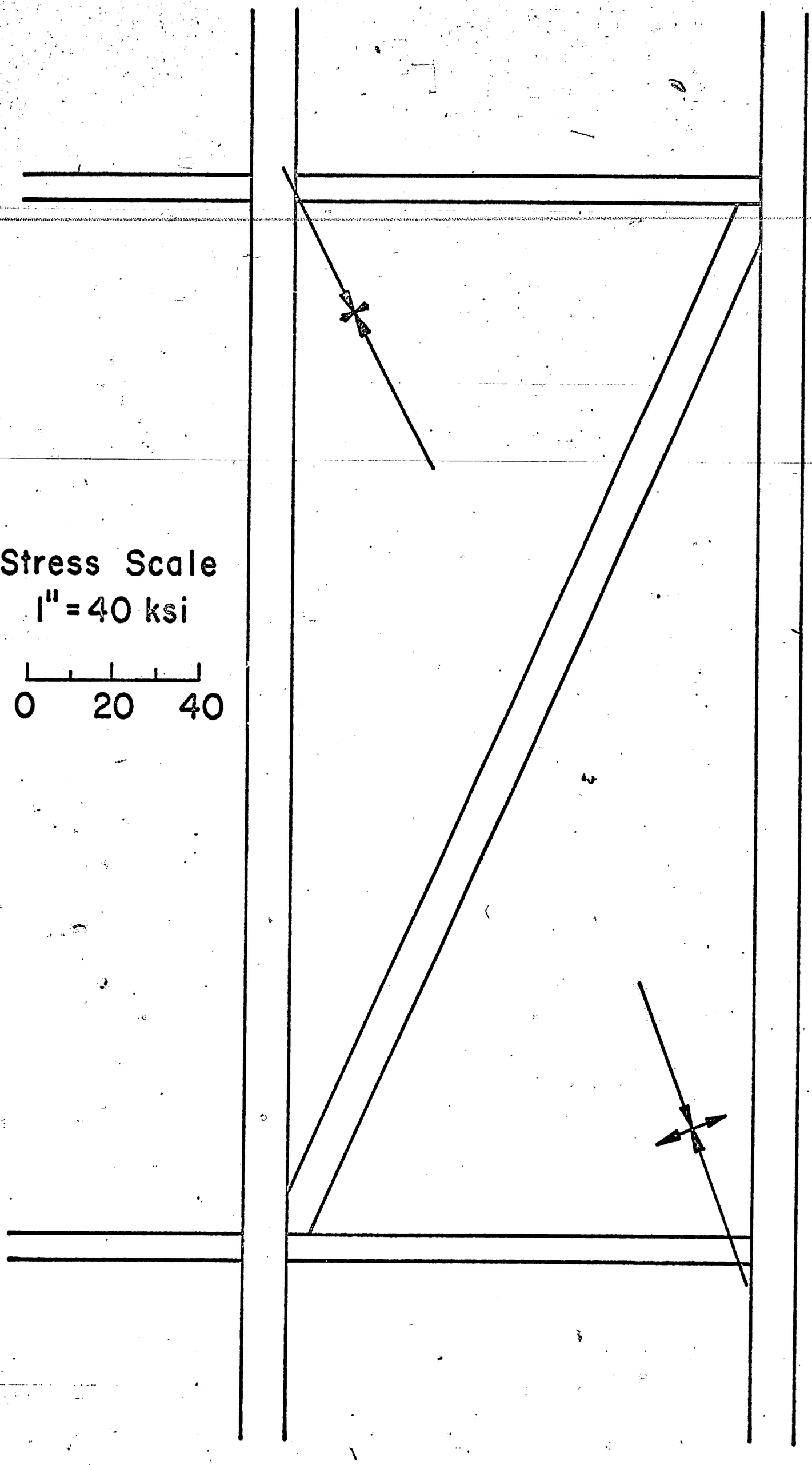

FIGURE 29. Principal Stresses in the Web Panel of a Connection with a Diagonal Stiffener Acting in Tension

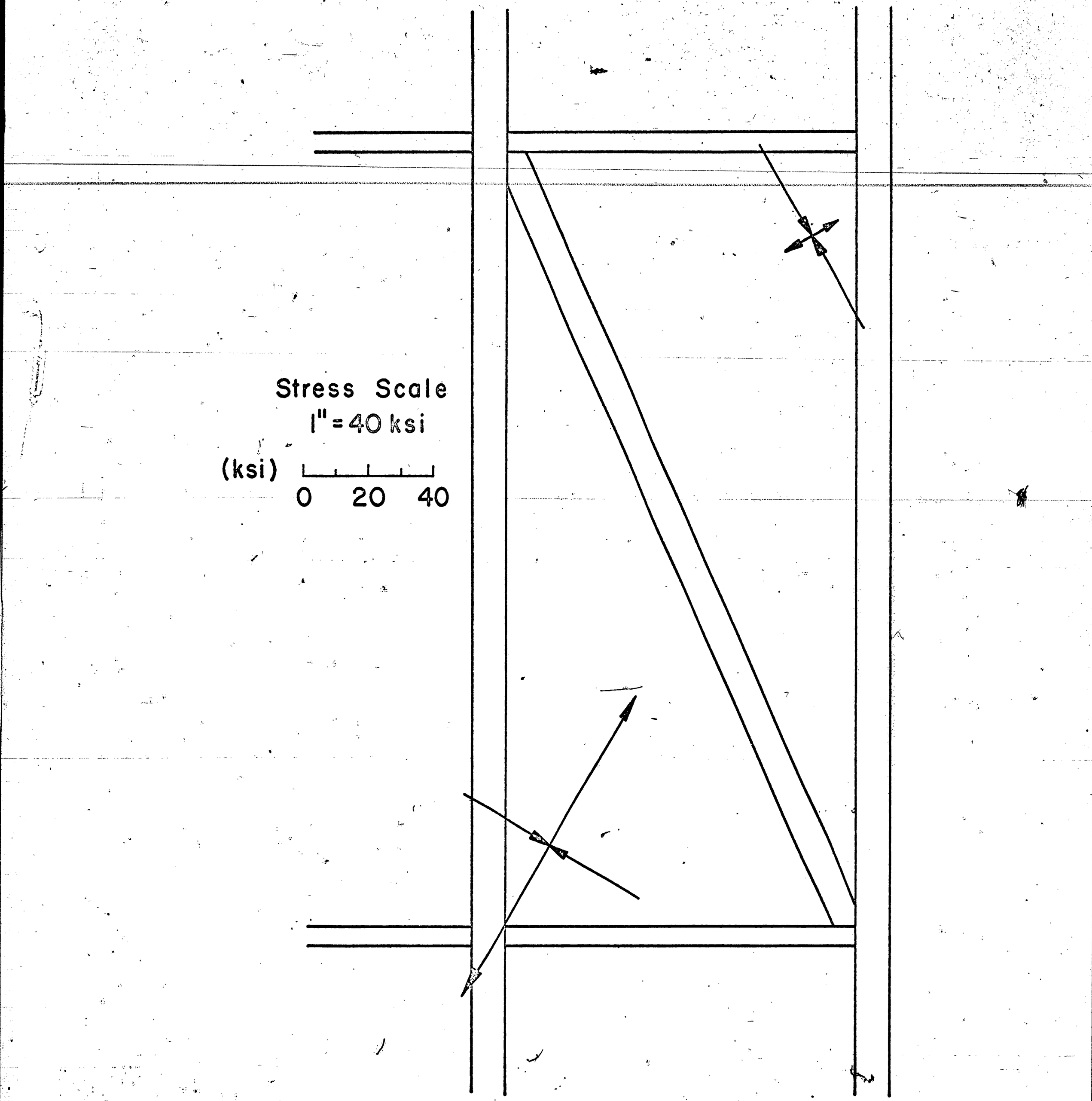

FIGURE 30. Principal Stresses Within the Web Panel of a Connection with a Diagonal Stiffener Acting in Compression

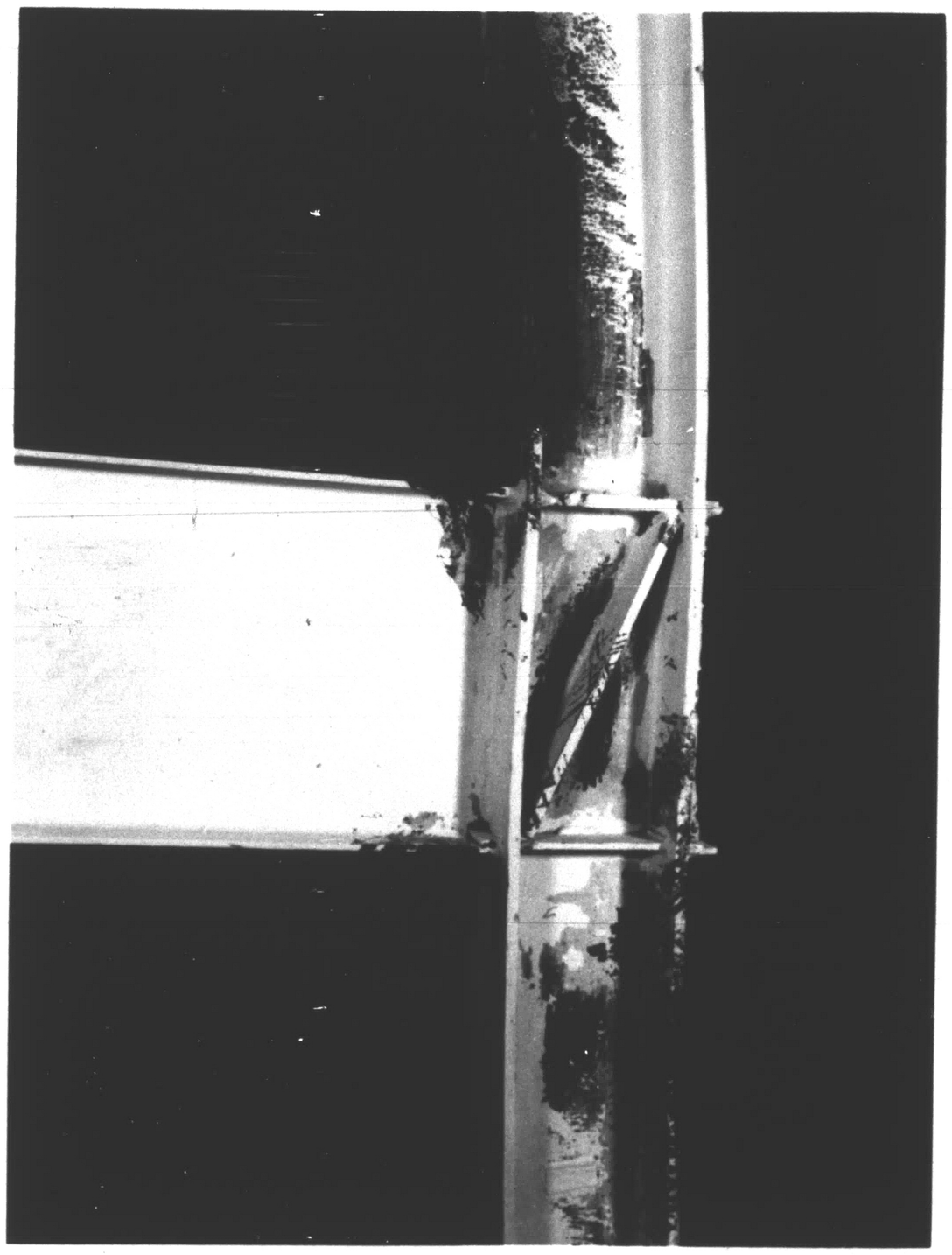

FIGURE 31. A Photograph of Test 333.A7 Showing a Diagonally Stiffened Connection and the way that Yielding Spreads in the Connection

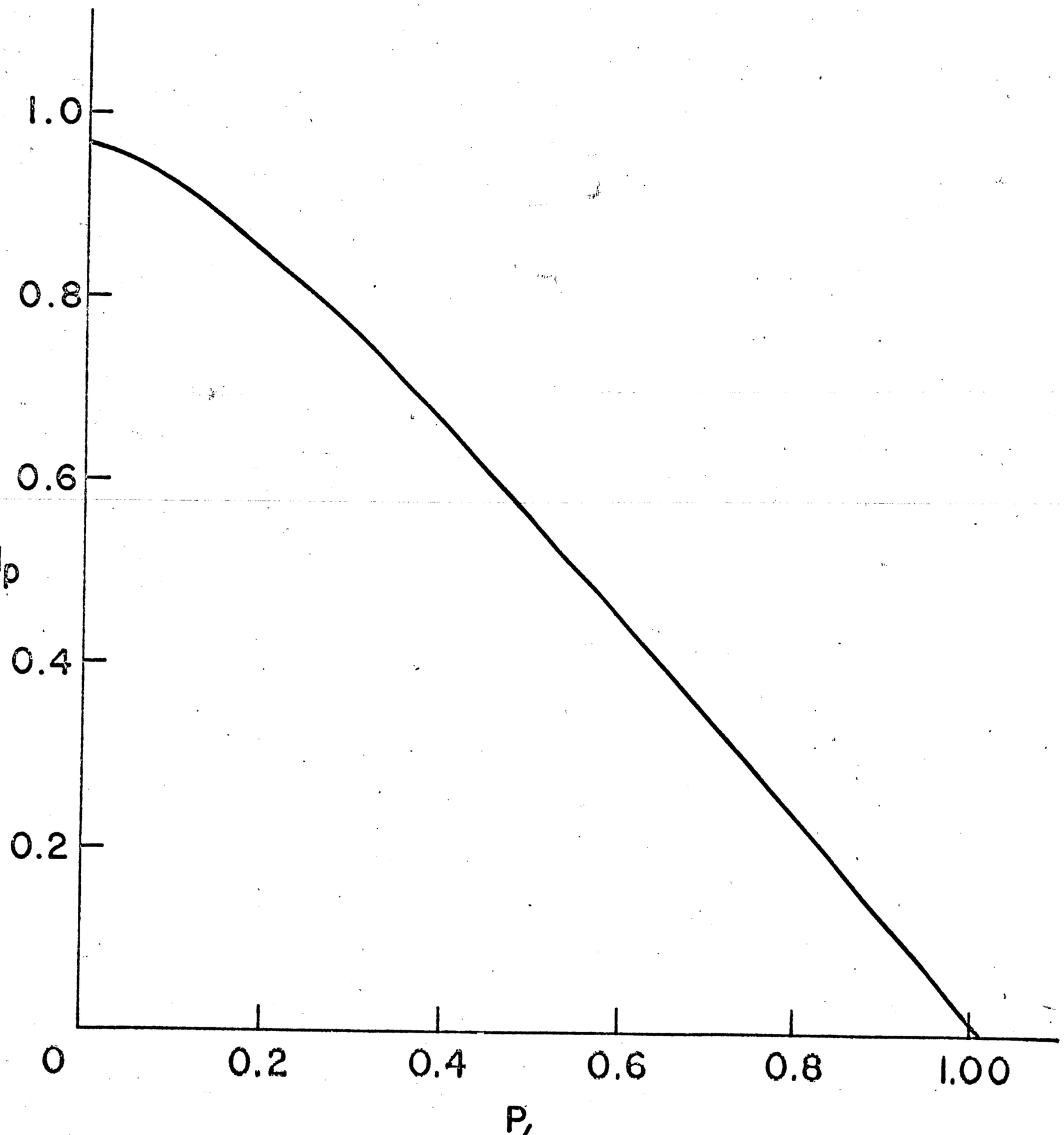

FIGURE 32. The Lowest Composite Interaction Curve Obtained from Selected Practical Sized Connections

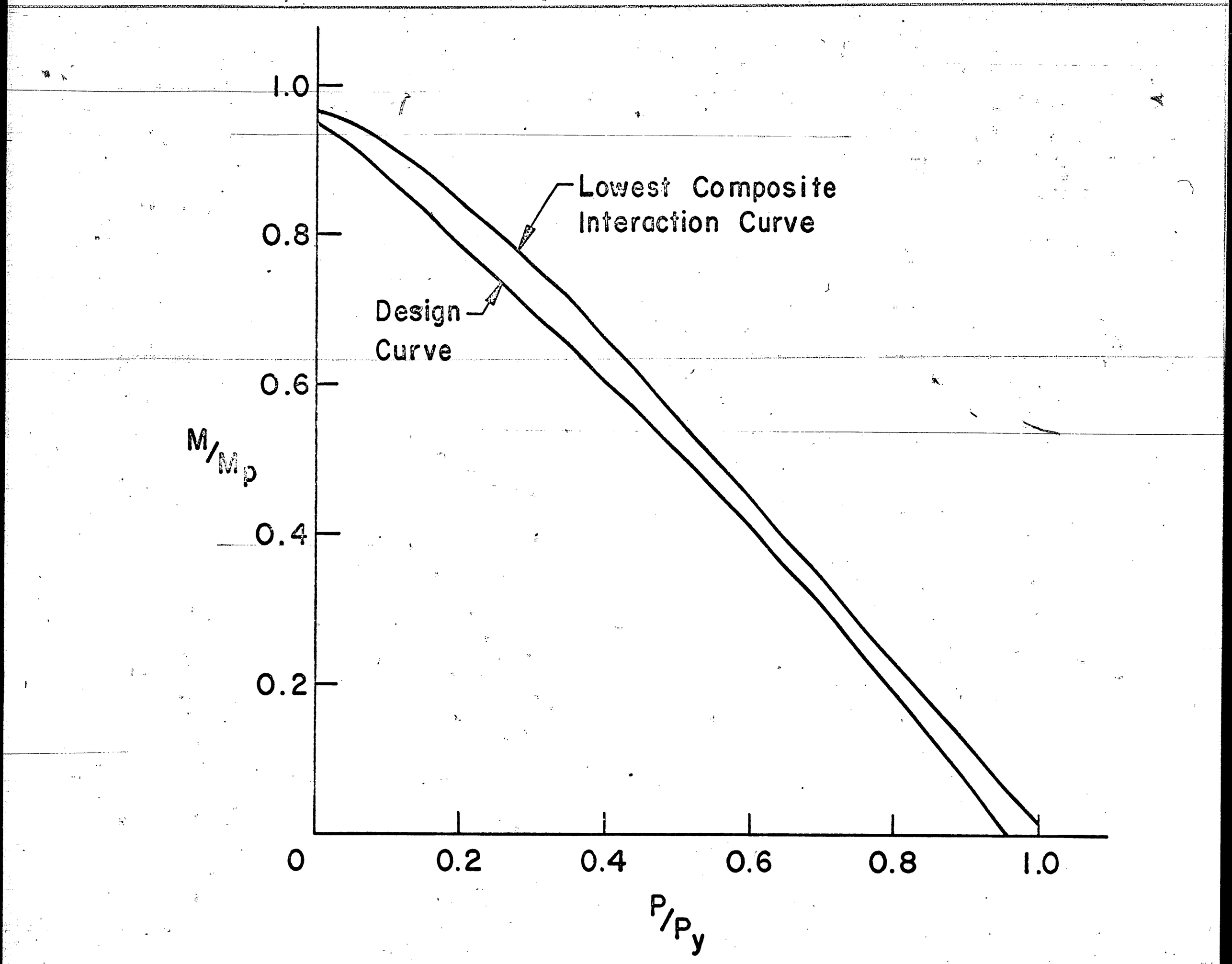

FIGURE 33. A Comparison of the Design Formula to Lowest Composite Interaction Curve of Selected Practical Sized Connections

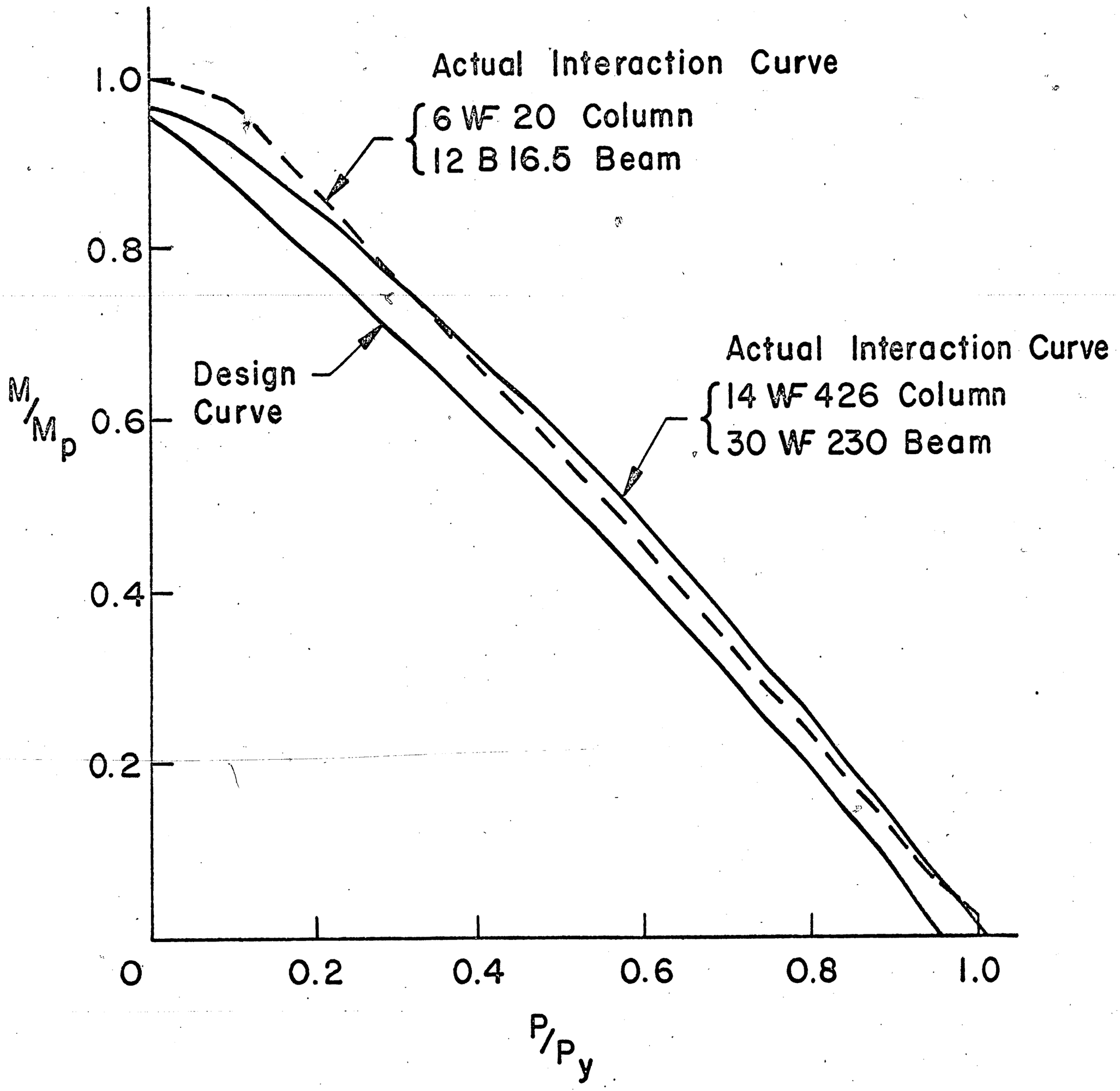

FIGURE 34. A Comparison of the Design Formula to the Actual Beam-to-Column Connection Interaction Curves Calculated from Part (2) of this Report

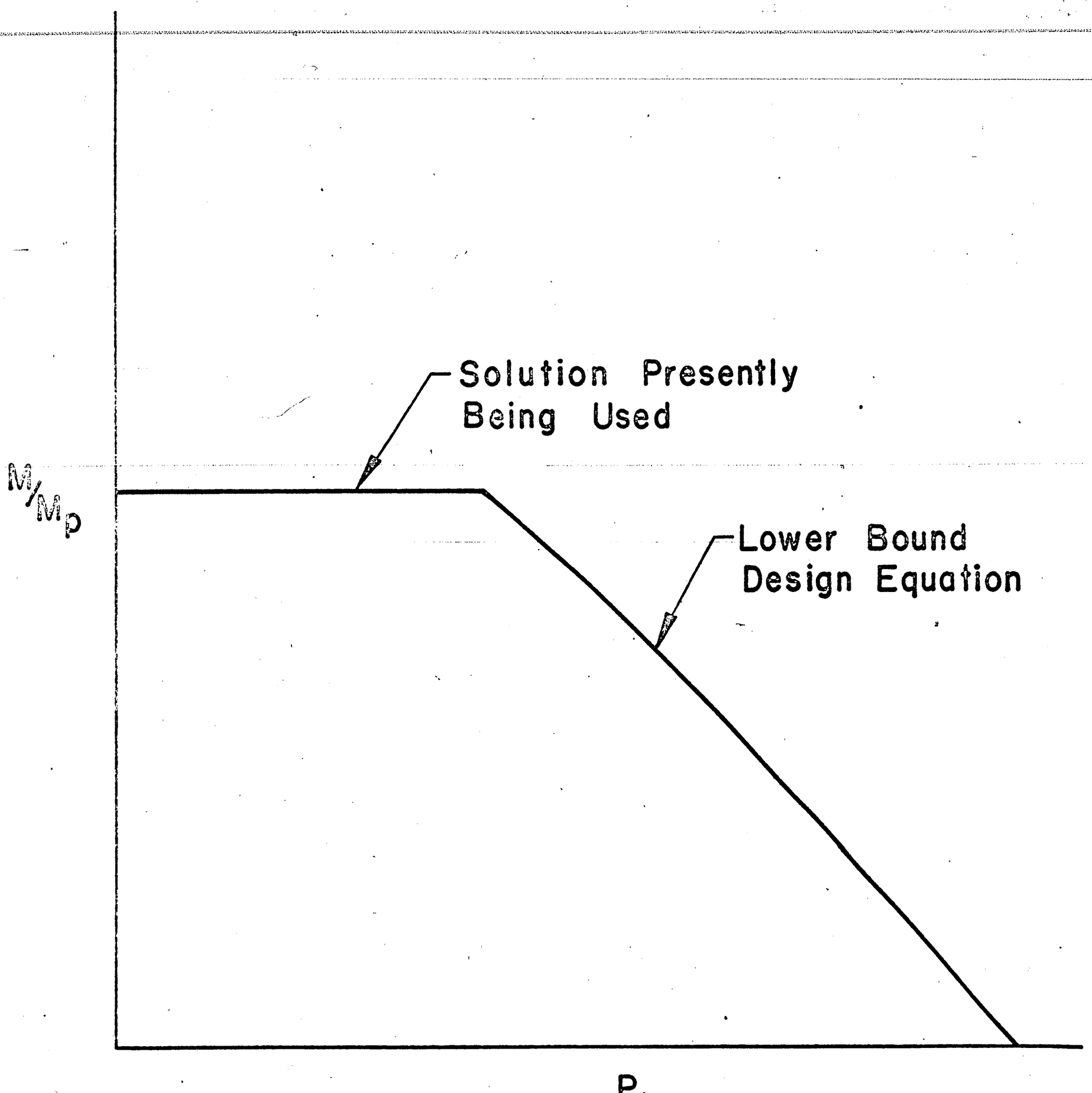

FIGURE 35. Final Design Interaction Curve for Beam-to-Column Connections

11. REFERENCES

1. Driscoll, G. C., Beedle, L. S., Galambos, T. V., Lu, L. W., Fisher, J. W., Ostapenko, A. and Daniels, J. H.
LECTURE NOTES--"PLASTIC DESIGN OF MULTI-STORY FRAMES", Fritz Laboratory Report No. 273.20, Lehigh University, 1965.

2. Fisher, J. W.
WELDED CONNECTIONS, Structural Steel Design, Chapter 19, ed. L. Tall, Ronald Press, New York, 1964.

3. Yura, J. A.
THE STRENGTH OF BRACED MULTI-STORY FRAMES, Fritz Laboratory Report No. 273.28, Lehigh University, September, 1965.

4. Beedle, L. S., Topractsoglou, A. A. and Johnston, B. G.
CONNECTIONS FOR WELDED CONTINUOUS PORTAL FRAMES, Progress Report No. 4, Welding Journal Research Supplement, July and August, 1951, November, 1952.

5. Graham, J. D., Sherbourne, A. N., Khabbaz, R. N. and Jensen, C. D.
WELDED INTERIOR BEAM COLUMN CONNECTIONS, WRC Bulletin Series No. 63, 1960.

6. Naka, T., Kato, B. and Watabe, M.
RESEARCH ON THE BEHAVIOR OF STEEL BEAM-TO-COLUMN CONNECTIONS, Laboratory for Steel Structure, University of Tokyo, 1966.

7. Horne, M. R.
THE FULL PLASTIC MOMENTS OF SECTIONS SUBJECTED TO SHEAR FORCE AND AXIAL LOAD, British Welding Research Association Report No. FE.1/51/57, March, 1957.

8. Kusuda, T. and Thurlimann, B.
STRENGTH OF WIDE FLANGE BEAMS UNDER COMBINED INFLUENCE OF MOMENT, AND AXIAL FORCE, PROGRESS REPORT No. 27. Fritz Laboratory Report No. 248.1, May, 1958.

9. Huber, A. W.
FIXTURES FOR TESTING PIN-ENDED COLUMNS, Fritz Laboratory Report No. 220A.24, Lehigh University, July, 1956.

10. Prager, W. and Hodge, P. G.
THEORY OF PERFECTLY PLASTIC SOLIDS, John Wiley and Sons, Inc., New York, 1961.

12. VITA

John Wilmer Peters, the son of Wilmer Jeremiah Peters and Virginia Louise Peters, was born on September 25, 1944, in Bethlehem, Pennsylvania.

He received his primary and secondary education in Bethlehem, Pennsylvania, graduating from Liberty High School in June of 1962. He then attended Lehigh University, obtaining his Bachelor of Science degree in Civil Engineering in June of 1966.

He entered Lehigh University Graduate School in September, 1966, as a research assistant in the Civil Engineering Department, and expects to receive his Master of Science degree in Civil Engineering in June of 1968.